National Library of Canada
Canadian Theses Service
Ottawa, Canada
K1A 0N4

Bibliothèque nationale du Canada
Service des thèses canadiennes

NOTICE

The quality of this microform is heavily dependent upon the quality of the original thesis submitted for microfilming. Every effort has been made to ensure the highest quality of reproduction possible.

If pages are missing, contact the university which granted the degree.

Some pages may have indistinct print especially if the original pages were typed with a poor typewriter ribbon or if the university sent us an inferior photocopy.

Previously copyrighted materials (journal articles, published tests, etc.) are not filmed.

Reproduction in full or in part of this microform is governed by the Canadian Copyright Act, R.S.C. 1970, c. C-30.

AVIS

La qualité de cette microforme dépend grandement de la qualité de la thèse soumise au microfilmage. Nous avons tout fait pour assurer une qualité supérieure de reproduction.

S'il manque des pages, veuillez communiquer avec l'université qui a conféré le grade.

La qualité d'impression de certaines pages peut laisser à désirer, surtout si les pages originales ont été dactylographiées à l'aide d'un ruban usé ou si l'université nous a fait parvenir une photocopie de qualité inférieure.

Les documents qui font déjà l'objet d'un droit d'auteur (articles de revue, tests publiés, etc.) ne sont pas microfilmés.

La reproduction, même partielle, de cette microforme est soumise à la Loi canadienne sur le droit d'auteur, SRC 1970, c. C-30.

NL-339 (r. 88/04)

Canada

THE UNIVERSITY OF ALBERTA

CHARACTERIZATION AND APPLICATION OF OXINE IMMOBILIZED ON CONTROLLED PORE GLASS FOR THE DETERMINATION OF FREE CALCIUM

by

PATRICK Y. T. CHOW

A THESIS

SUBMITTED TO THE FACULTY OF GRADUATE STUDIES AND RESEARCH IN

PARTIAL FULFILMENT OF THE REQUIREMENTS FOR

THE DEGREE OF DOCTOR OF PHILOSOPHY

DEPARTMENT OF CHEMISTRY

EDMONTON, ALBERTA

FALL 1988

Permission has been granted to the National Library of Canada to microfilm this thesis and to lend or sell copies of the film.

The author (copyright owner) has reserved other publication rights, and neither the thesis nor extensive extracts from it may be printed or otherwise reproduced without his/her written permission.

L'autorisation a été accordée à la Bibliothèque nationale du Canada de microfilmer cette thèse et de prêter ou de vendre des exemplaires du film.

L'auteur (titulaire du droit d'auteur) se réserve les autres droits de publication; ni la thèse ni de longs extraits de celle-ci ne doivent être imprimés ou autrement reproduits sans son autorisation écrite.

ISBN 0-315-45446-6

THE UNIVERSITY OF ALBERTA

RELEASE FORM

NAME OF AUTHOR PATRICK Y.T. CHOW

TITLE OF THESIS CHARACTERIZATION AND APPLICATION OF OXINE IMMOBILIZED ON CONTROLLED PORE GLASS FOR THE DETERMINATION OF FREE CALCIUM

DEGREE FOR WHICH THESIS WAS PRESENTED PH.D.

YEAR THIS DEGREE GRANTED 1988

Permission is hereby granted to THE UNIVERSITY OF ALBERTA LIBRARY to reproduce single copies of this thesis and to lend or sell such copies for private, scholarly or scientific research purposes only.

The author reserves other publication rights, and neither the thesis nor extensive extracts from it may be printed or otherwise reproduced without the author's written permission.

(Student's signiture)

32-P, Kim Tian Road
Singapore 0316
Republic of Singapore
(Student's permanent address)

DATE 14th Oct 1988

THE UNIVERSITY OF ALBERTA

FACULTY OF GRADUATE STUDIES AND RESEARCH

The undersigned certify that they have read, and recommend to the Faculty of Graduate Studies and Research for acceptance, a thesis entitled CHARACTERIZATION AND APPLICATION OF OXINE IMMOBILIZED ON CONTROLLED PORE GLASS FOR THE DETERMINATION OF FREE CALCIUM submitted by PATRICK Y.T. CHOW in partial fulfillment of the requirements for the degree of DOCTOR OF PHILOSOPHY.

Frederick F. Cantwell
F.F. CANTWELL, Supervisor

B. Kratochvil
B. KRATOCHVIL

J Harrison
D.J. HARRISON

George Kotovych
G. KOTOVYCH

G R Webster
G.R. WEBSTER

James L Fasching
J.L. FASCHING, External Examiner

DATE 12th Oct 1988

This thesis is dedicated to my late father, my mother, my brothers, and my sisters for their love, understanding and encouragement during the course of this program.

ABSTRACT

Many studies have been reported on the use of a sorbent consisting of 5-phenylazo-8-hydroxyquinoline bound to controlled pore glass (CPG-Oxine) for preconcentration and separation of metal ions. However, little has been done to provide a detailed characterization of this material. Therefore, one object of this thesis is to characterize a commercially available CPG-Oxine. The second objective is to determine the possibility of using CPG-Oxine for calcium speciation.

The theoretical basis of the CPG-Oxine column equilibration / atomic absorption spectrophotometry (AAS) method for measuring free calcium (Ca^{2+}) is described, and important experimental parameters are identified and optimized . The effects of pH, ionic strength and magnesium ion concentration on the sorption behavior of Ca^{2+} on CPG-Oxine are investigated. Studies of Ca^{2+} sorption isotherms show that the method is only useful for samples containing a relatively low ($\leq 10^{-4}$ M) Ca^{2+}.

A physico-chemical model for Ca^{2+} sorption on CPG-Oxine is presented, which is based on the "ionizable surface group" and "site-binding" models. Spectrophotometric measurements on CPG-Oxine allow determination of the degree of ionization of the phenolic hydroxyl group as a function of pH. Electrical properties of the surface of CPG-Oxine are obtained by applying the Gouy-Chapman theory to data obtained from capacity measurements and potentiometric titration of CPG-Oxine. The sorption model is used to quantitatively explain the dependence of Ca^{2+} sorption on both solution pH and ionic strength.

The use of CPG-Oxine in the column equilibration / AAS method for selectively determining $[Ca^{2+}]$ in aqueous solution in the presence of a variety of charged, kinetically labile metal-ligand complexes of calcium is demonstrated.

Finally, an attempt is made to use the CPG-Oxine column equilibration / AAS method for the determination of $[Ca^{2+}]$ in urine by measuring $[Ca^{2+}]$ in diluted urine

samples, and then extrapolating to the [Ca^{2+}] in the undiluted urine. The study shows that the dilution method is not suitable for this purpose. Determination of [Ca^{2+}] in urine requires the use of an immobilized ligand which is a weaker complexing agent for Ca^{2+} than 5-phenylazo-8-hydroxyquinoline.

ACKNOWLEDGEMENTS

I would like to express my deepest, sincerest appreciation and thanks to the following people.

My supervisor, Dr. Frederick F. Cantwell for his supervision, encouragement, and expert guidance throughout this research program and for his helpful suggestions in the preparation of this manuscript.

Dr. Anne K. Kolstad for help in carrying out the spectrophotometric measurements during her postdoctoring work with Dr. Cantwell.

Dr. Koichi Takamura and Mr. Ross Chow of the Alberta Research Council for helpful discussions and for the use of their electrophoresis equipment.

Dr. Byron Kratochvil and Dr. George Kotovych for such careful proofreading of this thesis.

TABLE OF CONTENTS

CHAPTER PAGE

ONE. INTRODUCTION.. 1

I.1 TRACE METAL SPECIATION........................... 1

I.2 CALCIUM SPECIATION................................ 2

I.2.1 The Role of Ca^{2+} in Biological System.................. 3

I.2.2 Approaches for Measuring Ca^{2+}....................... 3

I.2.2.1 Calcium Ion-Selective Electrode Methods......... 3

I.2.2.2 Spectrophotometric Methods................... 4

I.2.2.3 Ultrafiltration Methods....................... 5

I.2.2.4 Cation Exchange Methods.................... 5

I.3 BACKGROUND ON CONTROLLED PORE GLASS-OXINE.... 6

I.4 RESEARCH OBJECTIVES............................... 10

TWO CHARACTERIZATION OF CPG-OXINE / ATOMIC ABSORPTION SYSTEM FOR FREE CALCIUM DETERMINATION................ 12

II.1 THEORY OF THE COLUMN EQUILIBRATION TECHNIQUE... 12

II.2 EXPERIMENTAL...................................... 18

II.2.1 Chemicals and Reagents.............................. 18

II.2.2 Column Preparation.................................. 18

II.2.3 Apparatus.. 19

II.2.4 Preparation of Test Solutions......................... 22

II.2.5 Column Equilibration Procedure........................ 24

II.2.6 Measurement of Distribution Coefficient................ 25

II.3 RESULTS AND DISCUSSION............................ 26

II.3.1 Column Washing...................................... 26

II.3.2 Column Equilibration (Loading)........................ 30

II.3.3 Column Elution.............................. 41
II.3.4 Calcium Sorption Behavior.......................... 41
II.3.4.1 Sorption Isotherm........................... 41
II.3.4.2 Effect of Solution pH....................... 44
II.3.4.3 Effect of Ionic Strength...................... 44
II.3.4.4 Effect of Magnesium on Calcium Sorption........ 47
II.4 CONCLUSIONS.................................. 47
THREE PROPERTIES OF CPG-OXINE AND ITS SORPTION OF CALCIUM... 51
III.1 INTRODUCTION.................................. 51
III.2 THEORY.. 51
III.3 EXPERIMENTAL.................................. 57
III.3.1 Chemicals and Reagents.......................... 57
III.3.2 Apparatus...................................... 59
III.3.3 Capacity Measurements........................... 60
III.3.4 Determination of Chloride Content................. 61
III.3.5 Potentiometric Titrations.......................... 61
III.3.6 Spectrophotometric Measurement.................... 62
III.3.7 Microelectrophoresis............................. 62
III.4 RESULTS AND DISCUSSION........................... 63
III.4.1 Homogeneity..................................... 63
III.4.2 Capacity.. 63
III.4.3 Chloride Content................................ 65
III.4.4 Potentiometric Titrations.......................... 66
III.4.5 Spectrophotometry............................... 73
III.4.6 Microelectrophoresis............................. 77
III.4.7 Effect of pH on Ca^{2+} Sorption....................... 80
III.4.8 Effect of Ionic Strength on Ca^{2+} Sorption............. 82

III.5 CONCLUSIONS 84

FOUR SPECIFICITY OF THE CPG-OXINE COLUMN EQUILIBRATION / AAS METHOD FOR FREE CALCIUM SPECIES DETERMINATION IN AQUEOUS SOLUTIONS 87

IV.1 INTRODUCION 87

IV.2 EXPERIMENTAL 88

IV.2.1 Chemicals and Reagents 88

IV.2.2 Apparatus 89

IV.2.3 Preparation of Test Solution 89

IV.2.4 Determination of Free Calcium Concentration by the CPG-Oxine Column Equilibration Method 91

IV.3 DETERMINATION OF FREE CALCIUM CONCENTRATION BY THEORETICAL CALCULATIONS 91

IV.3.1 Ca^{2+} - CaL^{2-} System 91

IV 3.2 Ca^{2+} - CaL^{+} System 94

IV.3.3 Ca^{2+} - CaL System 97

IV.3.4 Ca^{2+} - CaL - $CaHL^{+}$ System 100

IV.3.5 Ca^{2+} - CaH_2L - $CaHL^{-}$ System 103

IV.4 RESULTS AND DISCUSSION 106

IV.4.1 Calcium ISE Method 106

IV.4.2 Column Equilibration Method 112

IV.4.2.1 Determination of Ca^{2+} in the Presence of CaL^{2-} complex 112

IV.4.2.2 Determination of Ca^{2+} in the Presence of CaL^{+} complex 113

IV.4.2.3 Determination of Ca^{2+} in the Presence of CaL complex 113

IV.4.2.4 Determination of Ca^{2+} in the Presence of both CaL and $CaHL^+$ complexes 116

IV.4.2.5 Determination of Ca^{2+} in the Presence of both $CaHL^-$ and CaH_2L complexes 116

IV.5 CONCLUSIONS 121

FIVE FEASIBILITY STUDIES OF MEASURING FREE CALCIUM IN REAL SAMPLES BY THE CPG-OXINE COLUMN EQUILIBRATION METHOD 122

V.1 INTRODUCTION 122

V.2 LIMITATIONS ON THE CPG-OXINE COLUMN EQUILIBRATION METHOD 123

V.3 DETERMINATION OF $[Ca^{2+}]$ BY THE DILUTION METHOD ... 124

V.3.1 Experimental 124

V.3.1.1 Chemicals and Reagents 124

V.3.1.2 Apparatus 124

V.3.1.3 Samples 125

V.3.1.4 Preparation of Diluted Samples and Ca^{2+} Standard Solutions 125

V.3.1.5 Determination of Total Calcium 125

V.3.1.6 Determination of Column Loading Time for Urine 126

V.3.1.7 Determination of $[Ca^{2+}]$ by the Column Equilibration Method 126

V.3.2 Results and Discussion 126

V.3.2.1 Total Calcium 126

V.3.2.2 Loading Study for Diluted Urine Samples 128

V.3.2.3 Effect of Dilution on $[Ca^{2+}]$ 133

V.3.3 Computer Simulation Studies of Dilution Effect on $[Ca^{2+}]$ in Model Solutions 143
V.3.3.1 Simulated Urine System 143
V.3.3.2 Results and Discussion 144
V.4 CONCLUSIONS 144
SIX FUTURE STUDIES 148

****

REFERENCE 150
APPENDIX I SORPTION ISOTHERM FOR Ca^{2+} ON CPG-OXINE (BATCH A) AT VARIOUS pH VALUES AND IONIC STRENGTHS 162
APPENDIX II COMICS PROGRAM 176

LIST OF TABLES

TABLE PAGE

1.1 Properties of sorbents composed of oxine bound to controlled pore glass 8

2.1 Instrumental conditions for monitoring calcium and sodium with the Model 4000 atomic absorption spectrophotometer 23

2.2 Effects of CO_2-free and untreated water washing on the eluted calcium peak height for a 20 mg CPG-Oxine column 28

2.3 Moles of Na^+ eluted from the 40 mg CPG-Oxine (125 - 177 μm particle size) column loaded with 0.10 M $NaClO_4$ containing 0.010 M HEPES buffer at pH 7.00 for various periods and washed for 18 min 39

2.4 Effect of pre-buffer loading time on the eluted calcium peak height obtained after 4 min loading of Ca^{2+} solution containing 0.10 M $NaClO_4$ at pH 7.00 on the 40 mg CPG-Oxine (125 - 177 μm particle size) column 40

2.5 The experimental conditions used in obtaining the isotherms and the approximate upper limit of $[Ca^{2+}]$ for trace loading CPG-Oxine 43

2.6 Effect of Mg^{2+} on the eluted calcium peak height under trace loading $[Ca^{2+}]$ for CPG-Oxine 48

2.7 Effect of Mg^{2+} on the eluted calcium peak height under non-trace loading $[Ca^{2+}]$ for CPG-Oxine 49

3.1 Variation of sorbed calcium with the weight of CPG-Oxine in column.... 64

3.2 Surface electrical properties and spectrophotometric measurement of ionization of bound 5-P-Oxine on CPG-Oxine (Batch B) at $c = 0.10$ M 74

3.3 Effect of pH on zeta potential at the surface of CPG-Oxine (Batch A) at $c = 0.10$ M 79

3.4 Surface electrical properties and calcium sorption by CPG-Oxine (Batch A) 81

4.1 Instrumental conditions for measuring calcium with the Model 290B atomic absorption spectrophotometer 90

4.2 Acid dissociation and stability constants for major calcium-EDTA complexes at 25° C 93

4.3 Complexation of Ca^{2+} with EDTA at pH 7.00 95

4.4 Acid dissociation and stability constants for major calcium-carnosinate and calcium-picolinate complexes at 25° C 96

4.5 Complexation of Ca^{2+} with carnosinate or picolinate at pH 7.00 98

4.6 Acid dissociation and stability constants for major calcium-phthalate and calcium-sulfate complexes at 25° C 99

4.7 Complexation of Ca^{2+} with phthalate or sulfate at pH 7.00 101

4.8 Acid dissociation and stability constants for major calcium-malate and calcium-tartrate complexes at 25° C 102

4.9 Complexation of Ca^{2+} with malate or tartrate at pH 7.00 104

4.10 Acid dissociation and stability constants for major calcium-citrate complexes at 25° C 105

4.11 Complexation of Ca^{2+} with citrate at pH 7.00 107

4.12 Calibration of the Orion 93-20 calcium ion-selective electrode for Ca^{2+} in 0.25 M $NaClO_4$ (pH 7.00) at 25 ± 1° C 110

4.13 Response of the Orion 93-20 calcium ion-selective electrode in various concentrations of picolinic acid containing 0.10 M $NaClO_4$ at 25 ± 1° C 111

4.14 Specificity of CPG-Oxine for Ca^{2+} in the presence of CaL^{2-} species 114

4.15 Specificity of CPG-Oxine for Ca^{2+} in the presence of CaL^+ species...... 115

4.16 Specificity of CPG-Oxine for Ca^{2+} in the presence of CaL species....... 117

4.17 Specificity of CPG-Oxine for Ca^{2+} in the presence of CaL + $CaHL^+$ species.. 118

4.18 Specificity of CPG-Oxine for Ca^{2+} in the presence of $CaHL^-$ + CaH_2L species.. 120

5.1 Total calcium content in urine and wine samples..................... 127

5.2 Loading times for unfiltered urine samples (pH 5.78) with various dilutions. Sample loading flow rate of 2 mL/min...................... 129

5.3 Analysis of [Ca^{2+}] in diluted urine (unfiltered, 5.78). Total calcium content in the original, undiluted urine was 4.11 (± 0.07) mM.......... 134

5.4 Analysis of [Ca^{2+}] in diluted urine (unfiltered, 5.88). Total calcium content in the original, undiluted urine was 6.05 (± 0.07) mM.......... 135

5.5 Analysis of [Ca^{2+}] in diluted urine (unfiltered, 6.13). Total calcium content in the original, undiluted urine was 2.40 (± 0.04) mM.......... 136

5.6 Analysis of [Ca^{2+}] in diluted wine (unfiltered, 3.30). Total calcium content in the original, undiluted wine was 2.14 (± 0.06) mM.......... 137

5.7 Mean values of maximum and minimum concentrations of some major components in typical urine sample (36)........................... 138

A.1 Equilibria in the simulated urine system (Section V.3.3.1)............ 186

LIST OF FIGURES

FIGURE PAGE

1.1 Structure of the immobilized derivative of 5-phenylazo-8-hydroxyquinoline.. 11

2.1 Concept of column equilibration technique. (a) CPG-oxine is at equilibrium with unperturbed sample solution. (b) Breakthrough curve.. 13

2.2 Diagram of Ca^{2+} equilibria in sample solution and CPG-Oxine column.. 15

2.3 Loading, washing and eluting profiles for a 40 mg CPG-Oxine column loading with Ca^{2+}.. 16

2.4 Diagram of a 1 cm CPG-Oxine (125 - 177 μm particle size) column..... 20

2.5 Diagram of operating system.. 21

2.6 Calibration plot of calcium peak height versus moles of Ca^{2+}.......... 27

2.7 Loading curves for Ca^{2+} in 0.10 M $NaClO_4$ at (a) pH 8.01; (b) pH 7.00 and (c) pH 6.51 on the 40 mg CPG-Oxine (125 - 177 μm particle size) column.. 31

2.8 Loading curves for Ca^{2+} in (a) 0.010 M; (b) 0.050 M; (c) 0.10 M and (d) 0.30 M $NaClO_4$ at pH 7.00 on the 40 mg CPG-Oxine (125 - 177 μm particle size) column.................... 32

2.9 Diagram of a 11 x 3 mm i.d. CPG-Oxine column with particle size of 50 - 75 μm.. 34

2.10 Loading curves for Ca^{2+} in (a) 0.10 M and (b) 0.30 M $NaClO_4$ at pH 7.00 on the 40 mg CPG-Oxine (50 - 75 μm particle size) column.. 35

2.11 Loading curve for Ca^{2+} in 0.010 M $NaClO_4$ at pH 8.01 on the

11 mg CPG-Oxine (125 - 177 μm particle size) column................ 36

2.12 Loading curve for Ca^{2+} in 0.10 M $NaClO_4$ at pH 7.00 on the 11 mg CPG-Oxine (125 - 177 μm particle size) column................ 37

2.13 Plot of λ_o *versus* pH for calcium sorbed by the 40 mg CPG-Oxine column under trace conditions at c = 0.10 M........................ 45

2.14 Plot of λ_o *versus* c for calcium sorbed by the 40 mg CPG-Oxine column under trace conditions at pH = 7.00........................ 46

3.1 Potentiometric titration curve of acid washed and vacuum dried CPG-Oxine (Batch A) at c = 0.010 M............................ 67

3.2 Potentiometric titration curve of acid washed and vacuum dried CPG-Oxine (Batch A) at c = 0.050 M............................ 68

3.3 Potentiometric titration curve of acid washed and vacuum dried CPG-Oxine (Batch A) at c = 0.10 M............................ 69

3.4 Potentiometric titration curve of acid washed and vacuum dried CPG-Oxine (Batch A) at c = 0.20 M............................ 70

3.5 Potentiometric titration curve of acid washed and vacuum dried CPG-Oxine (Batch A) at c = 0.30 M............................ 71

3.6 Potentiometric titration curve of acid washed and vacuum dried CPG-Oxine (Batch B) at c = 0.10 M............................ 72

3.7 Plot of spectrophotometric data from Run 1 for CPG-Oxine (Batch B) at c = 0.10 M according to Eq. 3.24...................... 76

3.8 Plot of spectrophotometric data from Run 2 for CPG-Oxine (Batch B) at c = 0.10 M according to Eq. 3.24...................... 78

3.9 Plot of λ_o *versus* $\overline{\alpha_{OX}}$ for CPG-Oxine (Batch A) at c = 0.10 M and varying pH for the data in Table 3.4................ 83

3.10 Plot according to Eq. 3.28 for CPG-Oxine (Batch A) at pH 7.00

and varying c for the data in Table 3.4........................... 85

4.1 Calibration of the Orion 93-20 calcium ion-selective electrode for Ca^{2+} in 0.10 M $NaClO_4$ (pH 7.00) at 25 ± 1° C.................... 108

5.1 Loading curve for unfiltered urine sample (pH 5.78) with 50 fold dilution.. 130

5.2 Loading curve for unfiltered urine sample (pH 5.92) with 50 fold dilution.. 131

5.3 Loading curve for filtered urine sample (pH 5.92) with 50 fold dilution.. 132

5.4 Plot of undiluted $[Ca^{2+}]$ versus dilution factor for urine sample at pH 5.78. Value of undiluted $[Ca^{2+}]$ was obtained by multiplying the value of $[Ca^{2+}]$ in the diluted urine by the corresponding dilution factor.. 139

5.5 Plot of undiluted $[Ca^{2+}]$ versus dilution factor for urine sample at pH 5.88. Value of undiluted $[Ca^{2+}]$ was obtained by multiplying the value of $[Ca^{2+}]$ in the diluted urine by the corresponding dilution factor.. 140

5.6 Plot of undiluted $[Ca^{2+}]$ versus dilution factor for urine sample at pH 6.13. Value of undiluted $[Ca^{2+}]$ was obtained by multiplying the value of $[Ca^{2+}]$ in the diluted urine by the corresponding dilution factor.. 141

5.7 Plot of undiluted $[Ca^{2+}]$ versus dilution factor for wine sample at pH 3.30. Value of undiluted $[Ca^{2+}]$ was obtained by multiplying the value of $[Ca^{2+}]$ in the diluted wine by the corresponding dilution factor.. 142

5.8 Plots of undiluted $[Ca^{2+}]$ versus dilution factor for simulated urine samples, with citrate to calcium ratios of 0.2, 0.7, 1.5, 3.0 and 6.0, at pH 5.5. Value of undiluted [Ca^{2+}] was obtained by multiplying the value of [Ca^{2+}] in the diluted urine by the corresponding dilution factor.. 145

5.9 Plots of undiluted [Ca^{2+}] versus dilution factor for simulated urine samples, with citrate to calcium ratios of 0.2, 0.7, 1.5, 3.0 and 6.0, at pH 6.0. Value of undiluted [Ca^{2+}] was obtained by multiplying the value of [Ca^{2+}] in the diluted urine by the corresponding dilution factor.. 146

A.1 Sorption isotherm for Ca^{2+} in 0.10 M $NaClO_4$ at pH 8.01 on the 11 mg CPG-Oxine column.................................. 164

A.2 Sorption isotherm for Ca^{2+} in 0.10 M $NaClO_4$ at pH 7.00 on the 11 mg CPG-Oxine column.................................. 165

A.3 Sorption isotherm for Ca^{2+} in 0.10 M $NaClO_4$ at pH 6.00 on the 11 mg CPG-Oxine column.................................. 166

A.4 Sorption isotherm for Ca^{2+} in 0.10 M $NaClO_4$ at pH 5.00 on the 11 mg CPG-Oxine column.................................. 167

A.5 Sorption isotherm for Ca^{2+} in 0.010 M $NaClO_4$ at pH 8.01 on the 11 mg CPG-Oxine column.................................. 168

A.6 Sorption isotherm for Ca^{2+} in 0.010 M $NaClO_4$ at pH 5.00 on the 11 mg CPG-Oxine column.................................. 169

A.7 Sorption isotherm for Ca^{2+} in 0.75 M $NaClO_4$ at pH 7.00 on the 11 mg CPG-Oxine column.................................. 170

A.8 Sorption isotherm for Ca^{2+} in 0.10 M $NaClO_4$ at pH 8.01 on the 40 mg CPG-Oxine column.................................. 171

A.9 Sorption isotherm for Ca^{2+} in 0.10 M $NaClO_4$ at pH 7.00 on the 40 mg CPG-Oxine column which has not been equilibrated......... 172

A.10 Sorption isotherm for Ca^{2+} in 0.10 M KCl at pH 5.00 on the

11 mg CPG-Oxine column.................................... 173

A.11 Sorption isotherm for Ca^{2+} in 0.10 M KCl at pH 3.00 on the 11 mg CPG-Oxine column.................................... 174

A.12 Sorption isotherm for Ca^{2+} in 0.30 M $NaClO_4$ at pH 6.00 and pH 7.40 on the 11 mg CPG-Oxine column.......................... 175

A.13 Schemes of COMICS method.................................... 177

A.14 Data input of "CALCIUM SPECIATION IN URINE" for the COMICS program.................................... 180

A.15 Data output of "CALCIUM SPECIATION IN URINE" for the COMICS program.................................... 181

A.16 Data input procedure for the COMICS programe.................... 184

LIST OF SYMBOLS

SYMBOL	DESCRIPTION
AAS	atomic absorption spectrophotomery
ISE	ion-selective electrode
CPG-Oxine	5-P-Oxine bound on Controlled Pore Glass
Ca^{2+}	free calcium ion
C_{Ca}	total calcium concentration in bulk solution
$[Ca^{2+}]$	Ca^{2+} concentration
a_{Ca}	activity of Ca^{2+} in bulk solution
γ_{Ca}	acivity coefficient for Ca^{2+}
$\overline{a_{Ca}}$	activity of Ca^{2+} at a distance **x** cm away from (but close to) the charge-surface
$\overline{n_{Ca}}$	moles of remaining dissolved calcium, not complexed by bound 5-P-Oxine, in the pores of CPG-Oxine that are incompletely removed by water washing
$\overline{N_{Ca}}$	total number of moles of sorbed calcium per gram of CPG-Oxine
$\overline{H_2OX^+}$	protonated bound 5-P-Oxine species
$\overline{HOX}$	neutral bound 5-P-Oxine species
$\overline{OX^-}$	anionic bound 5-P-Oxine species
a_H	acivity of hydrogen ion in the bulk solution
$\overline{a_{H,x}}$	activity of hydrogen ion at a distance **x** cm away from the charge-surface
$\overline{H^+}$	hydrogen ion near the charge-surface
$\overline{pH}$	pH immediately adjacent to the surface

K'_{a1}	first acid dissociation constant for oxine
K'_{a2}	second acid dissociation constant for oxine
$\overline{K'_{a1}}$	first acid dissociation constant for bound 5-P-Oxine
$\overline{K'_{a2}}$	second acid dissociation constant for bound 5-P-Oxine
$\overline{pK_a}$	negative value of log $\overline{K'_a}$
$\overline{\alpha_{OX}}$	fraction of bound 5-P-Oxine ionized
$\overline{\nu_{Oxine}}$	moles of bound 5-P-Oxine per gram of CPG-Oxine
V_x	volume per gram of CPG-Oxine in a thin layer of solution located at a distance **x** cm from the charge-surface
A_{sp}	specific surface area for CPG-Oxine
λ_o	distribution coefficient for Ca^{2+} on CPG-Oxine
c	ionic strength of the bulk solution
ψ_o	electrical potential of the charge-surface in volt
ψ_x	electrical potential at any distance **x** cm away from the charge-surface in volt
Q	surface concentration of ionized surface groups in mmol/g
σ_o	surface charge density in coul/cm^2
$1/\kappa$	"thickness" of the diffuse part of the electrical double layer
F	Faraday constant
R	ideal gas constant
Z	charge on the ionized surface group
T	absolute temperature
β	stability constant for calcium-ligand complex
β'	conditional stability constant for calcium-ligand complex
$\overline{CaOX^+}$	1:1 complex between Ca^{2+} and $\overline{OX^-}$
$\overline{\beta_1}$	stability constant for $\overline{CaOX^+}$

L	ligand
C_L	total ligand concentration in bulk solution
$[L']$	total concentration of uncomplexed ligand
ζ	zeta potential
u_H	electrophoretic mobility
ε	permittivity of the solution
η	viscosity of the solution
$A_{Scatter}$	absorbance due to scattering
A_{acid}	absorbance measured at pH 6.40
A_{alkali}	absorbance measured at pH 9.80
b	optical pathlength
$\varepsilon_{\overline{HOX}}$	molar absorptivity for $\overline{HOX}$ species
$\varepsilon_{\overline{OX}}$	molar absorptiviy for $\overline{OX^-}$ species

CHAPTER ONE

INTRODUCTION

Many elements are present in environmental or biological samples in a variety of physico-chemical forms (species). The distribution of an element among these species can affect its bioavailability, toxicity, bioaccumulation and transport. Measurement of the total concentration of each element does not provide enough information on these processes. In order to obtain meaningful data, it is essential that "chemical speciation" techniques be applied to determine each species formed by a particular element (1). In this thesis the term "speciation" will refer to determinations of one or more of the different species of an element (1,2).

I.1 TRACE METAL SPECIATION :

In environmental analysis, interest is often directed to trace heavy metal speciation in natural waters (1-4). This reflects the importance of these elements as common pollutants and the complexity of their species distributions.

The role of various species of heavy metals in natural waters has been discussed in many literature articles and books (1-4). There are two major reasons for performing trace heavy metal speciation studies:

(A) The biological activity of a metal can vary widely from one chemical species to another. For example, in the case of toxicity, it is believed that the free (ionized or hydrated) copper (II) ion is the form most toxic to aquatic life (1-5). However, metal-ligand complexes of copper (II) and copper (II) associated with colloid particles are less toxic. As another example the toxicity of mercury (II) to humans depends upon the form of mercury (II). Methylmercury is much more toxic than hydrated mercury (II) (1,6).

(B) The transport and fate of heavy metals in water systems is of importance to the control of pollution. They may depend markedly upon the distribution of the metal between the water itself and suspended particulate matter within it, and on the differences in physical properties such as volatility and solubility for various species of the metal present. It follows, therefore, that the efficiency of trace heavy metal removal by chemical or biological treatment processes may be influenced by the species distribution of the metal.

Many analytical techniques have been developed to study the chemical species distribution, especially of trace metals in waters (1-6). Basically, there are two different approaches to chemical speciation. The first involves calculation of the equilibrium concentrations of all the metal-ligand species using known values for total metal and ligand concentrations and published values of the relevent metal-ligand stability constants (1,7,8). The second approach is experimental, which includes a few measurement techniques such as ion-selective electrodes (ISE)(9,10) and anodic stripping voltammetry (11-13), as well as separation techniques such as dialysis, ultrafiltration (14,15) and ion-exchange/chelation (13,16-23).

1.2 CALCIUM SPECIATION :

Calcium is one of the major constituents present in natural waters and biological fluids. Among various ionic species in natural waters, calcium plays an important role in carbonate deposition in the oceans (24,25). Many papers on this topic have been included in the conference proceedings edited by Gould (26) and Jenne (8). However, most of the calcium speciation studies have been devoted to clinical or biomedical investigations. This is because calcium is well known to physiologists and biochemists as one of the most important bioelements (27). It has also been realized that in many biological systems only the free (ionized or hydrated) calcium ion has physiological activity. This was first demonstrated by McLean and Hasting (28). In this thesis Ca^{2+} will refer to the free calcium ion.

I.2.1 THE ROLE OF Ca^{2+} IN BIOLOGICAL SYSTEMS :

The free calcium ion is involved in various physiological and biochemical processes, such as bone formation, nerve conduction, cerebral function, cardiac conduction and contraction, membrane phenomena, muscle contraction and relaxation, blood coagulation, and enzyme activation (29-32); in the mechanism of calcium transport and binding (33-35); and in kidney stone formation (36,37). Free calcium ion values have been shown to be more relevant than total calcium values when studying the possibility of hypercalcaemic disorders (38-40). The advances in several fields of scientific research which relate to the involvement of calcium in the structure, development and function of biological systems have been discussed and reviewed (41-45). In order to investigate the role of Ca^{2+} in biological systems, it is important to develop a practical method for its measurement.

I.2.2 APPROACHES FOR MEASURING Ca^{2+} :

In general, Ca^{2+} concentration ($[Ca^{2+}]$) in human urine and serum has been reported to be about 50% of the total dissolved calcium concentration (28,46,47). The four major methodologies for determining $[Ca^{2+}]$ are : (a) Calcium ion-selective electrodes (30,43,47-51); (b) Spectrophotometric methods by using calcium indicators (43,51-57); (c) Ultrafiltration (58-62); and (d) Cation exchange (46,63-65). In addition, computer programs have also been used to study simulated biological systems (66).

1.2.2.1 CALCIUM ION-SELECTIVE ELECTRODE METHODS :

The calcium ion-selective electrode responds to the activity of Ca^{2+} in solution. Its major application is in the field of clinical and biomedical analysis (30,67-69) since most of the biological processes are thought to be dependent on the activity, rather than the concentration, of ionic species (30,68). Therefore, this technique has some theoretical advantages which could lead to more clinically relavent data. Recently, calcium microelectrodes have also been developed for measurement of intracellular Ca^{2+} activity (48,49,51,57,70).

There are a few commercially available calcium ion-selective electrodes (67,69). The Orion electrode is probably the only one which has been investigated extensively for use in the clinical laboratory. The calcium ion-selective electrode has several limitations when used in biological fluids. These limitations are often due to the following reasons : First, the lack of selectivity of the calcium electrodes, which experience interference by other cations such as magnesium and sodium (69,71,72). Second, the effect of variable ionic strength (68,69,73) and junction potential (69,74,75). And third, the presence of biochemicals or anionic surfactants that may interfere with electrode performance as well (76-81).

1.2.2.2 SPECTROPHOTOMETRIC METHODS :

Besides ion-selective electrodes, calcium indicators appear to be most widely used for the determination of extra- and intra-cellular Ca^{2+}. There are three major types of calcium indicators : (i) Photoproteins such as aequorin (43,51-53,57,82);
(ii) Metallochromic indicator dyes such as murexide (43,51,54,55) and arsenazo III (43,51,54,57); and (iii) Fluorescent indicators such as quin-2 (43,57).

In these methods, an indicator ligand that forms a weak but highly colored complex with Ca^{2+} is added to the sample under study. Changes in the luminescence of a photoprotein, the absorbance of a metallochromic dye, or the fluorescence of a fluorescent indicator is detected with suitable equipment, such as a photomultiplier, an image intensifier, or a fluorescent microscope. Like the calcium ion-selective electrode method, the spectrophotometric measurements also have several limitations (51,83) :

a) The indicator must not be bound to other metals or biological substances, except for Ca^{2+}, nor penetrate into organelles, nor hinder cell structure and function.

b) Disturbance of the natural equilibria involving Ca^{2+} due to the indicator must be minimized, i.e. only a small fraction of the Ca^{2+} (usually less than 1%) may be allowed to complex with the indicator.

c) The indicator and calcium-indicator complex must be soluble and stable in the biological fluids.

d) Other indicator properties such as acid-base properties compatible with the sample pH, high purity and sensitive optical properties are also important.

1.2.2.3 ULTRAFILTRATION METHODS :

Measurement of ultrafiltrable calcium (i.e. protein-free ionized plus complexed calcium) is more common in analysis of blood or serum than urine. It is an alternative approach to that of determining just Ca^{2+} but might provide a better index of calcium balance in certain clinical conditions (84). However, due to technical limitations such as contamination of sample in ultrafiltration (2), as well as a perceived lesser physiological importance of ultrafiltrable calcium, there are not many reports related to the measurement of ultrafiltrable calcium.

1.2.2.4 CATION EXCHANGE METHODS :

The use of cation exchange techniques to determine Ca^{2+} is based on the approach of Schubert (85). In this approach the sample solution under study is brought to equilibrium with a cation exchanger, then the amount of calcium bound by the exchanger is eluted and determined by either EDTA titration (46,63,65), or a radio-isotope technique (86), or flame photometry (87). The concentration of calcium in the eluate is linearly related to the $[Ca^{2+}]$ in the original sample solution. This technique provides a distinct advantage over the others : It is non-perturbing and can be used for measuring very low [Ca^{2+}] in samples containing interfering metal ions and ligands.

The cation exchange method is generally quite time-consuming due to the slow equilibration. The recent advent of the cation-exchange column equilibration technique (19-22) provides a more rapid and easier method for free metal ion determination, and it has been used to determine [Ca^{2+}] in urine (88). Unfortunately, the major drawback of all cation exchange speciation methods is that the sorption of positively charged calcium-containing species (e.g. calcium-containing labile complexes) has to be neglected. The limitations of the conventional cation exchangers have been discussed (22,89). It has been shown that they are capable of sorbing not only free metal ion but also positively charged, and even some neutral, complexes. Therefore, at present, this method is still considered non-selective for free metal ions in the presence of their cationic and, to some extent, neutral complexes.

I.3 BACKGROUND ON CONTROLLED PORE GLASS-OXINE :

The lack of selectivity of conventional cation exchange resins has led to the development of chelating ion exchange resins (90). Chelating ion exchange resins were first introduced by Gregor and his associates (91). The introduction of specific complexing groups onto silica or polymeric matrices makes them capable of selectively coordinating or chelating with one metallic element, in the presence of others, under certain experimental conditions (90-92). A variety of commercial chelating sorbents have been synthesized and applied to various analytical problems (90-93).

Oxine (or 8-Hydroxyquinoline, or 8-Quinolinol) is a well characterized ligand which forms complexes with over 20 metal ions (94,95). Oxine immobilized on silica gel or glass has been used for applications such as : (i) Removing trace concentrations of heavy metal ions from electrolyte solution (96), (ii) Preconcentrating trace metal ions prior to their quantitative measurement (97-105), and (iii) A column packing material for chromatographic separations (106-110).

A number of workers have immobilized oxine on controlled pore glass via covalent bonding. In Table 1.1 are summarized some properties of the resulting sorbents. The particle size, pore diameter, and specific surface area all refer to the underivatized controlled pore glass starting material. The apparent capacity refers to micromoles oxine per gram of derivatized controlled pore glass, and method refers to the chemical technique used to measure the apparent capacity. The measured apparent capacities range from about 3 to 390 μmol/g depending on synthetic procedure, pore size and specific surface area (97,111-114). In addition, as will be discussed later in this thesis, not all of the methods cited yield the correct capacity value (See Chapter Three).

There are several advantages in using controlled pore glass-immobilized oxine : (a) High mechanical strength (111,115); (b) Good swelling stability (required for use in high pressures and continuously changing solvent composition often encountered in liquid chromatographic systems); and (c) Fast metal sorption/desorption kinetics. The last two advantages are probably most important in comparing controlled pore glass-immobilized oxine with many organic polymer-based chelating ion exchangers (97,99,101,103,104, 111,112,116,117). The two main disadvantages are : (a) Extended operation at high pH results in hydrolysis of the glass substrate and cleavage of the bonded phase (99,108, 118); (b) Because of its relatively low capacity, controlled pore glass-immobilized oxine can be used only for samples containing either trace or low level concentrations (97,103, 111,112,118).

One of the most frequently used commercially available materials is manufactured by the Pierce Chemical Company with the name "Controlled Pore Glass-Oxine". It is the material used in the present reported work and will be referred it as CPG-Oxine. The preparation of CPG-Oxine has been described (118). Oxine is azo-linked to an arylamine which is coupled to controlled pore glass via γ-aminopropyltriethoxysilane. The structure

Table 1.1 : Properties of sorbents composed of oxine bound to controlled pore glass.

Manufacturer	Particle Size (µm)	Pore Diameter (nm)	Specific Surface Area (m^2/g)	Apparent Capacity (µmol/g)	Method	Reference
Laboratory-Made	37 - 74	7.4	152.7	173	?	112
"	"	51.5	41.6	58	?	"
"	"	190	10.2	5	?	"
"	"	55	70	53	?	"
"	"	4	125 - 250	95	Cu^{2+} (Titration)	104
"	"	51.5	41.6	58	Cu^{2+} (Extraction)	111
Pierce	74 - 125	?	?	3 - 3.5 (Breakthrough)	Cu^{2+} (Column)	98

Table 1.1 : Properties of sorbents composed of oxine bound to controlled pore glass (Continued).

Manufacturer	Particle Size (µm)	Pore Diameter (nm)	Specific Surface Area (m^2/g)	Apparent Capacity (µmol/g)	Method	Reference
Pierce	125 - 177	50	70	10	?	119
•	•	•	•	12.8	Fe^{2+}	120
•	•	•	•	5.5	Zn^{2+} (Column)	97
Laboratory-Made	•	54.4	57	389	Cu^{2+} (Extraction)	107
Pierce	177 - 380	55	80	57	Fe^{3+} (Extraction)	118
•	177 - 840	•	70	184	Cu^{2+} (Extraction)	107
Laboratory-Made	300 - 600	•	•	22	•	106
•	•	•	•	30	?	•

of CPG-Oxine is shown in Figure 1.1 in which it is seen that it is really not oxine but rather the derivative of 5-phenylazo-8-hydroxyquinoline (5-P-Oxine) which is immobilized on the controlled pore glass.

I.4 RESEARCH OBJECTIVES :

Numerous studies have been done which demonstrate the utility of oxine bound to controlled pore glass in preconcentration and separating metal ions (96-98,100,101,104, 105). Other studies demonstrate the dependence of metal ion sorption on solution properties such as pH (97,100,105,118). However, little has been done to provide an understanding of the underlying physico-chemical principles which explain this dependence on solution properties. Therefore, one objective of this thesis is to provide such a basic understanding in the form of a sorption model for Ca^{2+} on CPG-Oxine which quantitatively explains the dependence of Ca^{2+} sorption on both solution pH and ionic strength. The sorption model is based on the "ionizable surface group" and "site-binding" models (121-124) which involve the electrical double layer theory (125). This subject is discussed in Chapter Three.

A second object of this thesis is to see whether CPG-Oxine can be substituted for a cation exchange resin in the column equilibration / atomic absorption technique to more selectively determine $[Ca^{2+}]$ in aqueous solution in the presence of a variety of charged, kinetically labile metal-ligand complexes of calcium. This subject is discussed in Chapters Two and Four.

In Chapter Five, the feasibility of applying the CPG-Oxine column equilibration / atomic absorption method to the determination of Ca^{2+} in urine is explored.

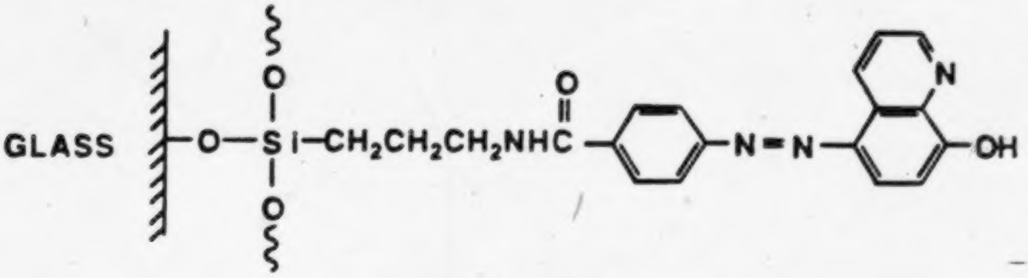
GLASS
O
Si
CH₂CH₂CH₂NHC
O
N=N
N
OH

Figure 1.1 : Structure of the immobilized derivative of 5-phenylazo-8-hydroxyquinoline.

CHAPTER TWO

CHARACTERIZATION OF CPG-OXINE / ATOMIC ABSORPTION SYSTEM FOR FREE CALCIUM DETERMINATION

In this chapter the principles underlying the column equilibration technique are presented. The apparatus used to measure Ca^{2+} by the column equilibration method is described. The conditions to be used for loading, washing and eluting the CPG-Oxine column are determined. Calcium sorption isotherms are measured in order to determine trace loading conditions.

II.1 THEORY OF THE COLUMN EQUILIBRATION TECHNIQUE :

The principle of the column equilibration technique for determining the concentration of free metal ion has been presented for the case in which a sulfonated cation exchange resin is the sorbent (19). By analogy, when CPG-Oxine is the sorbent, the Ca^{2+}-containing sample and standard solutions must be made to have the same inert salt concentration and their pH must be controlled at a value equal to the pH of the sample.

Consider a metal ion (M^{n+}) and a ligand (L^-) forming a series of complexes in a test solution : $M \overset{L}{\rightleftharpoons} ML \overset{L}{\rightleftharpoons} ML_2 \overset{L}{\rightleftharpoons} \cdots\cdots ML_n$ (For simplicity, charges on the complexes are ignored). These metal-containing complex species can be either kinetically "labile" or "inert", and all the labile species and M^{n+} are in rapidly reversible equilibrium with one another. Therefore, the techniques employed in the determination of M^{n+} are only allowed which do not significantly perturb all the existing equilibria in the solution. The theory of the column equilibration technique is illustrated in Figure 2.1, which

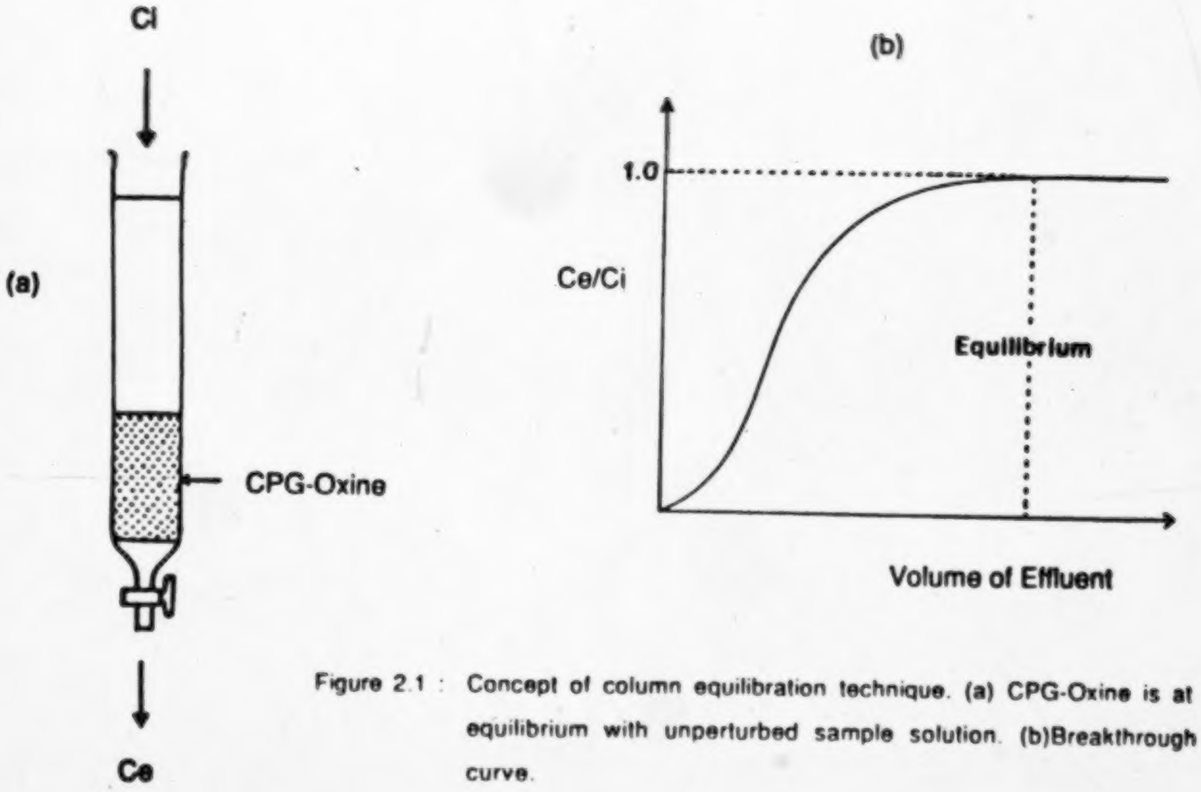
(a)
Ci
CPG-Oxine
Ce
(b)
1.0
Ce/Ci
Equilibrium
Volume of Effluent

Figure 2.1 : Concept of column equilibration technique. (a) CPG-Oxine is at equilibrium with unperturbed sample solution. (b)Breakthrough curve.

involves passing the test solution through a known weight of a sorbent, such as CPG-Oxine (Figure 2.1a), until the total metal concentration in the effluent (Ce) is the same as that of the test solution (Ci). This concept is illustrated by the "breakthrough curve" in Figure 2.1b, which is a plot of Ce/Ci ratio versus volume of column effluent. At the initial loading step, where Ce < Ci, the breakthrough curve shows that the Ce/Ci < 1. As the loading is continued, equilibrium is established between the CPG-Oxine column and metal ion when Ce = Ci, i.e. the plateau of the breakthrough curve at Ce/Ci = 1, which is so-called "complete breakthrough". Thus the CPG-Oxine in the column has been brought to equilibrium with the unperturbed test solution. In other words, the CPG-Oxine is in equilibrium with a solution in which no metal species of any form have been taken up by the sorbent. For the sake of simplicity, consider a monobasic acid (HL) that forms a single complex (CaL^+) with Ca^{2+}. The concept of non-perturbation can also be understood by the equilibria presented in Figure 2.2. A Ca^{2+}-containing solution is pumped through a CPG-Oxine column until complete breakthrough of Ca^{2+} has occurred and equilibrium has been achieved between $\overline{OX^-}$ and the unperturbed sample solution. After a water wash, the calcium sorbed on the column is eluted and measured by atomic absorption spectrophotometry (AAS).

Figure 2.3 presents the loading, washing, and eluting profile for calcium. The loading profile, recorded directly on chart by pumping a Ca^{2+} solution through a CPG-Oxine column directly into the AA flame, showed that equilibrium is established when the Ca^{2+} loading signal has reached a plateau value equal to that expected from its total concentration, i.e. the Ca^{2+} has completely broken through and the composition of the column effluent is identical with the influent. After switching to water for column washing, it was found that about 0.8 mL water was required in order to establish a flat AA base line signal. Switching to eluent (diluted acid) then produced the AA peak for calcium eluted from the CPG-Oxine column. It is interesting to note that the breakthrough

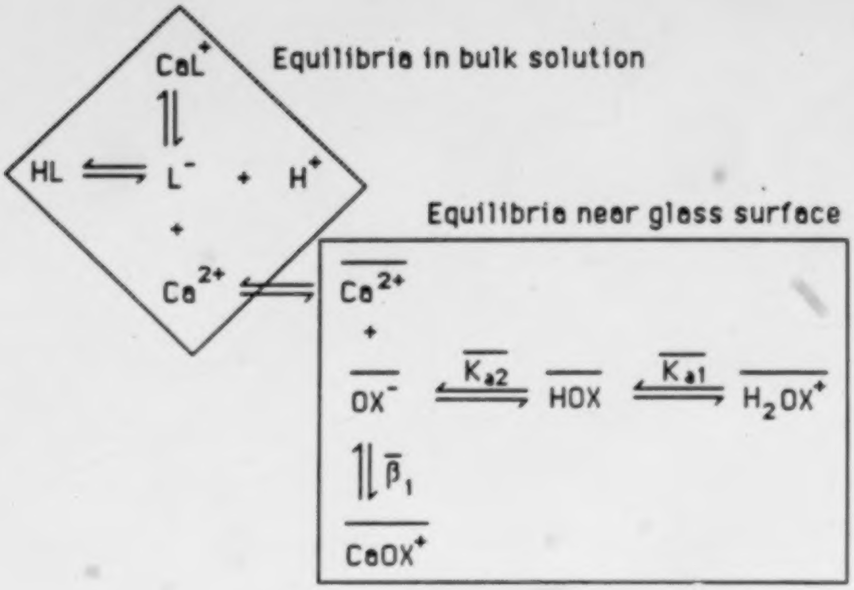
Equilibria in bulk solution
CaL⁺
HL
L⁻
H⁺
Ca²⁺
Equilibria near glass surface
Ca²⁺
OX⁻
Ka2
HOX
Ka1
H₂OX⁺
β₁
CaOX⁺

Where the bar indicates a species in the vicinity of the glass surface.

$\overline{K_{a1}}$ is the acid dissociation constant for protonated bound oxine ($\overline{H_2OX^+}$).

$\overline{K_{a2}}$ is the acid dissociation constant for neutral bound oxine ($\overline{HOX}$).

$\overline{\beta}_1$ is the stability constant for $\overline{CaOX^+}$ complex, assuming 1 : 1 complexation.

Figure 2.2 : Diagram of Ca^{2+} equilibria in sample solution and CPG-Oxine column.

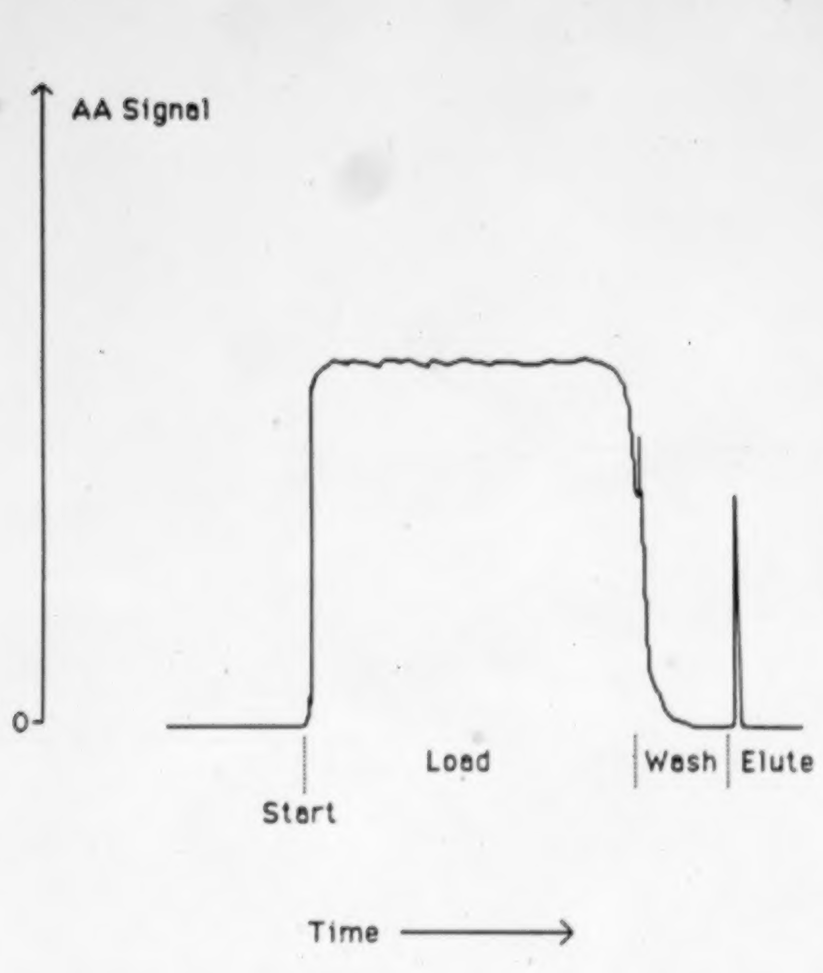

Figure 2.3 : Loading, washing and eluting profiles for a 40 mg CPG-Oxine column loading with Ca^{2+}.

for Ca^{2+} on CPG-Oxine appeared almost instantly, which is contradictory to the slow reaching equilibrium in the theoretical plot of Figure 2.1b. However, this does not imply the CPG-Oxine column has reached equilibrium instantly because a very small change from Ci to Ce during the loading step may not contribute to a significant change in the absorbance of the AA signal. The column equilibration rate may depend on a number of factors, e.g. pore size of CPG-Oxine, column size and as well the kinetics involved in the column such as particle and film diffusion (128). These subjects are discussed later in Section II.3.2.

In the column equilibration technique, it is desirable to maintain trace loading conditions such that, at equilibrium, only a small fraction (< 1%) of the bound oxine groups are coordinated to Ca^{2+}, i.e.

$$[\overline{CaOX^+}] \ll [\overline{HOX}] + [\overline{OX^-}] + [\overline{CaOX^+}] \qquad (2.1)$$

The distribution coefficient for Ca^{2+} is defined as

$$\lambda_o = \frac{\text{Moles of Sorbed Calcium per gram CPG-Oxine}}{[Ca^{2+}]} \qquad (2.2)$$

Under conditions of constant pH, constant ionic strength (c) and trace loading, the value of λ_o is a constant which can be measured by the column equilibration experiment using a standard of known $[Ca^{2+}]$ with the same pH and c as the sample solution (Section II.2.6). As $[Ca^{2+}]$ in the sample or standard solution is made larger and larger, $[\overline{CaOX^+}]$ increases proportionally and λ_o remains constant under the trace loading conditions. Eventually, trace loading will be exceeded. The effect of this is the same as would be the effect of decreasing the bound oxine capacity ($\overline{v_{Oxine}}$). It causes λ_o to decrease with increasing $[Ca^{2+}]$.

II.2 EXPERIMENTAL :

II.2.1 CHEMICALS AND REAGENTS :

CPG-Oxine (Pierce Chemical Co.), batch 071982-81, with particle diameter 125 - 177 μm and pore diameter 50 nm, was used throughout the studies in this chapter.

All solutions were prepared with doubly distilled water that was deionized by passing through a mixed bed ion exchange resin column (Amberlite MB-1, analytical reagent, Mallinckrodt Inc., Paris, Kentucky). The doubly distilled-deionized water was also used for column washing in all column equilibration experiments.

Calcium stock solutions were prepared by dissolving analytical grade $CaCO_3$ (British Drug Houses) in perchloric acid.

4-(2-Hydroxyethyl)-1-piperazineethanesulfonic acid, HEPES, 99% (Aldrich Chemical Co.), was used as a buffer.

Sodium perchlorate (hydrated), $NaClO_4 \cdot H_2O$ (G. Frederick Smith Chemical Co.) and potassium chloride, KCl (Fisher Scientific Co.), both reagent grade, were used as the inert electrolytes.

Nitric acid, HNO_3 (British Drug Houses), analytical reagent grade, was used to prepare the eluent.

Sodium hydroxide, NaOH (British Drug Houses), and perchloric acid, $HClO_4$ (British Drug Houses), both analytical reagent grade, were used to adjust pH.

Magnesium stock solution was prepared by dissolving magnesium ribbon (Fisher Scientific Co.) in $HClO_4$.

II.2.2 COLUMN PREPARATION :

The CPG-Oxine particles are orange in color. The commercial material originally contained some opaque white particles which the manufacturer believed were underivatized glass beads (119). Before packing the CPG-Oxine column, most of the opaque particles were individually removed after spreading the material in a thin layer. Then the fines were removed by repeated suspension and decantation with water. The cleaned CPG-Oxine was air-dried and ready to be used.

Three CPG-Oxine columns, approximately 1 cm, 2 cm and 4.5 cm, were used in this chapter. The preparation of the 1 cm column is described in the following procedure :

An 11 mg amount of CPG-Oxine was weighed and packed into a 5 cm length of 1.5 mm i.d. Teflon tubing flared at both ends (Figure 2.4). This length of tubing was required to accommodate the Cheminert end fittings (LDC). The 11 mg CPG-Oxine was slurry packed into the tube as follows : Approximately 2 mm long glass frits were made by drilling cores from a sintered glass plate (nominal pore size 50 µm). One frit was pressed about 1.4 cm into the tube and butted up against a 0.8 mm i.d. Teflon retaining tube. With this inner frit in place a slurry of CPG-Oxine was slowly and carefully filled into the tube with a disposable pasteur capillary pipette. When all the CPG-Oxine was packed into the tube (about 1 cm long packing bed), a second 2 mm long glass frit was pressed into place. A tiny space was left between the second glass frit and CPG-Oxine to avoid excessively compacting the packed bed.

II.2.3 APPARATUS :

The operating system is shown in Figure 2.5. It is very similar to that previously used with a cation exchange resin system (20), except the peristaltic pump has been placed in front of valve V1. The variable speed peristaltic pump (Minipuls 2, Gilson, Villiers-le-Bel, France) was fitted with Clear Standard (PVC) tubes (Technicon Corp.). One tube pumped sample (or standard) Ca^{2+}-containing solution and the other pumped either water or eluent, depending on the position of the 4-way Teflon slider valve V1 (CAV4031, LDC). Pump rates were measured with a home-made flow meter (10-mL

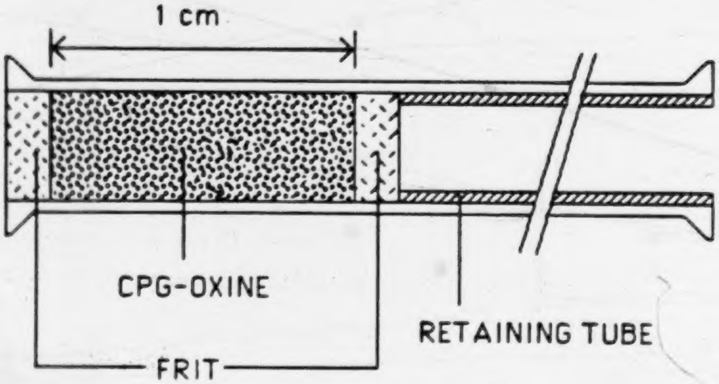
1 cm
CPG-OXINE
RETAINING TUBE
FRIT

Figure 2.4 : Diagram of a 1 cm CPG-Oxine (125-177 μm particle size) column.

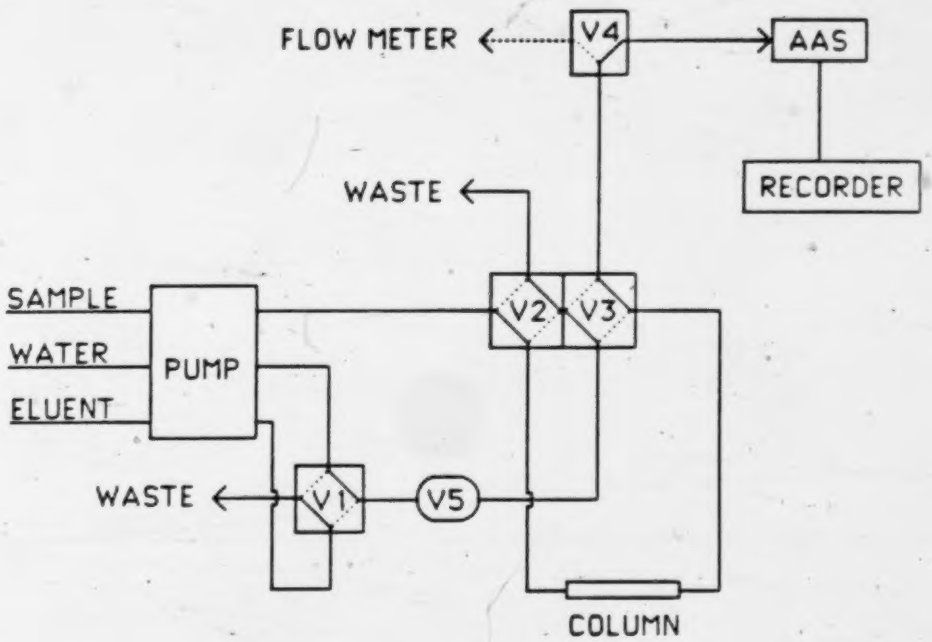
FLOW METER
V4
AAS
RECORDER
WASTE
SAMPLE
WATER
ELUENT
PUMP
V2
V3
WASTE
V1
V5
COLUMN

Figure 2.5 : Diagram of operating system.

buret) and stopwatch by diverting the flow through another 4-way Teflon slider valve V4. By means of the two coupled 4-way Teflon slider valves V2 and V3, the flow from either pump tube could be directed through the CPG-Oxine column while the other was diverted to waste. A 10 µL Teflon slider injection valve V5 (CSV-2, LDC) was connected as necessary to inject standard Ca^{2+} solutions to obtain calibration plots of calcium peak height versus moles of Ca^{2+} injected (Section II.2.6). A Haake circulating thermostat Model R20 was used to provide a constant temperature at 25 ± 1°C for the water jacket surrounding the CPG-Oxine column.

In the present studies, calcium and sodium concentrations were monitored by a Model 4000 atomic absorption spectrophotometer (AAS) (Perkin-Elmer Corp.). The peristaltic pump rate and the AAS conditions are listed in Table 2.1.

Measurements of pH were made with separate glass and calomel electrodes using an Accumet Model 525 digital pH meter (Fisher Scientific Co.) with a precision estimated at ± 0.01 pH unit.

II.2.4 PREPARATION OF TEST SOLUTIONS :

All Ca^{2+}-containing standard solutions were prepared at the desired pH using 0.010 M HEPES buffer. HEPES does not complex with Ca^{2+} (126). The total ionic strengths were adjusted to the specified value by adding the necessary amount of $NaClO_4$. Therefore ionic strength and sodium ion concentration were identical to one another. Blank solutions were prepared similarly along with each set of standard solutions.

The preparation of 25.0 µM Ca^{2+} in 0.10 M $NaClO_4$ at pH 7.00 was described as follows : 49.00 mL of $NaClO_4$ stock solution (1.0 M) and 5 mL of HEPES buffer solution (1.0 M) were added into a cleaned 600 mL beaker. About 300 mL of water was added and the pH was adjusted to 7.00 with dilute NaOH. Then 5 mL of Ca^{2+} diluted standard solution (2.50 mM) was added and the solution was mixed by using a glass

Table 2.1 : Instrumental conditions for monitoring calcium and sodium with the Model 4000 AAS.

Wavelength	422.7 nm (Ca); 589.0 nm (Na)*
Spectral Slit Width	0.7 nm (Ca); 0.2 nm (Na)*
Lamp Current	12 mA
Flame	Oxidizing (lean, blue)
Acetylene Pressure	13.5 psig
Air Pressure	23 psig
Aspiration Rate	3.4 mL/min
Pumping Flow Rate	3.4 mL/min
Recorder Type	Hewlett-Packard, Model 7101BM
Voltage Range	Varied
Chart Speed	1.2 cm/min

* : Sodium was determined by atomic emission (AE) spectrophotometry

rod. The mixture was then quantitatively transferred into a cleaned 500 mL volumetric flask, diluted to almost 500 mL with water and shaken well. The pH of the solution was rechecked and readjusted if necessary using small volumes of very dilute NaOH or $HClO_4$. The volume of the final solution was adjusted to the mark, shaken well and was then ready to use.

II.2.5 COLUMN EQUILIBRATION PROCEDURE :

The Ca^{2+}-containing solution was first pumped through the column via V2 and V3 (solid lines in Figure 2.5). The time (or sample volume) required for this loading step was determined from the equilibration study in Section II.3.2. The effluent load solution was diverted to waste through the flow meter via V4 (dashed lines in Figure 2.5) during equilibration.

After equilibrium was achieved V2 and V3 were switched (dashed lines in Figure 2.5) and the column was backwashed with water for about 15 s to remove most of the interstitial calcium solution. Next, V4 was switched to divert the washing to the atomic absorption spectrophotometer (AAS) and the water washing was continued in order to remove the remainder of interstitial solution. The total volume of water used for washing, about 2.0 ml, was determined from the column washing study in Section II.3.1. In the present system, the wash-water was sparged with N_2 or He before use to remove dissolved CO_2.

After the water washing, the absorbance of the spectrophotometer should be zero (i.e. a base line AA signal is established). Then V1 was switched (dashed line in Figure 2.5) to the eluent (1% HNO_3) to start the elution step. Dilute HNO_3 is a suitable eluent for calcium; its concentration is not critical because chelation between Ca^{2+} and $\overline{OX^-}$ is rather weak. After the elution was completed and the base line was reestablised, V1 was switched back to the wash position. Valves V2, V3 and V4 were then switched back to their initial position for the next test solution.

The width of the asymmetric eluted calcium peak, measured from the point of departure of the AA signal from the base line to the point that it rejoins the base line, was about 8 s. Quantification of eluted calcium was based on AA peak height because integrated peak areas were found to be less precise measures of peak size for these narrow and asymmetric peaks.

II.2.6 MEASUREMENT OF DISTRIBUTION COEFFICIENT :

In order to determine the distribution coefficient (λ_o), defined as Eq. 2.2, it is necessary to measure the number of moles of sorbed Ca^{2+} on a particular CPG-Oxine column under a constant pH and a constant ionic strength. This can be done as follows :

(a) By using the column equilibration method to determine the calcium eluted peak height obtained from a standard solution containing trace loading of $[Ca^{2+}]$ at the particular pH and c.

(b) By using the calibration plot of calcium peak height versus number of moles of Ca^{2+}, which was obtained under the same instrumental and operating conditions, to determine the number of moles of Ca^{2+} sorbed on the column corresponding to that eluted peak height.

(c) Subsequently, the number of moles of sorbed Ca^{2+} per gram of CPG-Oxine can be calculated for the particular column used for the experiment. With this calculated number and the known value of $[Ca^{2+}]$, λ_o at the particular pH and c can be calculated by Eq. 2.2.

The calibration plot of calcium peak height versus number of moles of Ca^{2+} can be obtained by the flow through method (127). The experimental procedure was described as follows : A series of Ca^{2+} standard solutions was injected separately via the 10 µL injection valve (Figure 2.5) into the eluent stream which delivered the calcium plug through the column and then aspirated it into the AA flame. The eluted calcium signal was detected as a peak. The width of the eluted peak must be identical to the eluted calcium peak obtained by the column equilibration method with the same AAS and instrumental conditions. Figure 2.6 is the calibration plot obtained by injecting 10 μL of each of the standard solutions containing 0.125, 0.250, 0.500, 1.00 and 1.25 mM Ca^{2+}.

II.3 RESULTS AND DISCUSSION :

II.3.1 COLUMN WASHING :

Basically, the experiment was done by loading a 20 x 1.5 mm i.d. column containing 20 mg CPG-Oxine (125 - 177 μm particle diameter) with Ca^{2+} solution for an arbitrary period of time, 4 min, then washing the column with water for various periods of times. After that, the calcium sorbed on the column was eluted and the peak height was measured. The purpose of this study is to find the washing conditions that will remove Ca^{2+}-containing solution from the bed of CPG-Oxine and associated frits and tubing without removing Ca^{2+} that has been complexed to $\overline{OX^-}$. The total hold-up volume of Ca^{2+}-containing solution involved is about 70 μL.

It is understood that the chelating between Ca^{2+} and $\overline{OX^-}$ is weak. Therefore it was thought that washing the column with water containing dissolved CO_2, and therefore of a lower pH, might be more likely to elute Ca^{2+} that is complexed to $\overline{OX^-}$ than washing with CO_2-free water. Therefore the column washing experiments were performed using both ordinary untreated doubly distilled-deionized water and the same water which was freed of CO_2 by bubbling with N_2 or He. A solution containing 50.0 μM Ca^{2+} in 0.10 M $NaClO_4$ at pH 7.00 was prepared for the experiments.

Table 2.2 presented the eluted calcium peak height as a function of volume of wash water for both CO_2-free and untreated (CO_2-dissolved) water. Two conclusions can be drawn. First, the interstitial Ca^{2+}-containing solution is washed out of the column by less than 1 mL of water. Second, neither the untreated nor the CO_2-free water seem to remove significant amounts of sorbed Ca^{2+} up to a volume of about 3 mL. This is seen from the

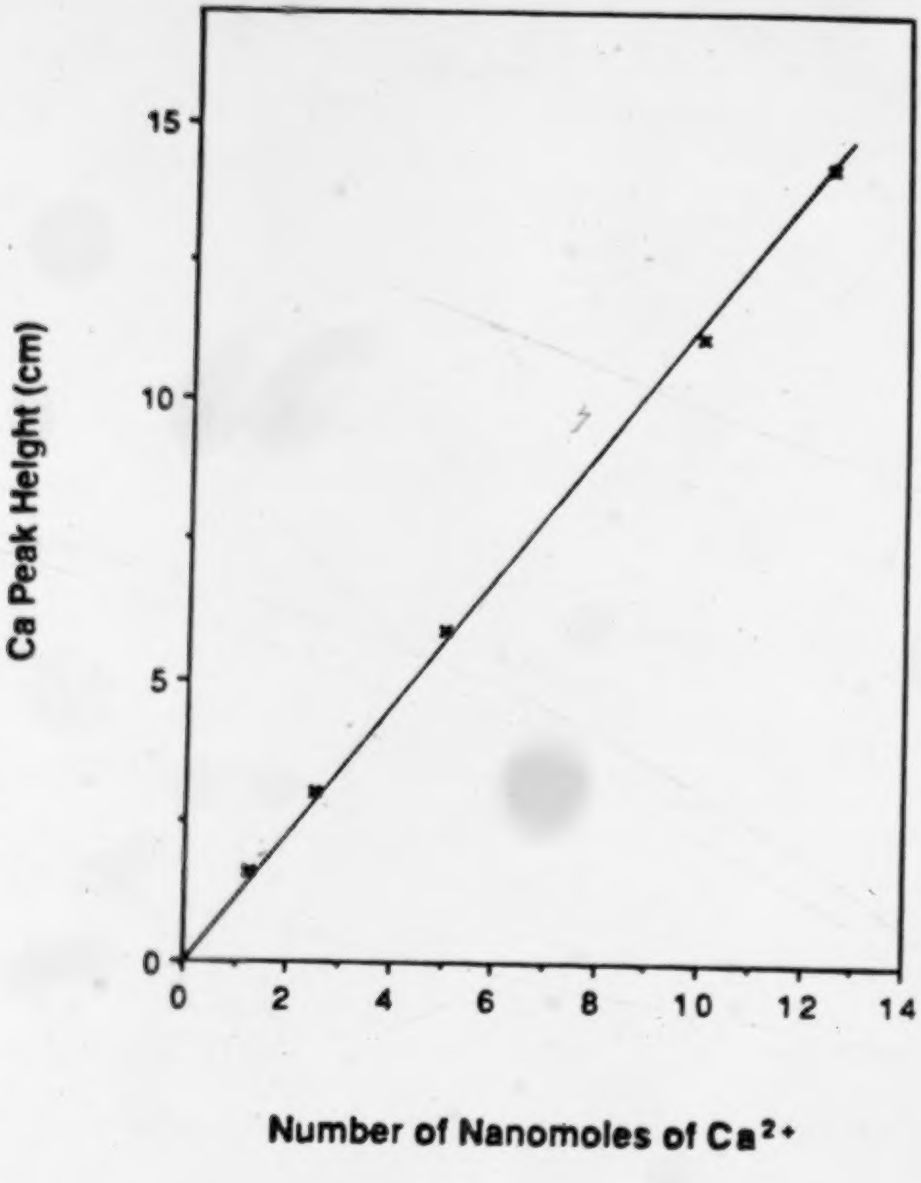

Figure 2.6 : Calibration plot of calcium peak height versus moles of Ca^{2+}.

Table 2.2 : Effects of CO_2-free and untreated water washing on the eluted calcium peak height for a 20 mg CPG-Oxine column.

	Eluted Calcium Peak Height (cm)	
Wash Volume (mL)	CO_2- Free Water	Untreated Water
0.85	3.8 ± 0.1	3.8 ± 0.1
1.1	3.8 ± 0.0	3.8 ± 0.0
1.4	3.8 ± 0.0	3.8 ± 0.0
2.0	3.7 ± 0.0	3.8 ± 0.1
3.1	3.7 ± 0.1	3.8 ± 0.0

Note : The ± value indicates the standard deviation.

fact that the eluted calcium peak height remains constant up to at least this volume. Although this experiment demonstrates that it is not necessary to use CO_2-free water in the washing step, for most experiments in this thesis the wash water was freed of CO_2 anyway. In routine use of the column equilibration method, the column effluent was diverted to waste during the loading step in order to prevent fouling of the AA nebulizer or burner by solutions containing high salt concentrations. However, it is interesting to carry out the following experiments to find out what happens to the eluted calcium peak height if the effluent is not diverted to waste. During the 4 min loading the effluent was directed to the AA nebulizer; the column was next washed for 35 s with CO_2-free water. Upon elution with 1% HNO_3 it was observed that the eluted calcium peak height was 5.1 cm in contrast to a peak height of 3.7 cm obtained for the same load solution when the load effluent is diverted to waste in the usual way. This suggested that calcium accumulates somewhere in the system when the effluent is diverted to the nebulizer. To verify this, the experiment was repeated but after the water washing step the pump was shut off, the column was removed from the system and the column influent and effluent tubes were connected together. When 1% HNO_3 was pumped through the system with the column removed, a 1 cm eluted calcium peak was recorded. The pump was shut off again and the column was replaced. Elution of the calcium sorbed on the column gave a peak height of 3.8 cm, which is close to the peak height obtained in the experiment in which the effluent load solution is diverted to waste. These results suggest that when the effluent load solution was aspirated directly into the flame, Ca^{2+} was deposited somewhere, probably along with the residual of $NaClO_4$ in the AA nebulizer or burner. This residual calcium was dissolved later as the column was eluted with HNO_3. Consequently, the eluted calcium peak height was increased. Therefore, all column equilibration experiments must be carried out in such a way that the effluent is diverted to waste during the loading step, in order to avoid either fouling or deposition of metal residues in the AA nebulizer and burner.

II.3.2 COLUMN EQUILIBRATION (LOADING) :

The column of principal interest in this work contained 40 mg of 125 - 177 μm particle diameter CPG-Oxine (45 x 1.5 mm i.d.). In this study, rather than measuring the breakthrough curve as shown in Figures 2.1b and 2.3, the loading curve was measured by loading the column for various times while diverting the effluent to waste, then washing with 2.0 mL of CO_2-free water and measuring the peak height obtained when the column is eluted with 1% HNO_3. The flow rate used for the loading step in most of the studies was 3.4 mL/min. The loading time (or volume) required to equilibrate the column with Ca^{2+} was determined by pumping the Ca^{2+}-containing load solutions prepared at various pH and ionic strength values. These column equilibration experiments were time-consuming, therefore each run was performed without replication. However, a 4 min loading was carried out in between each run in order to check the instrumental precision. Standard deviation for the eluted peak height obtained after 4 min loading was about ± 0.1 cm.

Figure 2.7 shows the loading curves for solutions containing 25.0 μM Ca^{2+} in 0.10 M $NaClO_4$ at pH 6.51, 7.00 and 8.01. It was observed that the calcium loading reaches a maximum in about 4 min and then begins to decrease and slowly approach a plateau value at about 60 min. This latter plateau is the true equilibrium value. Loading curves were also studied as a function of ionic strength at a fixed pH of 7.00. The results are presented in Figure 2.8 which show that the curves have the same general shapes as observed in Figure 2.7. However, the time required for equilibrating the solutions containing ionic strength less than 0.1 M was doubled (i.e. about 2 hours). Obviously, both Figures 2.7 and 2.8 suggest that the equilibration rate for the 40 mg CPG-Oxine column is very slow. In order to understand the cause of the slow equilibrium and to explain the shape of these loading curves, the following experiments were carried out :

The first experiment involved studies of loading curves for a 40 mg column containing smaller diameter particles of CPG-Oxine. The cleaned CPG-Oxine (125 - 177

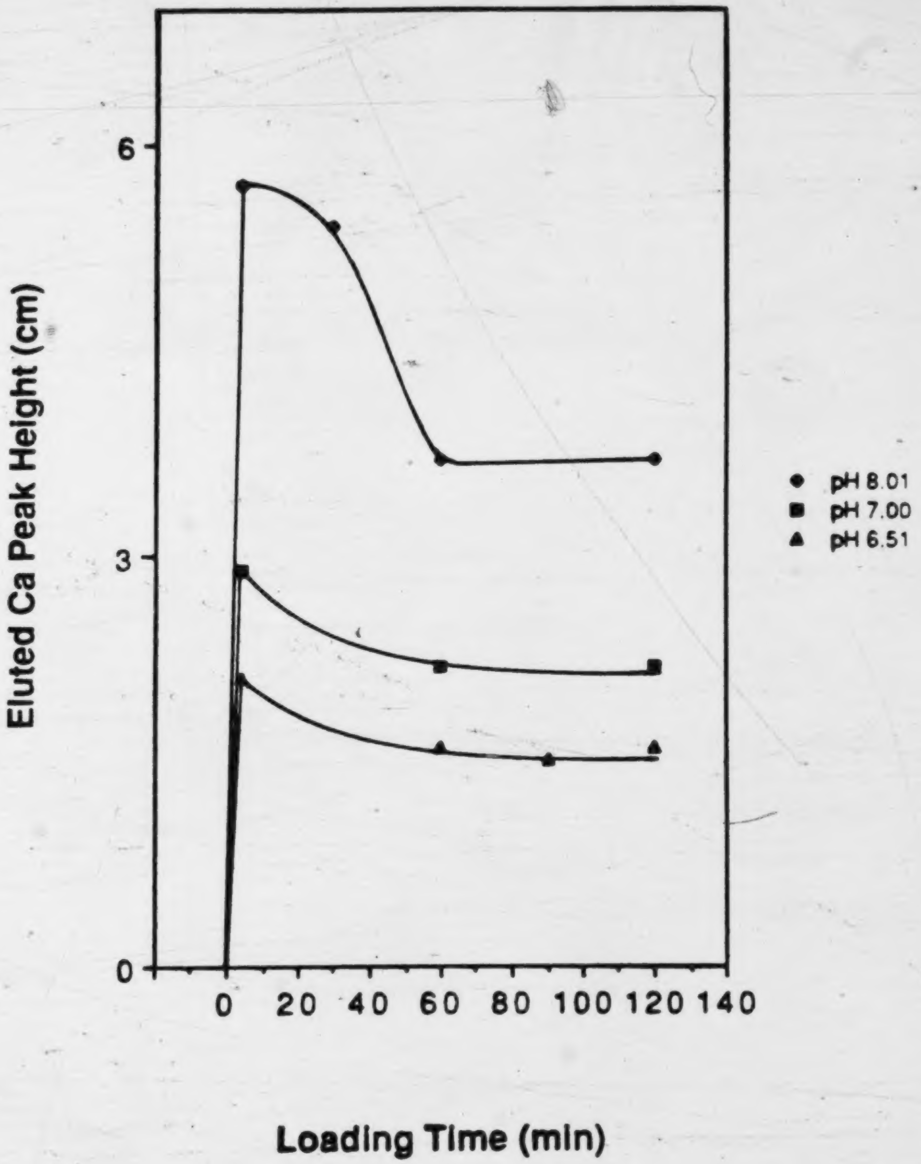

Figure 2.7 : Loading curves for Ca^{2+} in 0.10 M $NaClO_4$ at (a) pH 8.01; (b) pH 7.00 and (c) pH 6.51 on the 40 mg CPG-Oxine (125 - 177 µm particle size) column.

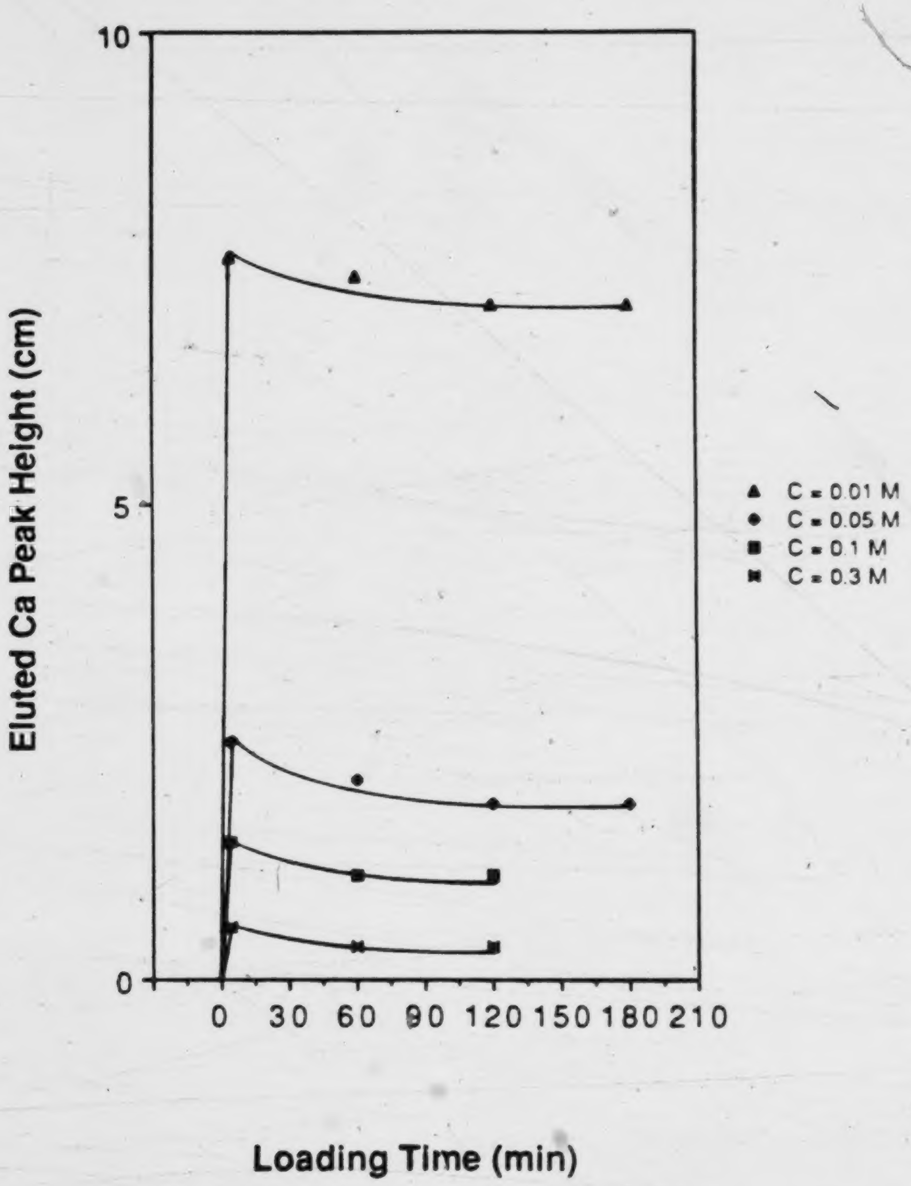

Figure 2.8 : Loading curves for Ca^{2+} in (a) 0.010 M; (b) 0.050 M; (c) 0.10 M and (d) 0.30 M $NaClO_4$ at pH 7.00 on the 40 mg CPG-Oxine (125 - 177 µm particle size) column.

μm particle diameter) was ground and sieved to a particle size range of 50 - 75 μm. When these particles were packed into the ordinary 1.5 mm i.d. column, the resistance to flow increased. Therefore, a column with a larger diameter was constructed. 40 mg of the CPG-Oxine were packed into an 11 x 3 mm i.d. Teflon tubing flared at both ends (Figure 2.9) which was attached and sealed to two G-nuts (LDC) by the split rings plus epoxy glue. Each end of the column was covered with a 5 mm diameter Teflon filter membrane (30 - 60 μm pores) which was backed with a 5 mm Teflon end disc with a 2 mm hole through its center. Then both ends were connected via ordinary Cheminert end fittings (LDC) to 0.3 mm i.d. Teflon tubes. Using the same peristaltic pump setting, the flow rate through this wider column packed with smaller diameter particles was 2 mL/min instead of 3.4 mL/min. Figure 2.10 shows that the use of smaller particles of CPG-oxine gave no significant improvement in the equilibration rate as compared to the column with larger particles. Therefore, this suggests that the equilibration rate is independent of the particle size of CPG-Oxine.

The second experiment studied the effect of column size on the equilibration rate of CPG-Oxine. A 10 x 1.5 mm i.d. column containing 11 mg CPG-Oxine (125 - 177 μm particle diameter) was used in this study. The flow rate for the loading step was 2 mL/min. Figures 2.11 and 2.12 show the loading curves for 2.50 μM Ca^{2+} in 0.010 M $NaClO_4$ at pH 8.01 and 25.0 μM Ca^{2+} in 0.10 M $NaClO_4$ at pH 7.00, respectively. This column completely reached equilibrium in only about 4 min, and it was very much faster than the columns containing 40 mg CPG-Oxine. The large increase in equilibration time for a relatively small (e.g. 4 times) increase in amount of CPG-Oxine in the column is surprising. It was thought that it might somehow be associated with slow diffusion of the species Ca^{2+}, HEPES, and Na^+ into the pores of the CPG-Oxine particles. When HEPES first encounters the glass surface lining the pores, it reacts with acid-base groups to ionize them. This increase in surface charge density requires a readjustment of HEPES and Na^+ in the pores, with reacted HEPES diffusing out and fresh HEPES and Na^+

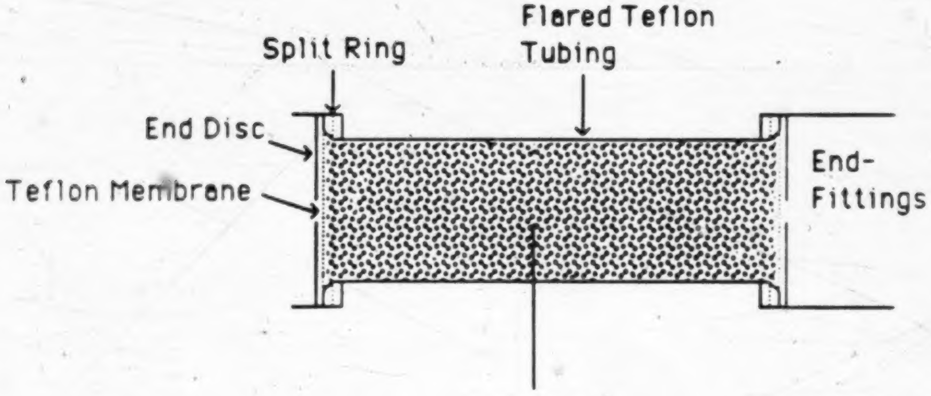
Flared Teflon Tubing
Split Ring
End Disc
Teflon Membrane
End-Fittings
CPG-Oxine

Figure 2.9 : Diagram of a 11 x 3 mm i.d. CPG-Oxine column with particle size of 50 - 75 μm.

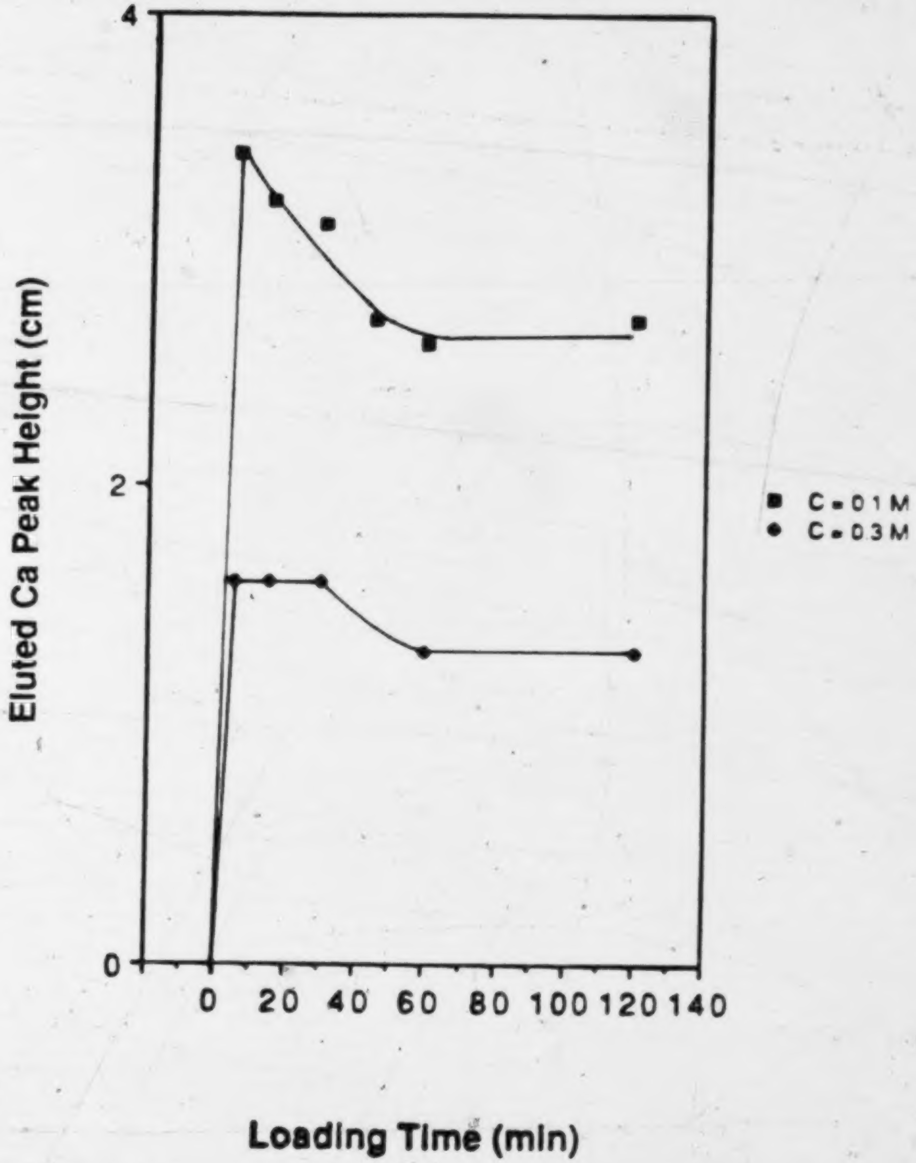

Figure 2.10 : Loading curves for Ca^{2+} in (a) 0.10 M and (b) 0.30 M $NaClO_4$ at pH 7.00 on the 40 mg CPG-Oxine (50 - 75 μm particle size) column.

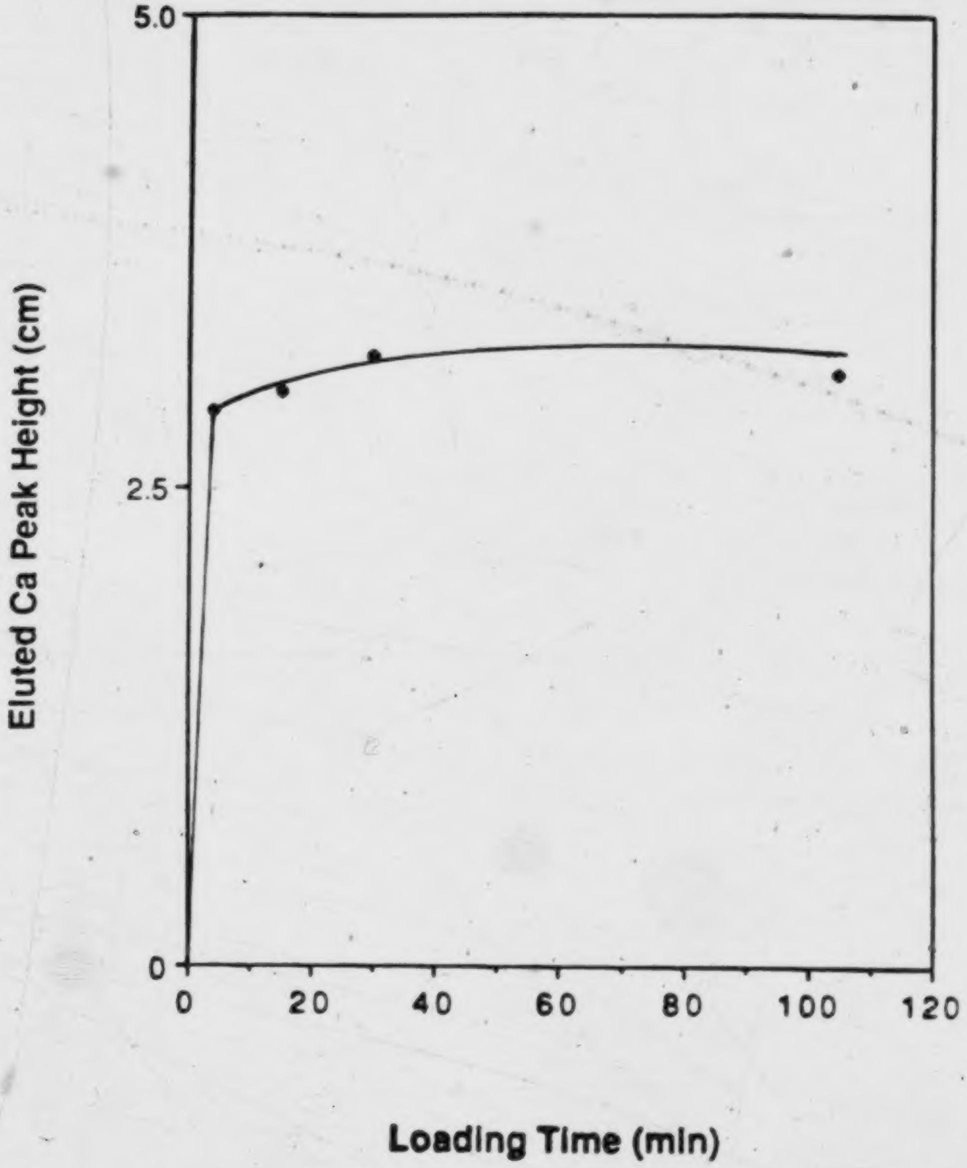

Figure 2.11 : Loading curve for Ca^{2+} in 0.010 M $NaClO_4$ at pH 8.01 on the 11 mg CPG-Oxine (125 - 177 μm particle size) column.

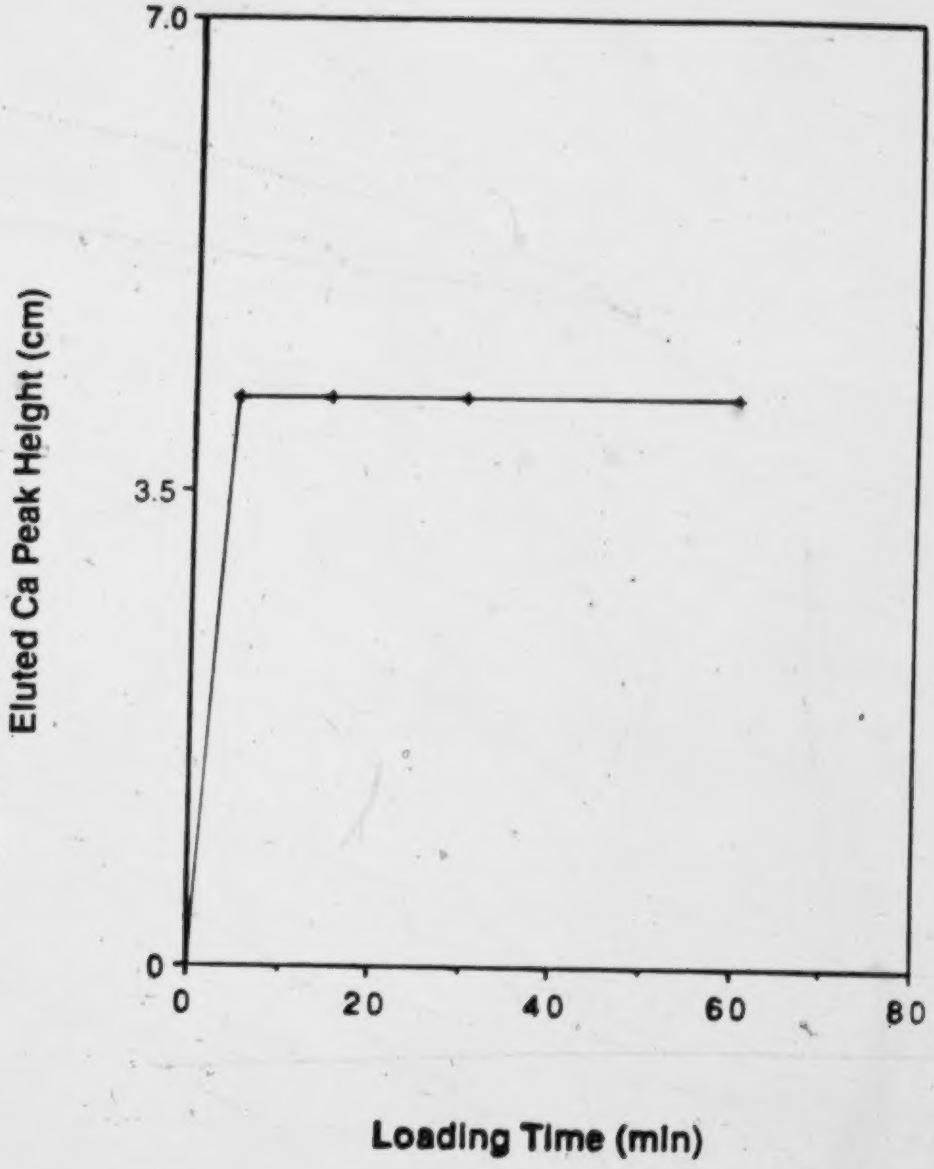

Figure 2.12 : Loading curve for Ca^{2+} in 0.10 M $NaClO_4$ at pH 7.00 on the 11 mg CPG-Oxine (125 - 177 µm particle size) column.

diffusing in. In order to understand this phenomenon, the third and fourth experiments were performed as described below.

The third experiment carried out by loading the 40 mg column (125 - 177 μm particle diameter) with 0.10 M $NaClO_4$ containing 0.010 M HEPES at pH 7.00 for various periods of times. Then the column was washed for 18 min and eluted with 1% HNO_3 into a 10 mL volumetric flask. The sodium content was analyzed by atomic emission mode on the Model 4000 AAS. A calibration curve was prepared from NaCl in 1% HNO_3. The results presented in Table 2.3 show that the amount of sorbed sodium increases with increasing loading time. This suggests that the diffusion of Na^+ from the bulk solution into the diffuse layer of CPG-Oxine is probably very slow.

The fourth experiment was done by first loading the same column with 0.010 M HEPES at pH 7.00 for various periods of times, and then loading with 2.5 μM Ca^{2+} in 0.10 M $NaClO_4$ at pH 7.00 for 4 min. The column was next washed for 35 s and eluted with 1% HNO_3. The results presented in Table 2.4 shows that the eluted calcium peak height decreased with increasing loading time of the buffer, and then remained constant after 60 min loading. It agreed with the loading curve in Figure 2.7 and therefore suggests that the diffusion of HEPES buffer from the bulk solution into the diffuse layer of CPG-Oxine was also very slow.

Experiments three and four suggest that the slow rate of equilibration in the 40 mg column may be caused by the time required for HEPES or Na^+ to diffuse through the particles. While this phenomenon would have to be investigated more fully to be understood, the results of experiments three and four suggest that ionization of the surface groups by HEPES may occur more rapidly than Na^+ achieves its equilibrium concentration in the pores. Thus before the system is fully equilibrated, the surface charge has reached its maximum value but the ionic strength near the surface is lower than its equilibrium value. This would lead to a higher surface potential ψ_0 (See

Table 2.3 : Moles of Na^+ eluted from the 40 mg CPG-Oxine (125 - 177 μm particle size) column loaded with 0.10 M $NaClO_4$ containing 0.010 M HEPES buffer at pH 7.00 for various periods and washed for 18 min.

$NaClO_4$ Loading Time	Moles of Na^+ Eluted
4 min	1.20×10^{-8}
30 min	1.96×10^{-8}
60 min	2.72×10^{-8}

Table 2.4 : Effect of pre-buffer loading time on the eluted calcium peak height obtained after 4 min loading of Ca^{2+} solution containing 0.10 M $NaClO_4$ at pH 7.00 on the 40 mg CPG-Oxine (125 - 177 μm particle size) column.

Pre-Buffer Loading Time	Eluted Calcium Peak Height
4 min	2.9 ± 0.1 cm
30 min	2.7 cm
60 min	2.5 cm
90 min	2.4 cm

Note : The ± value indicates the standard deviation.

Chapter Three) and thus to the sorption of more Ca^{2+} than would eventually be sorbed at equilibrium.

The exact reason for the 40 mg column approaching equilibrium so much more slowly than the 11 mg column is not known, but may have to do with the extent to which the sample solution is shifted from its influent composition (i.e. pH, HEPES, Na^+ and Ca^{2+}) in the early stages of the loading operation. Further work is necessary to fully understanding the kinetics of sample loading.

II.3.3 COLUMN ELUTION :

Diluted HNO_3 was used as eluent. It works by protonating the $\overline{OX^-}$ groups to form $\overline{H_2OX^+}$, thereby eliminating the ligand-active oxine species $\overline{OX^-}$. In previous work it was found that 1% HNO_3 readily eluted Cu^{2+} from a strong cation exchange resin column (22). Therefore, 1% HNO_3 was used throughout the experiments in this thesis. In fact, the eluent concentration used for eluting the sorbed Ca^{2+} from the CPG-Oxine column is not critical because the chelating of Ca^{2+} by CPG-Oxine is relatively weak and $\overline{OX^-}$ is a relatively weak base which is readily protonated.

II.3.4 CALCIUM SORPTION BEHAVIOR :

In this study, the columns were loaded completely to equilibrium. The flow rate used for the loading step was 2 mL/min.

II.3.4.1 SORPTION ISOTHERM:

A test of whether trace loading conditions have been achieved in the column equilibration is to see whether the distribution coefficient (λ_0) is independent of $[Ca^{2+}]$ with load solution. In other words, trace loading conditions prevail in the linear region of the calcium sorption isotherm. In the present study, the calcium sorption isotherm is obtained by measuring the moles of calcium sorbed on the CPG-Oxine column at equilibrium (in terms of eluted peak height) at various concentrations of Ca^{2+} in the standard solutions with which the column has been equilibrated.

Figures A.1 - A.11 in Appendix I present sorption isotherms for calcium on columns containing either 11 mg or 40 mg of CPG-Oxine (125 - 177 μm particle diameter) at various combinations of solution pH and ionic strength. The purpose of these isotherms is merely to identify the linear regions so that future studies can be performed within these linear regions (i.e. under trace loading conditions). Therefore, the vertical axis in these figures has not been converted to sorbed calcium concentration (mmoles per gram of CPG-Oxine), which would have required running a calibration curve, like Figure 2.6, with each isotherm measurement. The first point of interest in Figures A.1 - A.10 is that the calcium sorption isotherm is, indeed, linear at lower $[Ca^{2+}]$ values. Additional conclusions from the isotherm are best understood by reference to Table 2.5 in which are presented the experimental conditions used in obtaining the isotherms and the approximate upper $[Ca^{2+}]$ limit to which the isotherm is linear (i.e. trace loading $[Ca^{2+}]$ limit). Comparing entry #A.1 with #A.5 and comparing #A.4 with #A.6 show that at both high pH (8.01) and low pH (5.00) an increase in ionic strength from 0.010 M to 0.10 M increases the upper limit. Comparing #A.2 with #A.7 at pH 7.00 shows that, in contrast, increasing ionic strength from 0.10 M to 0.75 M has little effect on the upper limit. Comparing #A.1 with #A.8 at pH 8.01 and ionic strength 0.10 M shows that increasing the size of the column form 11 to 40 mg has little effect on the upper limit. Comparing #A.4 with #A.10 at pH 5.00 and ionic strength 0.10 M shows that using KCi in place of $NaClO_4$ to adjust ionic strength has little effect on the upper limit.

The final conclusion to be drawn from the data in Table 2.5 can be seen by comparing #A.2 on a 11 mg column with #A.9 on a 40 mg column (a 4 min loading time was used in both cases). It will be recalled that in 4 min the 11 mg column has come

Table 2.5 : The experimental conditions used in obtaining the isotherms and the approximate upper limit of [Ca^{2+}] for trace loading CPG-Oxine

Figure #	Weight of CPG-Oxine	pH	c	Loading Time	Flow Rate	Approx. Upper Limit of [Ca^{2+}] for Trace Loading	Equilibrium
A.1	11 mg	8.01	0.10 M $NaClO_4$	4 min	2 mL/min	1.5×10^{-5} M	Yes
A.2	•	7.00	•	•	•	2.5×10^{-5} M	•
A.3	•	6.00	•	•	•	6.5×10^{-5} M	•
A.4	•	5.00	•	•	•	7.5×10^{-5} M	•
A.5	•	8.01	0.010 M $NaClO_4$	•	•	0.25×10^{-5} M	•
A.6	•	5.00	•	•	•	2.0×10^{-5} M	•
A.7	•	7.00	0.75 M $NaClO_4$	•	•	2.5×10^{-5} M	•
A.8	40 mg	8.01	0.10 M $NaClO_4$	60 min	3.4 mL/min	1.5×10^{-5} M	•
A.9	•	7.00	•	4 min	•	2.5×10^{-5} M	No
A.10	11 mg	5.00	0.10 M KCl	•	2 mL/min	7.5×10^{-5} M	Yes

completely to equilibrium (Figure 2.12) but the 40 mg column had not (Figure 2.7 and 2.8). Nevertheless, the upper limit is about the same on these two columns.

In all future studies, except where noted, experiments were performed within the linear parts of the appropriate isotherm (i.e. under trace loading conditions).

II.3.4.2 EFFECT OF SOLUTION pH :

In this study, the Ca^{2+} solutions were prepared in 0.10 M $NaClO_4$ at various pH values, and each of these solutions was brought to complete equilibrium with the column containing 40 mg CPG-Oxine (125 - 177 µm particle diameter). The value of λ_0 at each pH was calculated from the measured peak height *via* the calibration curve run at the same time (Figure 2.6). Figure 2.13 is a plot of λ_0 *versus* pH for solutions at a constant ionic strength of 0.10 M. Since there are no dissolved ligands in these solutions, the observed increase in λ_0 with pH is associated exclusively with the effect of pH on bound 5-P-Oxine. Similar behavior has been reported for calcium sorption on silica-bound (103) and CPG-bound (97) 5-P-Oxine, and also for the sorption of other divalent metal cations (97,103,106,118). The influence of pH on calcium sorption on CPG-Oxine is explained in Chapter Three.

II.3.4.3 EFFECT OF IONIC STRENGTH :

These experiments were carried out in an identical manner to that just described in Section II.3.4.2 except that the solution pH was held constant at 7.00 and the ionic strength was varied. In Figure 2.14 it can be seen that λ_0 decreases markedly with ionic strength at pH 7.00. In contrast to the influence of pH, the influence of ionic strength on metal ion sorption by immobilized 5-P-Oxine seems to have been ignored or taken little into account in past studies of metal sorption. The physico-chemical origin of the influence of ionic strength on calcium sorption is also explained in Chapter Three.

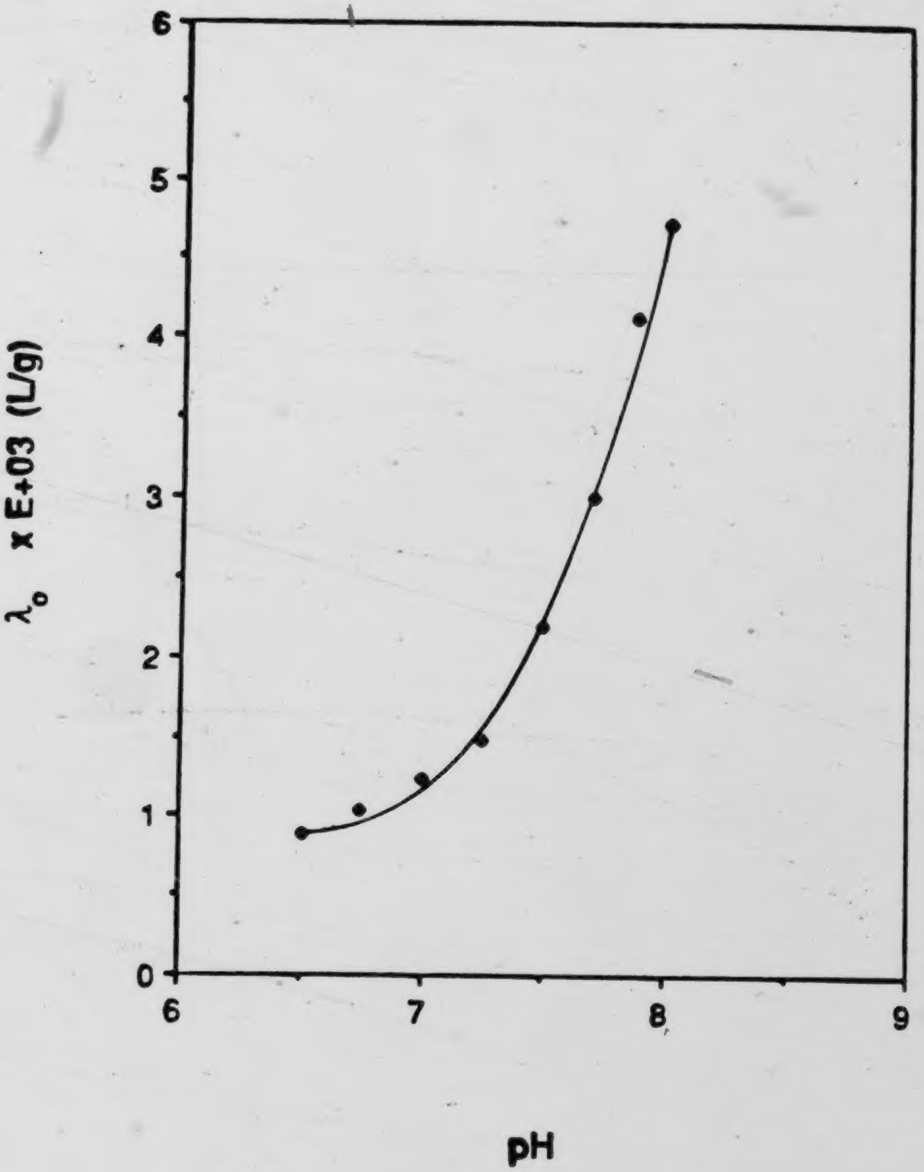

Figure 2.13 : Plot of λ_0 versus pH for calcium sorbed by the 40 mg CPG-Oxine column under trace conditions at c = 0.10 M.

c

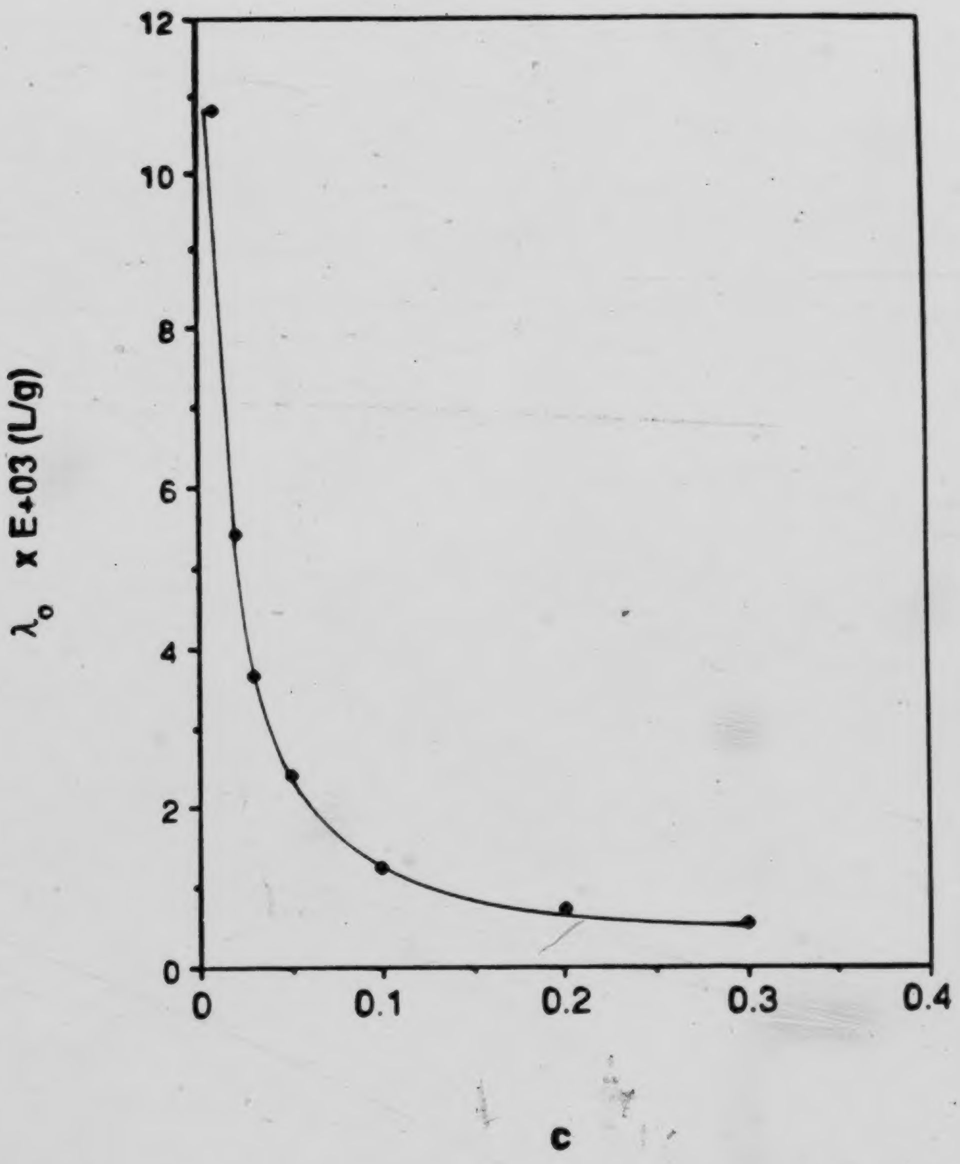

Figure 2.14 : Plot of λ_o versus c for calcium sorbed by the 40 mg CPG-Oxine column under trace conditions at pH = 7.00.

II.3.4.4 EFFECT OF MAGNESIUM ON CALCIUM SORPTION :

In solution, the log β_1 values for chelate formation between oxine and Fe^{3+}, Cu^{2+}, Zn^{2+}, Mg^{2+} and Ca^{2+} are 14.52, 12.56, 8.56, 4.74 and 3.27, respectively (94). While 5-P-Oxine would have somewhat different values of β_1 with these metals, one would expect that the sequence of stabilities for complexes with these metals would be similar to what it is for oxine. It is therefore expected that excess of either Fe^{3+}, or Cu^{2+}, or Zn^{2+} would displace Ca^{2+} from the column. Generally, however, in environmental and biological samples Ca^{2+} is present in much higher concentration than most transition metals and Zn^{2+}. However, Mg^{2+} can be a problem because it is usually present in amounts comparable to Ca^{2+}. In Table 2.6 are shown the results of experiments performed at both pH 7.00 and 3.00 with ionic strength 0.10 M in which the mole ratio of Mg^{2+} to Ca^{2+} in the sample is varied, with $[Ca^{2+}]$ always being in the linear regions of its isotherm as indicated in Figure A.2 and A.11 of Appendix I. The results demonstrated that under the trace loading conditions for Ca^{2+}, the eluted calcium peak height remained almost constant in the presence of various $[Mg^{2+}]$ levels up to a mole ratio of Mg^{2+} to Ca^{2+} of 3. On the other hand, in Table 2.7 are presented the results of experiments performed at both pH 6.00 and 7.40 with ionic strength 0.30 M in which the sample contained either no Mg^{2+} or equal molar Ca^{2+} and Mg^{2+}, with $[Ca^{2+}]$ at the non-linear regions of its isotherm as indicated in Figure A.12 of Appendix I. The results demonstrated that under non-trace loading conditions for Ca^{2+}, the peak height was reduced significantly in the presence of Mg^{2+}. Therefore, when using the column equilibration technique to measure $[Ca^{2+}]$ in the presence of Mg^{2+}, it is important to maintain trace loading conditions such that any interference due to Mg^{2+} can be ignored.

II.4 CONCLUSIONS :

Table 2.6 : Effect of Mg^{2+} on the eluted calcium peak height under trace loading $[Ca^{2+}]$ for CPG-Oxine.

Column	$[Ca^{2+}]$	$[Mg^{2+}]/[Ca^{2+}]$	pH	c	Eluted Calcium Peak Height
40 mg	2.50×10^{-5} $\underline{M}$	0	7.00	0.10 $\underline{M}$	1.3 ± 0.2 cm
"	"	0.49	"	"	1.6 ± 0.1 cm
"	"	0.66	"	"	1.5 ± 0.1 cm
"	"	1.3	"	"	1.5 ± 0.1 cm
11 mg	7.50×10^{-5} $\underline{M}$	0	3.00	0.10 $\underline{M}$	0.9 ± 0.1 cm
"	"	1	"	"	0.9 ± 0.0 cm
"	"	2	"	"	0.8 ± 0.1 cm
"	"	3	"	"	0.8 ± 0.0 cm

Note : The ± value indicates the standard deviation for 2 runs.

Table 2.7 : Effect of Mg^{2+} on the eluted calcium peak height under non-trace loading $[Ca^{2+}]$ for CPG-Oxine.

Column	$[Ca^{2+}]$	$[Mg^{2+}]/[Ca^{2+}]$	pH	c	Eluted Calcium Peak Height
11 mg	6.20×10^{-4} $\underline{M}$	0	6.00	0.30 $\underline{M}$	5.1 ± 0.0 cm
"	"	1	"	"	4.3 ± 0.1 cm
11 mg	6.20×10^{-4} $\underline{M}$	0	7.40	0.30 $\underline{M}$	9.6 ± 0.1 cm
"	"	1	"	"	7.7 ± 0.0 cm

Note : The ± value indicates the standard deviation for 2 runs.

The system and experimental conditons described in this study are used in latter chapters of this thesis for measuring [Ca^{2+}]. The loading step in the column equilibration method should be carried out in such a way that the column effluent is diverted to waste in order to avoid either fouling or deposition of metal residues in the AA nebulizer and burner. Untreated doubly distilled-deionized water is suitable for column washing; however, CO_2-free water was used for most experiments in this thesis. The eluent used for all experiments was 1% HNO_3.

The use of a short CPG-Oxine column in the present system permits faster equilibration than the long column. However, the equilibration rate may not be improved by reducing the particle size of CPG-Oxine in the long column because the kinetics involved in the equilibration process of CPG-Oxine are controlled by the diffusion of Na^+, H^+ and Ca^{2+} from the bulk solution into the diffuse double layer on CPG-Oxine.

Trace loading conditions (linear isotherms) for calcium on CPG-Oxine are required in order to maintain constant λ_0 and to prevent any interference due to the presence of high [Mg^{2+}] in the sample. The fact that the calcium sorption isotherms reached their upper limits of linearity at relatively low [Ca^{2+}] under most conditions studied restricts the use of CPG-Oxine to samples in which the [Ca^{2+}] is relatively low (e.g. $\leq 10^{-4}$ M). In samples containing $> 10^{-4}$ M Ca^{2+} the [Ca^{2+}] cannot be measured using CPG-Oxine. An immobilized ligand with a lower "conditional" stability constant for calcium would have to be used for such samples.

CHAPTER THREE

PROPERTIES OF CPG-OXINE AND ITS SORPTION OF CALCIUM

III.1 INTRODUCTION :

The objective of this study is to determine the acid-base and Ca^{2+} complexation behavior of CPG-Oxine and to describe them in terms of the "ionizable surface-group" (121,128,129) and "site-binding" models (121-124).

It was noted above that the immobilized oxine, incorporated on the surface of silica gel or controlled pore glass (CPG), is not oxine itself but rather one or another 5-phenylazo derivatives of oxine (99,104,107,108,111-114,118). In order to explain the observed dependence of metal ion sorption on solution pH and ionic strength, it is necessary to know the acid-base properties of the bound 5-phenylazo-8-hydroxyquinoline (5-P-Oxine, Figure 1.1). Spectrophotometric measurements on CPG-Oxine give the degree of ionization of the phenolic hydroxyl group as a function of pH. It allows determination of the second acid dissociation constant of the bound 5-P-Oxine. Capacity measurements combined with information from potentiometric titration curves and microelectrophoresis permit calculations of surface charge density and surface potential as a function of pH and ionic strength.

III.2 THEORY :

5-P-Oxine is an ampholyte containing both a weakly basic heterocyclic nitrogen as well as a weakly acidic phenol group. In homogenous aqueous solution, the degree of ionization of the compound depends on the pH of the solution. However in CPG-Oxine, it is the pH immediately adjacent to the surface ($\overline{pH}$) which determines the degree of ionization of the 5-P-Oxine bound to the surface. The $\overline{pH}$ generally is not the same as the pH in bulk solution (128,130,131).

In previous studies (132) $\overline{\mathrm{pH}}$ for small-pore diameter (3.2 nm) CPG was related to pH via the polyelectrolyte gel model (133-136). In the present case, however, the pores in CPG-Oxine are 50 nm. In 0.1 M electrolyte the "thickness" ($1/\kappa$) of the electrical double layer near the charged surface lining the pores is 1 nm (125,137) so that solution in the middle of the pores is uninfluenced by the surface potential. In this case the ionization of the bound 5-P-Oxine can be understood in terms of the "ionizable surface-group model".

In this model the relationship between surface charge density (σ_o, coul/cm^2) and electrical potential of the charge-surface (Ψ_o, volt) is given by the Gouy-Chapman equation (121,137,138) which, at 25° C, has the form :

$$\sinh\left(\frac{Z F \psi_o}{2 RT}\right) = 8.53 \times 10^4 \ c^{-1/2} \ \sigma_o \tag{3.1}$$

where Z is the charge on the ionized surface group, R is the ideal gas constant, F is the Faraday constant, T is the absolute temperature and c is the ionic strength of the bulk solution. The value of σ_o can be calculated from the surface concentration of ionized surface groups (Q, mmol/g) as follows :

$$\sigma_o = \frac{Z F Q}{1000 A_{sp}} \tag{3.2}$$

where A_{sp} is the specific surface area (7.0×10^5 cm^2/g for CPG-Oxine, (115)).

The potential Ψ_x at any distance **x** cm away from the charge-surface can be calculated (125). The simplified form of the relationship which is valid at relatively low values of Ψ_o is :

$$\Psi_x = \Psi_o \exp(-3.29 \times 10^7 c^{-1/2} x) \qquad (3.3)$$

When σ_o is constant, changing c alters Ψ_o via Eq. 3.1 which, in turn, alters Ψ_x via Eq. 3.3.

The relationship between the activity of hydrogen ion at a distance **x** cm away from the charge-surface ($\overline{a_{H,x}}$) and in the bulk solution (a_H) is given by the Boltzmann equation (121,128,137) :

$$\overline{a_{H,x}} = a_H \exp\left(-\frac{F\Psi_x}{RT}\right) \qquad (3.4)$$

In homogeneous aqueous solution 5-phenylazo-8-hydroxyquinolinium cation has pK_{a1} = 3.2 (for cation to neutral species) pK_{a2} = 8.6 (for neutral to anionic species) (139). Substituents at the o-, m- and p-positions of the phenylazo group do not change these values by more than ± 0.7 units unless they are highly electron-withdrawing or -donating (139). Thus, by analogy with homogeneous solution behavior, covalently bound 5-P-Oxine is expected to have $\overline{pK_{a1}}$ in the range 2.5 - 3.9 and $\overline{pK_{a2}}$ in the range 7.9 - 9.3. Deprotonation of cationic groups on bound 5-P-Oxine is therefore complete at pH > 6 so that 5-P-Oxine can be treated as a monoprotic acid at pH > 6, vis :

$$\overline{HOX} + \overline{H_2O} \rightleftharpoons \overline{OX^-} + \overline{H_3O^+} \qquad (3.5)$$

The bar indicates a species in the vicinity of the charge-surface (i.e. the silica surface of CPG). The species $\overline{HOX}$ is the neutral species, shown in Figure 1.1. The second dissociation constant corresponds to the deprotonation from the phenolic hydroxyl group on the 8-hydroxyquinoline moiety in the bound 5-P-Oxine and is given by (121,137) :

$$\overline{K_{a2}} = \frac{[\overline{OX^-}]_x \, \overline{a_{H,x}}}{[\overline{HOX}]_x} \tag{3.6}$$

Substituting for $\overline{a_{H,x}}$ in Eq. 3.6 from Eq. 3.4 gives :

$$\overline{K'_{a2}} = \overline{K_{a2}} / \exp(-\frac{F\psi_x}{RT}) = \frac{[\overline{OX^-}]_x \, a_H}{[\overline{HOX}]_x} \tag{3.7}$$

in which $\overline{K'_{a2}}$ is the acidity quotient in terms of the bulk solution a_H. While $\overline{K_{a2}}$ should be independent of Ψ_X, $\overline{K'_{a2}}$ varies with Ψ_X.

The "ionizable surface-group model" can be extended to describe "site-binding" of counterions such as the formation of a metal-ligand complex between the immobilized $\overline{OX^-}$ species and Ca^{2+}. Previous evidence suggests that Ca^{2+} forms a 1:1 complex with bound $\overline{OX^-}$ (106,140,141) :

$$\overline{Ca^{2+}} + \overline{OX^-} \rightleftharpoons \overline{CaOX^+} \tag{3.8}$$

where the bar indicates a species in the vicinity of the charge-surface. The stability constant for the complex is :

$$\overline{\beta_1} = \frac{[\overline{CaOX^+}]_x}{[\overline{OX^-}]_x \, \overline{a_{Ca}}} \tag{3.9}$$

The Boltzmann equation (121,124) relates the activity of Ca^{2+} at a distance x cm away from (but close to) the charge-surface ($\overline{a_{Ca}}$) to its activity in bulk solution (a_{Ca}) (121,124):

$$\overline{a_{Ca}} = a_{Ca} \exp\left(-\frac{2F\psi_x}{RT}\right) \qquad (3.10)$$

The value of Ψ_x is calculated from the surface charge density σ_0 by combining Eq. 3.1, which gives the surface potential Ψ_0, with Eq. 3.3.

In the column equilibration experiment CPG-Oxine is first equilibrated with bulk solution containing Ca^{2+} with an activity a_{Ca} and is then washed briefly with water to remove bulk solution from the pores and between the particles. The total number of moles of sorbed calcium per gram of CPG-Oxine ($\overline{N_{Ca}}$) is defined by the expression :

$$\overline{N_{Ca}} = [\overline{CaOX^+}]_x V_x + \overline{n_{Ca}} \qquad (3.11)$$

where V_x is the volume per gram of CPG-Oxine in a thin layer of solution located at a distance x cm from the charge-surface and $[\overline{CaOX^+}]_x$ is the concentration of complexed calcium in this thin layer of solution. $[\overline{CaOX^+}]_x$ can be expressed by Eq. 3.9, i.e.

$$[\overline{CaOX^+}]_x = \overline{\beta_1}\,[\overline{OX^-}]_x\,\overline{a_{Ca}} \qquad (3.12)$$

where $\overline{a_{Ca}}$ is given by Eq. 3.10, and

$$[\overline{OX^-}]_x = \frac{\overline{\alpha_{OX}}\;\overline{v_{Oxine}}}{V_x} \qquad (3.13)$$

Substituting for $\overline{a_{Ca}}$ and $[\overline{OX^-}]_x$ in Eq. 3.12 from Equations 3.10 and 3.13 gives

$$[\overline{CaOX^+}]_x = \overline{\beta_1}\,\frac{\overline{\alpha_{OX}}\;\overline{v_{Oxine}}}{V_x}\,a_{Ca} \exp\left(-\frac{2F\psi_x}{RT}\right) \qquad (3.14)$$

where

$$\overline{\alpha_{OX}} = \frac{\overline{K'_{a2}}}{\overline{K'_{a2}} + a_H} \qquad (3.15)$$

which is the fraction of bound 5-P-Oxine ionized, and $\overline{v_{Oxine}}$ is the moles of bound 5-P-Oxine per gram of CPG-Oxine.

The quantity $\overline{n_{Ca}}$ in Eq. 3.11 is the moles of remaining dissolved calcium, not complexed by bound 5-P-Oxine, in the pores of CPG-Oxine that are incompletely removed during the water wash. $\overline{n_{Ca}}$ can be expressed by the proportionality :

$$\overline{n_{Ca}} \;\alpha\; \frac{a_{Ca}}{\kappa} \qquad (3.16)$$

in which $1/\kappa$ is the "thickness" of the diffuse part of the electrical double layer (125,137). During the washing step, dilution of electrolyte in the pore solution decreases ionic strength, which causes an increase of ψ_x. From Figure 2.14 it can be seen that the decrease in ionic strength increases λ_0. Therefore the amount of sorbed (complexed) Ca^{2+} increases. The distance into the pore solution, measured from the glass surface, that will experience the effect of increasing ψ_x (i.e. λ_0) is proportional to the thickness ($1/\kappa$) of the diffuse layer before washing is started.

$$\kappa \;\alpha\; c^{1/2} \qquad (3.17)$$

Eq. 3.16 becomes

$$\overline{n_{Ca}} = k \frac{a_{Ca}}{c^{1/2}} \qquad (3.18)$$

and

$$a_{Ca} = [Ca^{2+}]\,\gamma_{Ca} \qquad (3.19)$$

where k is a constant and γ_{Ca} is the ionic activity coefficient for Ca^{2+}. Finally, Eq. 3.11 can be combined with Equations 3.14, 3.18 and 3.19 to give the expression :

$$\overline{N_{Ca}} = \overline{\beta_1}\ \overline{\alpha_{OX}}\ \overline{v_{Oxine}}\ [Ca^{2+}]\,\gamma_{Ca} \exp\left(-\frac{2F\psi_x}{RT}\right) + k\,[Ca^{2+}]\,\frac{\gamma_{Ca}}{c^{1/2}} \qquad (3.20)$$

The distribution coefficient for calcium λ_o, defined by Eq. 2.2 as $\overline{N_{Ca}}/[Ca^{2+}]$, can be obtained by rearranging Eq. 3.20 :

$$\lambda_o = \overline{\beta_1}\ \overline{\alpha_{OX}}\ \overline{v_{Oxine}}\ \gamma_{Ca} \exp\left(-\frac{2F\psi_x}{RT}\right) + k\,\frac{\gamma_{Ca}}{c^{1/2}} \qquad (3.21)$$

Under conditions of constant pH, constant c and trace loading, λ_o is a constant. The value of λ_o is measured by the column equilibration experiment using a standard solution of known $[Ca^{2+}]$ and with the same pH and c as in the sample solution.

III.3 EXPERIMENTAL :

III.3.1 CHEMICALS AND REAGENTS :

CPG-Oxine (Pierce Chemical Co.), batch 071982-81, called Batch A, and batch 850605085, called Batch B; both batches with particle size 125 - 177 µm and pore diameter 50 nm.

Controlled Pore Glass (CPG), CPG/500, is underivatized from the Pierce Chemical Co., batch 841101081. It has a particle size of 37 - 74 µm and pore diameter of 50 nm.

Both CPG-Oxine and CPG were washed with 1% HNO_3, then rinsed with water and air dried with vacuum suction prior to use.

All solutions were prepared with doubly distilled-deionized water.

$CaCO_3$, HEPES, $NaClO_4 \cdot H_2O$, NaOH, $HClO_4$ and HNO_3 used in this study were described in Section II.2.1.

Copper stock solution was prepared by dissolving copper foil (Matheson, Coleman and Bell, Richmond, N.J.) in HNO_3.

Iron stock solution was prepared by using analytical grade ferric nitrate, $Fe(NO_3)_3 \cdot 9\ H_2O$ (British Drug Houses).

0.1 M acetate buffer (pH 5.00) was prepared by first adding 6.804 g of sodium acetate, $NaC_2H_3O_2 \cdot H_2O$ (Fisher Scientific Co.) and 2.87 mL of glacial acetic acid, $HC_2H_3O_2$ (Fisher Scientific Co.) to about 450 mL of water. The pH was checked and adjusted to 5.00 by adding small amounts of either NaOH or acetic acid. Finally, the solution was diluted to 500 mL with water. Both chemicals were reagent grade.

Eluent used in the determination of capacity of CPG-Oxine was prepared from analytical reagent grade hydrochloric acid, HCl (British Drug Houses), and HNO_3 in the concentrations described below.

The 0.9 M ammonium nitrate (NH_4NO_3) / 0.05 M ammonium hydroxide (NH_4OH) buffer (pH 8.00) used for eluting the sorbed Cl^- on CPG-Oxine was prepared by combining suitable quantities of the two reagent grade chemicals (Fisher Scientific Co.), diluting with water, adjusting to pH 8.00 by adding either NH_4OH or HNO_3 and finally diluting to volume.

Buffers used in the spectrophotometric determination of $\overline{pK_{a2}}$ were prepared in the pH range 6.40 to 9.80 to contain 0.10 M ionic strength. They were composed of various combinations of analytical grade $NaH_2PO_4 \cdot H_2O$ (J.T. Baker Chemical Co.), reagent grade Na_2HPO_4 (American Scientific & Chemical), reagent grade NH_4OH (Fisher Scientific Co.) and reagent grade NH_4Cl (Fisher Scientific Co.).

0.1 M NaOH titrant was prepared by dissolving 4.0 g of reagent grade NaOH in 1 litre of water. It was standardized by titrating against potassium hydrogen phthalate.

Potassium chloride, KCl (Fisher Scientific Co.), potassium nitrate, KNO_3 (J.T. Baker Chemical Co.), silver nitrate, $AgNO_3$ (Terochem Laboratory Ltd.) and potassium hydrogen phthalate, $HOCOC_6H_4COOK$ (Anachemic Ltd.), were all reagent grade.

III.3.1.2 APPARATUS :

A Model 4000 atomic absorption spectrophotometer (Perkin-Elmer) was used to determine copper and iron. The instrumental parameters are the same as those listed in Table 2.1 except that the wavelengths were 324.8 nm and 248.3 nm, slit widths were 0.7 nm and 0.2 nm and lamp currents were 15 mA and 20 mA, respectively. Calibration curves were obtained from the copper and iron standard solutions prepared in the 1% HNO_3.

The concentration ("H-type") cell used for null-point potentiometric titration has been described (142). EMF measurements were made between two Ag/AgCl electrodes in the cell with 2 M KNO_3 salt bridge using a Model 461-2 digital multimeter (Simpson Electric Co., U.S.A.).

Measurements of pH were made with either separate glass and calomel electrodes using an Accumet Model 525 digital pH meter (Fisher Scientific Co.) with a precision estimated at ± 0.01 pH unit, or a combination glass/reference electrode using an Accumet Model 520 pH/ion meter (Fisher Scientific Co.).

pH titrations of CPG-Oxine were carried out in a plastic beaker. Stirring was done with a Teflon propeller attached via a glass rod to a stirring motor. A propeller was used in order to minimize crushing of the CPG-Oxine particles.

Spectrophotometric measurements on CPG-Oxine were made by A.K. Kolstad. They were performed at 520 nm, with a Model 8451A diode array spectrophotometer (Hewlett-Packard Corp.), in a modified variable pathlength flow cell with 1.5 inch diameter round windows (Beckman Instruments). Inlet and outlet holes of the cell were threaded to accept standard Cheminert end-fittings (Applied Science) and a porous Teflon filter was installed in the outlet hole to permit slurry packing and flushing with buffer. The actual cell geometry was established by cutting a 4 mm wide rectangular slot through the 0.13 mm thick Teflon spacer disk placed between the cell windows. The ends of the slot terminated at the inlet and outlet holes so that liquid was pumped through the length of the packed bed. The bed of particles was packed by pumping a slurry from a stirred reservoir. A Milton Roy Minipump (Applied Science) was used for slurry packing and flushing the bed with buffer. All absorbance measurements were made on a stainless steel plate which was designed to fit and position the cell window in the light path.

Electrophoretic mobility was measured in a particle microelectrophoresis apparatus (Rank Brothers Mark II, Cambridge, England) with a rectangular cell.

III.3.3 CAPACITY MEASUREMENTS :

Capacity by Copper Uptake :

The experiment was performed by equilibrating 0.4 g, accurately weighed, CPG-Oxine (Batch A) overnight with 50 mL acetate buffer (pH 5.00) containing an excess of Cu^{2+} (6.25×10^{-4} M). The CPG-Oxine was filtered out next day and rinsed with water until no copper was detected in the rinsings. The bound Cu^{2+} was then eluted into a 100 mL volumetric flask with an acid eluent mixture containing 1 M HCl and 1 M HNO_3, and the Cu^{2+} content in the eluate was determined by AAS. The analysis was performed in four replicates. Copper uptake has previously been used for capacity measurement and is considered reliable (106,107,111,114).

Capacity by Iron Uptake :

Batch A CPG-Oxine was used. The experimental procedure was similar to the determination of copper uptake but used a buffered Fe^{3+} (5.5×10^{-4} M) solution at pH 5.00. However, the sorbed Fe^{3+} was completely eluted into a 500 mL volumetric flask in this case, and the analysis was performed in duplicate. This procedure is based on a literature method (118).

Capacity by Carbon and Nitrogen Determinations:

The microanalysis of Batch A CPG-Oxine was performed using standard methods by the Microanalytical Laboratory of the University of Alberta, Department of Chemistry. The analysis was performed in duplicate.

III.3.4 DETERMINATION OF CHLORIDE CONTENT :

The experiment was performed on both Batches A and B by first equilibrating 1 g, accurately weighed, of CPG-Oxine with 1 M HCl overnight and then drying in vacuum for 5 - 6 hours without water washing, to remove all unreacted and interstitial HCl. The Cl^- sorbed on CPG-Oxine was eluted into a 50 mL volumetric flask with NH_3/NH_4NO_3 buffer (pH 8.00). Completeness of elution was checked with $AgNO_3$. The 50 mL Cl^- sample was filled into one arm of the "H-type" cell which contained 50 mL of the NH_3/NH_4NO_3 buffer and a small magnetic stirrer bar in the other arm. Small increments of standardized 0.1 M KCl were added to the stirred buffer using a 2 mL micrometer buret (Roger Gilmont, Great Neck, New York) until the voltage difference between the two arms was zero. The Cl^- content in the sample was then determined from the added amount of 0.1 M KCl. The analysis was performed in four replicates.

III.3.5 POTENTIOMETRIC TITRATIONS :

Both Batches A and B were used in this study. One gram of the HCl-washed and vacuum dried CPG-Oxine (Section III.3.4) was accurately weighed into a plastic beaker and then 100 mL of the appropriate $NaClO_4$ solutions (0.010 M, 0.050 M, 0.10 M, 0.20 M, and 0.30 M) was added. The pH electrodes and stirring rod were then placed in the solution; the mixture was stirred for 5 min and left overnight under N_2 atmosphere. The initial pH of the bulk solution was recorded next day, and a 0.02 mL increment of standardized 0.1 M NaOH was delivered into the solution by using a 2-mL micrometer buret (Roger Gilmont, Great Neck, N.Y.). The mixture was stirred for 5 min after the addition, the stirrer was shut off and the pH was recorded when the reading was stable (about 15 min). Although the experiment was carried out under N_2 atmosphere, the titration was not continued to very high pH to avoid the possibility of dissolution of silica from CPG-Oxine. The experiment was performed in duplicate.

III.3.6 SPECTROPHOTOMETRIC MEASUREMENTS (Performed by A.K. Kolstad):

Both CPG-Oxine (Batch B) and CPG were ground and sieved under water. The 38 - 45 μm fraction of each was slurry packed into the 0.13 mm pathlength flow cell and the appropriate buffer was pumped through the packed bed until well after the pH of the effluent was equal to that of the influent. The visible spectrum was recorded for each pH. Changing to the next buffer solution was accomplished without disturbing the packing structure of the bed. Ten consecutive absorbance measurements at 520 nm were also made at each pH by taking the cell out and then replacing again in the same position. The relative standard deviation of these measurements was 0.2%.

III.3.7 MICROELECTROPHORESIS :

CPG-Oxine (Batch A) was ground to very fine particles such that they remained suspended in water for about 20 min. The ground CPG-Oxine particles were washed with 1% HNO_3 by centrifuging and decanting. Next, it was washed with doubly distilled-deionized water several times until the pH of the washing became neutral.

Sodium solutions containing 0.010 M HEPES were prepared either in 0.10 M $NaClO_4$ at the appropriate pH values (6.51, 6.75, 7.00, 7.25, 7.50, and 8.01), or in the appropriate $NaClO_4$ concentrations (0.010 M and 0.050 M) at pH 7.00. An aliquot of the neutralized particles was suspended in the appropriate Na$^+$ solution and left overnight. The pH of each mixture was checked and readjusted, if necessary, before the electrophoresis experiment.

The microelectrophoresis experiments were performed by the author at the Alberta Research Council, Oil Sands Research Department, Edmonton. The mobilities of 20 - 40 particles were measured at 30° C. It was difficult to measure the mobilities at $c > 0.1$ M Na$^+$, and sometimes at $c = 0.1$ M as well, due to the formation of bubbles at the electrodes surface.

III.4 RESULTS AND DISCUSSION :

III.4.1 HOMOGENEITY :

Column equilibration experiments were performed on four newly packed 10 x 1.5 mm i.d. CPG-Oxine (Batch A) columns by using a 25.0 µM Ca^{2+} solution in 0.10 M NaClO$_4$ at pH 7.00. The old column containing 11 mg CPG-Oxine (Batch A), which has been described in Chapter Two, was also used in this study for comparison.

As seen in Table 3.1, the eluted calcium peak heights obtained from the four new columns were almost identical, which indicated that CPG-Oxine is essentially a homogeneous packing material. The reason for obtaining a higher calcium eluted peak height from the old column is unknown.

III.4.2 CAPACITY :

The variation in literature values for capacities of CPG-Oxine are shown in Table 1.1. In addition to real differences between batches, several reasons have been proposed to explain the variation, such as effect of pore size (112,113); adsorption or precipitation of the metal ion, which is used to measure the capacity, on the glass; binding to either the

Table 3.1 : Variation of sorbed calcium with the weight of CPG-Oxine in column.

Column	Weight of CPG-Oxine	Moles of Calcium Sorbed
1	11.2 mg	5.7×10^{-10}
2	11.2 mg	5.0×10^{-10}
3	11.2 mg	5.0×10^{-10}
4	11.4 mg	6.7×10^{-10}
Old	11.1 mg	2.7×10^{-9}

azo nitrogens or the residual silanol groups (97,111,143); and the possibilities of formation of a 2:1 complex between the metal ion and bound oxine (111).

The capacity of Batch A was determined by the established literature method involving sorption of Cu^{2+} (106,107,111,114). In this experiment copper forms a 1:1 complex with bound 5-P-Oxine (106,140,141). The measured capacity was 0.00362 ± 0.00005 mmol 5-P-Oxine/g. On the other hand, capacity obtained by measuring Fe^{3+} uptake was 0.0573 ± 0.0003 mmol per gram CPG-Oxine. However, the value based on Fe^{3+} uptake is probably unreliable. At pH 5.0 Fe^{3+} is prone to hydrolysis which causes precipitation of Fe^{3+} on the glass. Also, surface silanol groups have the ability to extract Fe^{3+} down to pH 1 (111,143). The capacity based on the more well established Cu^{2+} uptake method is taken as reliable.

Measurement of bound 5-P-Oxine capacity cannot be based upon micro-determination of nitrogen or carbon because the synthetic scheme for CPG-Oxine is known to leave a lot of N- and C- containing byproducts as impurities covalently bound to the glass surface (113,114). For example, from the measured nitrogen content of 0.16 mmol N/g and from the measured carbon content of 1.18 mmol C/g the calculated content of bound 5-P-Oxine has an erroneously high value of 0.040 and 0.062 mmol 5-P-Oxine per gram, respectively.

III.4.3 CHLORIDE CONTENT :

In order to calculate σ_O, as discussed below, it is necessary to know the concentration of cationic protonated nitrogens present on the acid-washed CPG-Oxine at the start of the titration. Since cationic groups arising from protonation of basic nitrogens have associated with them an equivalent amount of Cl^-, the former may be determined by measuring the latter. In this experiment vacuum drying, rather than water washing, was used to remove excess HCl from acid-washed CPG-Oxine in order to avoid loss of protons from NH^+ groups via hydrolysis. The Cl^- content was found to be 0.011 ± 0.001 mmol Cl^-/g for Batch A and 0.008 ± 0.003 mmol Cl^-/g for Batch B. This is the quantity needed for calculating σ_0.

It is interesting to calculate the fraction of protonatable (basic) nitrogens in CPG-Oxine that are associated with bound 5-P-Oxine. It has been shown that in strong acid solution the compound 5-phenylazo-8-hydroxyquinoline can be protonated on two sites, the first on the heterocyclic nitrogen and a second on one of the azo nitrogens (139,144). Thus, based on the measured capacity of 0.0036 mmol/g, the bound 5-P-Oxine could account for between 0.0036 and 0.0072 mmol basic N/g, which represents between 33% and 65% of the total basic nitrogen content of 0.011 mmol/g in CPG-Oxine. In addition, the fact that the total basic nitrogen content (0.011 mmol/g) is far less than the total nitrogen content (0.16 mmol/g) indicates that the majority of the nitrogens in the impurity groups on CPG-Oxine are not basic. This is consistent with the facts that an aromatic amide is the major synthetic byproduct (108,113,114,118) and that aromatic amides are extremely weak bases (145).

III.4.4 POTENTIOMETRIC TITRATIONS :

Several attempts have been made to measure $\overline{pK_{a1}}$ and $\overline{pK_{a2}}$ for 5-P-Oxine bound to silica gel and CPG using potentiometric (pH) titration of aqueous suspensions (106,107,111,140). Titration curves are typically ill-defined and yield $\overline{pK_a}$ values showing considerable variability (111,140).

Figures 3.1-3.5 are the represented titration curves for Batch A acid-washed CPG-Oxine in 0.010 M, 0.050 M, 0.10 M, 0.20 M and 0.30 M $NaClO_4$ solutions, respectively; and Figure 3.6 is one of the titration curves for Batch B acid-washed CPG-Oxine that was obtained in 0.10 M $NaClO_4$ solution. As far as bound 5-P-Oxine is concerned, protons are removed from cationic protonated azo and heterocyclic nitrogens in the early stages of the titration and from the neutral phenolic group later in the titration.

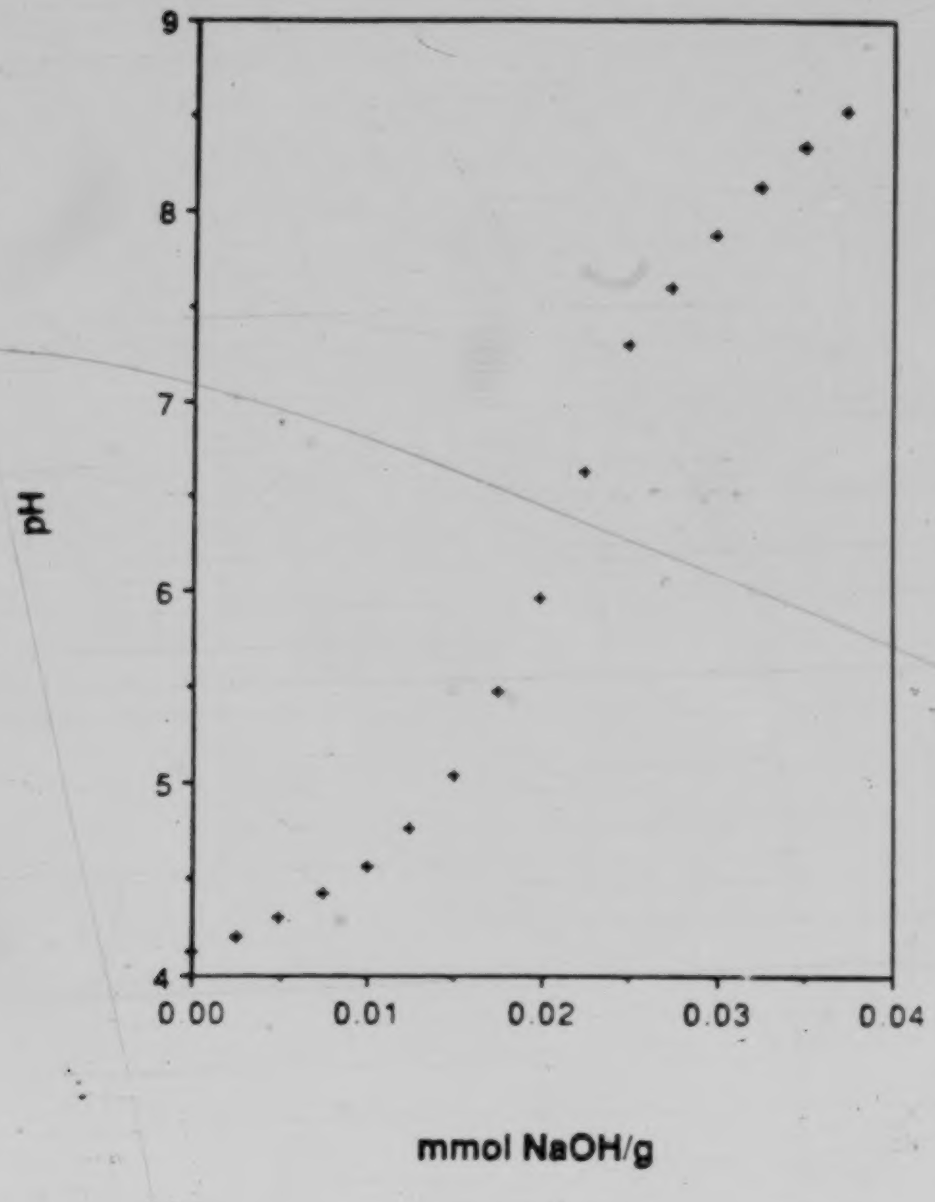

Figure 3.1 : Potentiometric titration curve of acid washed and vacuum dried CPG-Oxine (Batch A) at c = 0.010 M.

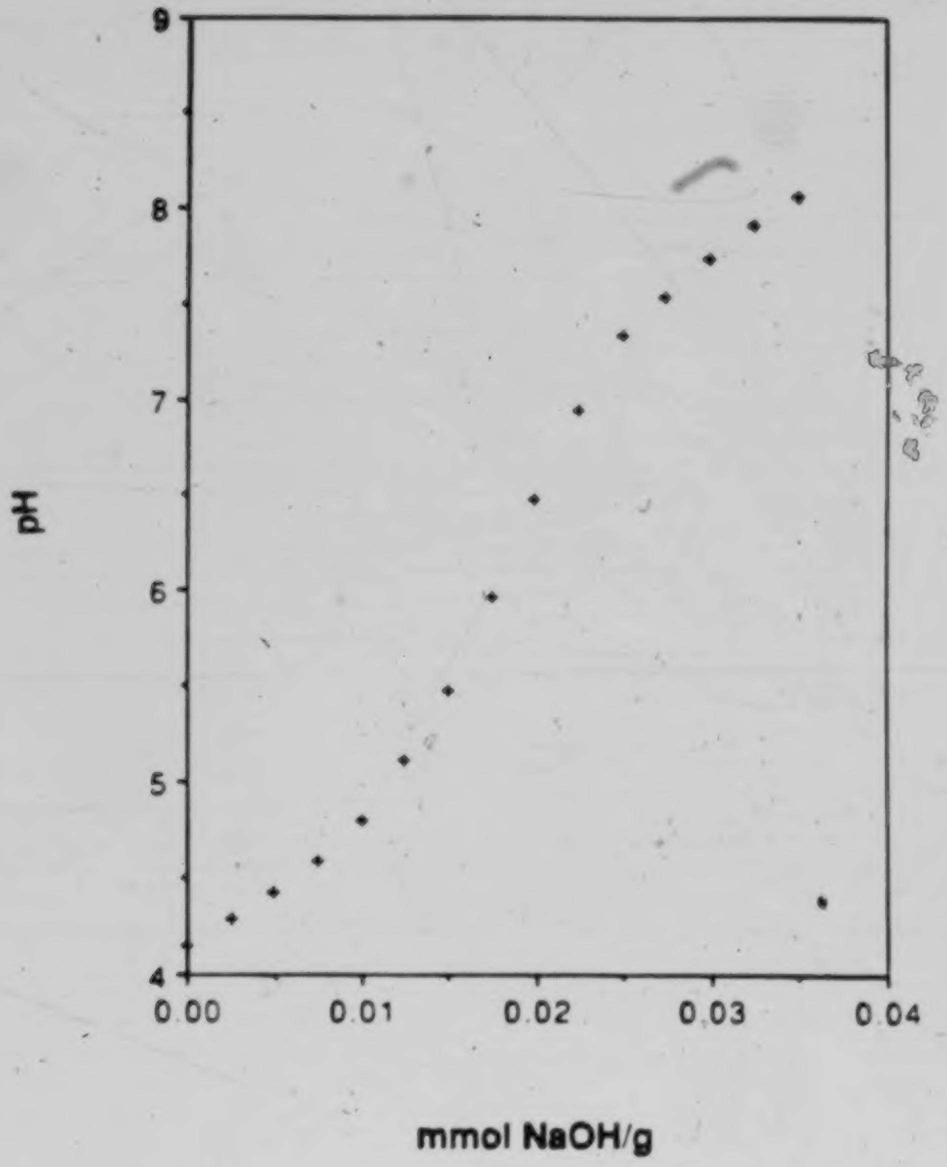

Figure 3.2 : Potentiometric titration curve of acid washed and vacuum dried CPG-Oxine (Batch A) at c = 0.050 M.

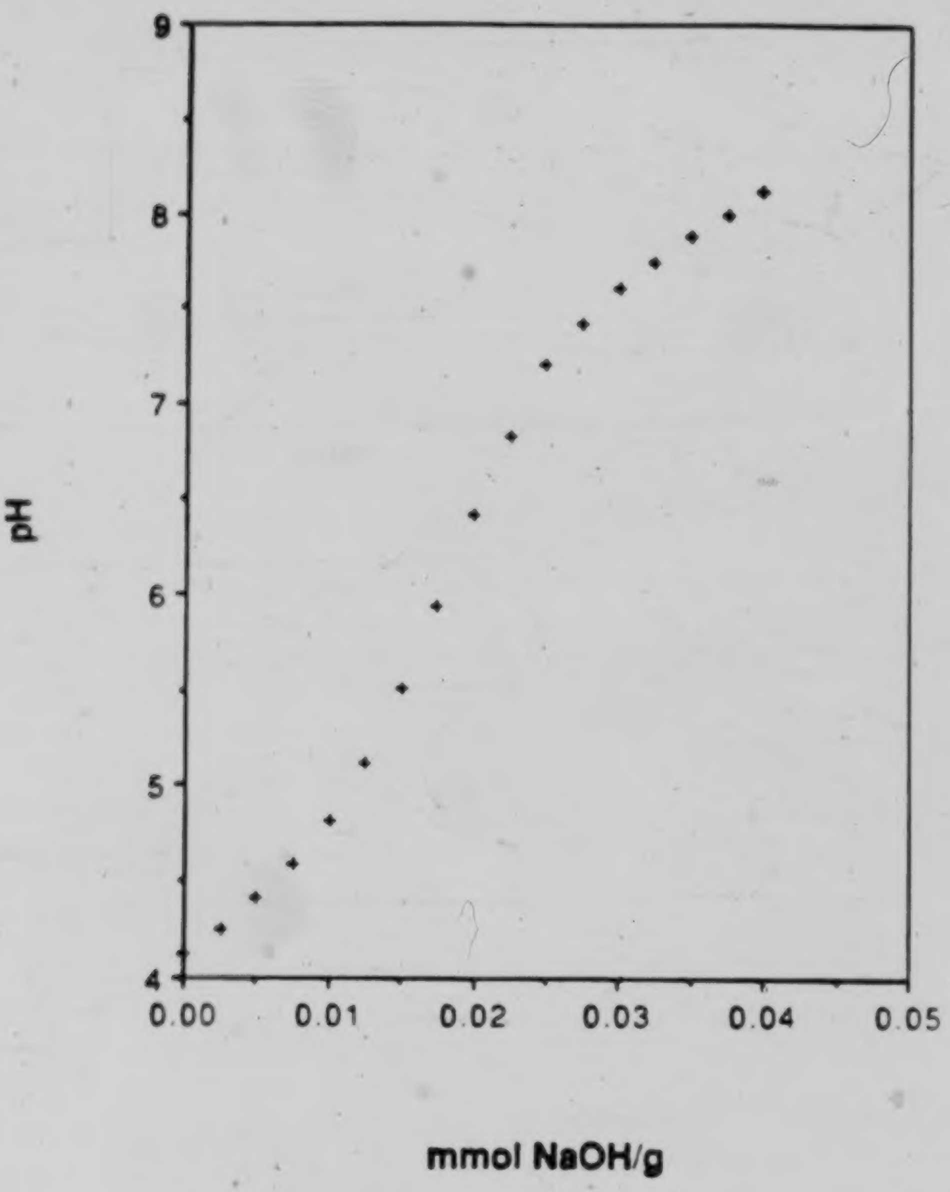

Figure 3.3 : Potentiometric titration curve of acid washed and vacuum dried CPG-Oxine (Batch A) at c = 0.10 M.

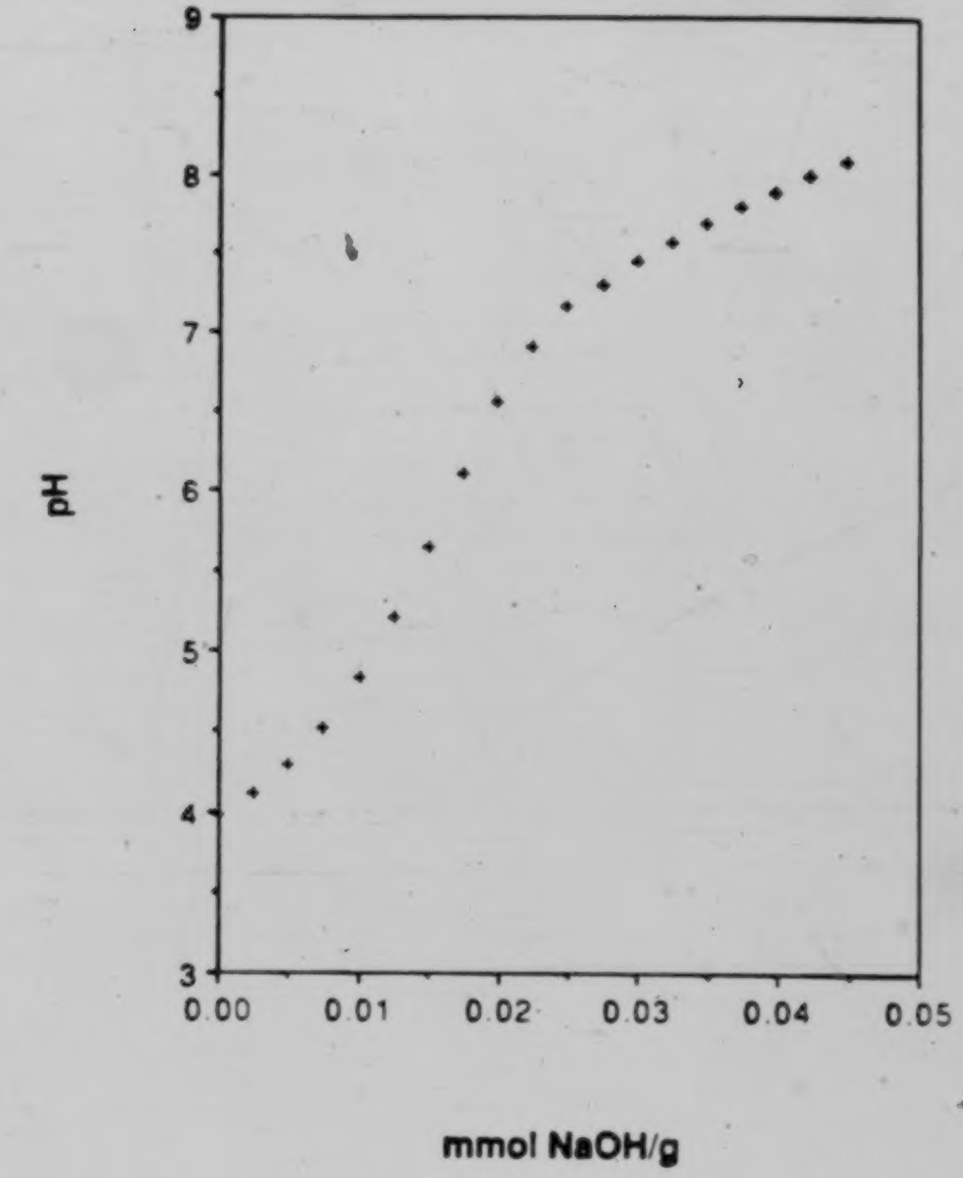

Figure 3.4 : Potentiometric titration curve of acid washed and vacuum dried CPG-Oxine (Batch A) at c = 0.20 M.

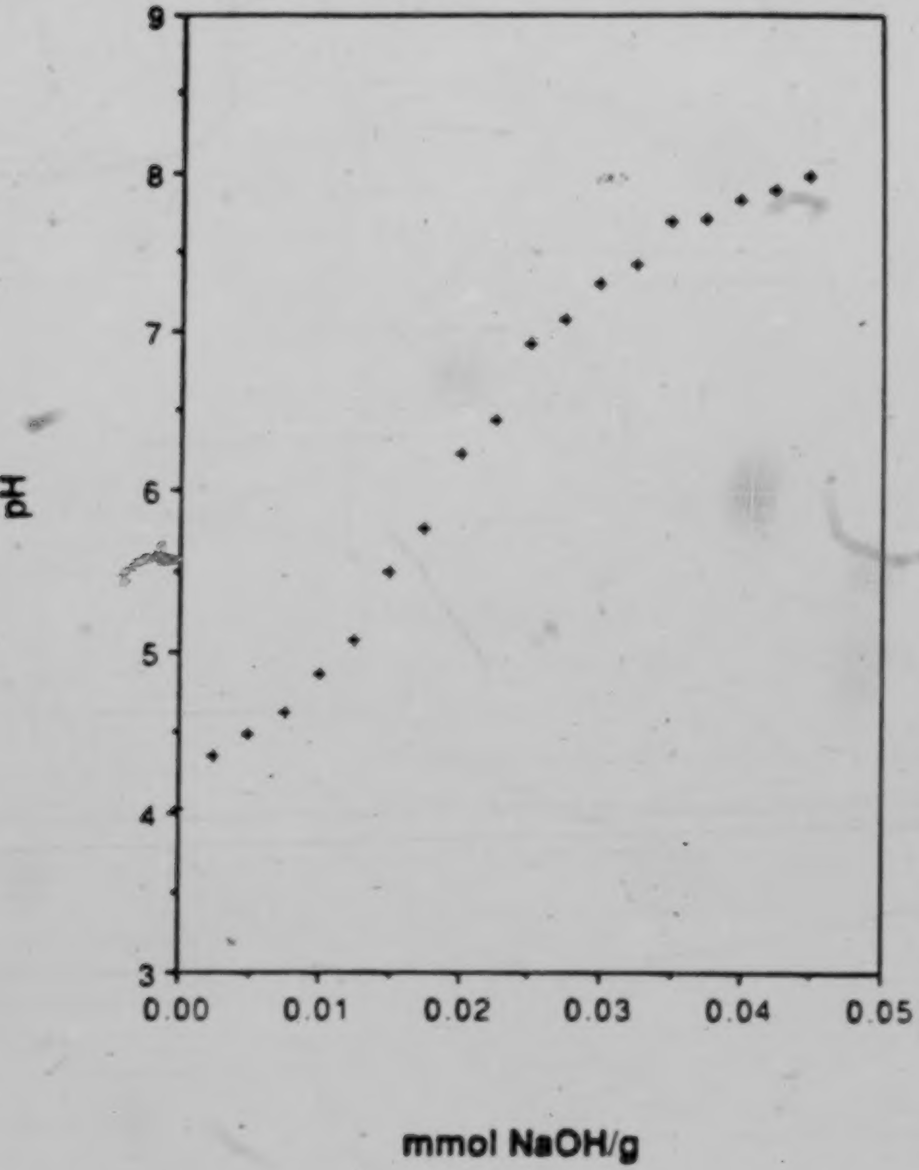

Figure 3.5 : Potentiometric titration curve of acid washed and vacuum dried CPG-Oxine (Batch A) at c = 0.30 M.

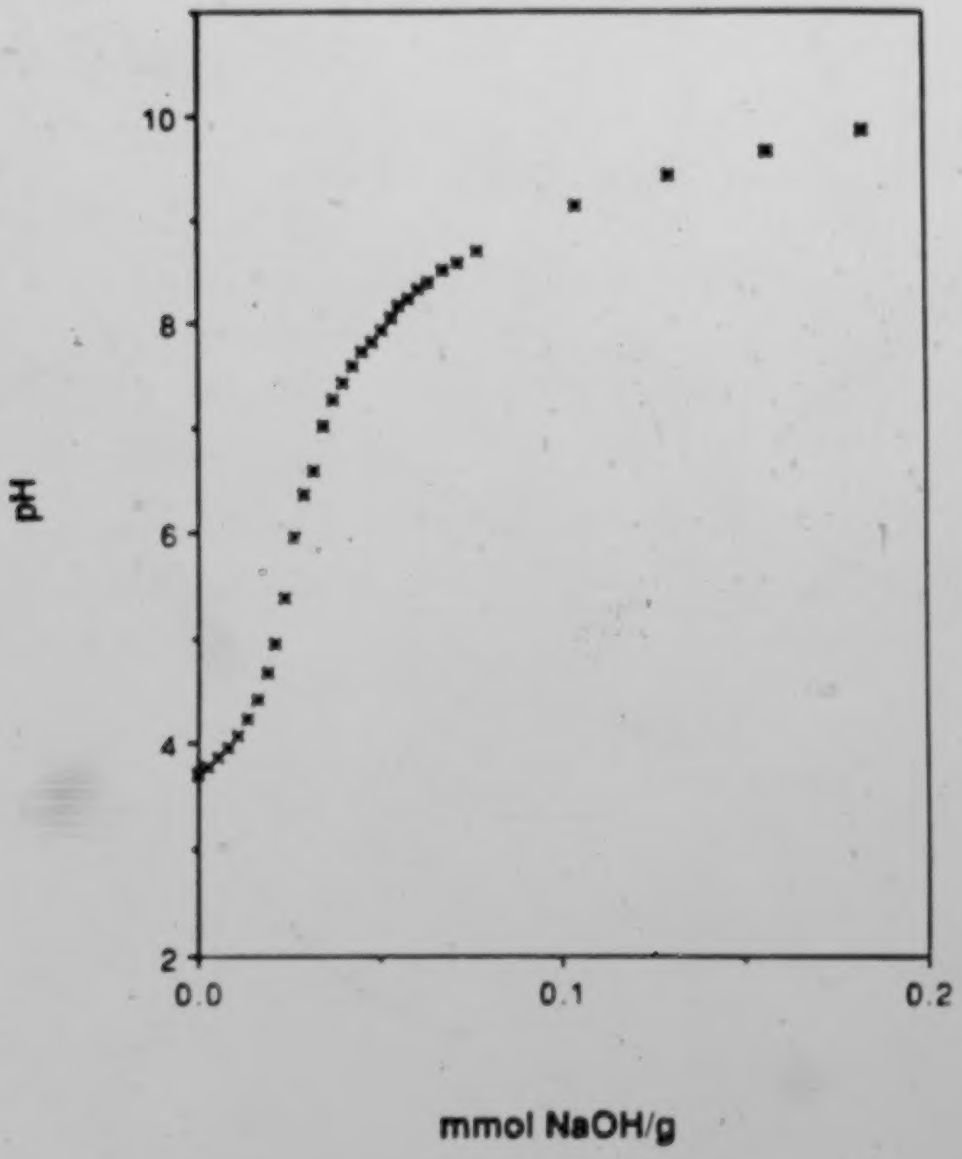

Figure 3.6 : Potentiometric titration curve of acid washed and vacuum dried CPG-Oxine (Batch B) at c = 0.10 M.

However, the situation is complicated by the fact that protons are being removed from other acidic groups, such as residual surface hydroxyl groups in SiOH and BOH sites, throughout the titration. In fact, it has been shown these surface hydroxyl groups exhibit a range of apparent $\overline{pK_a}$ values and their dissociation begins at pH values well below 6 and continues at pH values well above 6 (111,131,146,147). This precludes the use of titration curves to obtain the values of $\overline{pK_a}$, especially $\overline{pK_{a2}}$. As revealed by the titration curves (Figures 3.1-3.6), a great fraction of the negative surface charge that develops on CPG-Oxine at pH > 6 comes from deprotonation of surface hydroxyl groups rather than from deprotonation of the phenolic hydroxyl groups of bound 5-P-Oxine. The charge surface, at which σ_O and Ψ_O are defined, is thus identified with the hydroxyl-bearing glass surface of the CPG.

The total negative surface-charge on CPG-Oxine at any pH value above 6, at which deprotonation of cationic groups is complete, can be obtained from the titration curves. The concentration of negative surface groups, Q, is equal to the mmol NaOH/g taken up by CPG-Oxine in reaching a given pH, calculated by the method of Berube and de Bruyn (148), minus mmol NaOH/g required to neutralize the protonated cationic sites. The mmol NaOH/g required to neutralize the protonated sites at pH > 6 is equal to the measured mmol Cl^-/g (i.e. 0.011 for Batch A and 0.008 for Batch B). Consequently, σ_O and Ψ_O can be calculated via Equations 3.2 and 3.1, respectively. Calculated values of Q, σ_O and Ψ_O are presented in Table 3.2.

III.4.5 **SPECTROPHOTOMETRY** :

Uncertainty about the value of the second acid dissociation constant prompted an investigation of the acid-base behavior of CPG-Oxine, and the development of a spectrophotometric technique to measure $\overline{pK'_{a2}}$.

Absorbance measurements made through a thin layer of CPG-Oxine particles were subjected to light scattering. However, it was found by using the same size particles of

Table 3.2 : Surface electrical properties and spectrophotometric measurement of ionization of bound 5-P-Oxine on CPG-Oxine (Batch B) at ionic strength 0.10 M

pH	Q (mmol/g)	σ_o (coul/cm^2)	ψ_o (volt)	Absorbance [c]		$\overline{\alpha_{ox}}$ [d]	
				Run 1	Run 2	Run 1	Run 2
6.40	0.021_2	-2.9×10^{-6}	- 0.037	0.929 [a]	0.929 [a]	0	0
7.49	0.032	-4.4×10^{-6}	- 0.052	0.934	0.934	0.070	0.063
7.76	0.036	-5.0×10^{-6}	- 0.057	0.938	0.938	0.12_7	0.11_4
7.98	0.042	-5.7×10^{-6}	- 0.063	0.943	0.943	0.19_7	0.17_7
8.20	0.047	-6.4×10^{-6}	- 0.068	0.951	0.951	0.31_0	0.27_8
8.50	0.057	-7.9×10^{-6}	- 0.077	0.961	0.961	0.45_1	0.40_5
8.61	0.061	-8.4×10^{-6}	- 0.080	0.966	0.966	0.52_1	0.46_8
9.80	0.15	-2.0×10^{-5}	- 0.12	1.000 [b]	1.008 [b]	1.00	1.00

a. Absorbance at pH = 6.40 = A_{acid}.
b. Absorbance at pH = 9.80 = A_{alkali}.
c. $\underline{A_{scatter}}$ = 0.360 at pH 6.40 and 0.363 at pH 9.80 for CPG.
d. $\overline{\alpha_{ox}}$ is defined in Eq.3.26.

CPG without bound 5-P-Oxine, that the absorbance due to scattering ($A_{scatter}$) alone was independent of solution pH (see footnote c, Table 3.2). Thus, it was possible to use the change in absorbance as a function of solution pH to measure $\overline{pK'_{a2}}$ for bound 5-P-Oxine. At a fixed wavelength the absorbance, A, at any pH is given by :

$$A = [\overline{HOX}]\, b\, \varepsilon_{\overline{HOX}} + [\overline{OX^-}]\, b\, \varepsilon_{\overline{OX}} + A_{scatter} \qquad (3.22)$$

where b is the optical pathlength; and $\varepsilon_{\overline{HOX}}$ and $\varepsilon_{\overline{OX}}$ are the molar absorptivities for $\overline{HOX}$ and $[\overline{OX^-}]$ species, respectively. By measuring the absorbances A_{acid} at pH << $\overline{pK'_{a2}}$ and A_{alkali} at pH >> $\overline{pK'_{a2}}$ and combining Eq 3.22 with Eq 3.7 the following expression is obtained :

$$\frac{1}{a_H} = \frac{\exp\left(-\frac{F\psi_x}{RT}\right)}{\overline{K_{a2}}} * \frac{A - A_{acid}}{A_{alkali} - A} \qquad (3.23)$$

in which it is assumed that the phenolic group on bound 5-P-Oxine is located at a distance x cm from the charge-surface. A_{acid} was measured at pH 6.40 and A_{alkali} was measured at pH 9.80. A plot of $1/a_H$ versus ($A - A_{acid}/A_{alkali} - A$) should have a slope of $\exp(-F\psi_x/RT)/\overline{K_{a2}}$ at any pH. Such a plot for one of the duplicate runs is shown in Figure 3.7.

It can be observed in Table 3.2 that the quantity $-\Psi_o$ increases with pH. If the distance x remains constant, independent of pH, then $-\Psi_x$ should also increase with pH (Eq. 3.3) and the plot in Figure 3.7 should be curved (i.e. changing slope). However, the plot is linear with slope $(3.7 \pm 0.1) \times 10^8$ and zero intercept $(1 \pm 5) \times 10^6$, where ± indicates standard deviation, which suggests that Ψ_x is constant and independent of pH between 6.40 - 9.80. By substituting Eq. 3.7 into Eq. 3.23, the following expression is obtained :

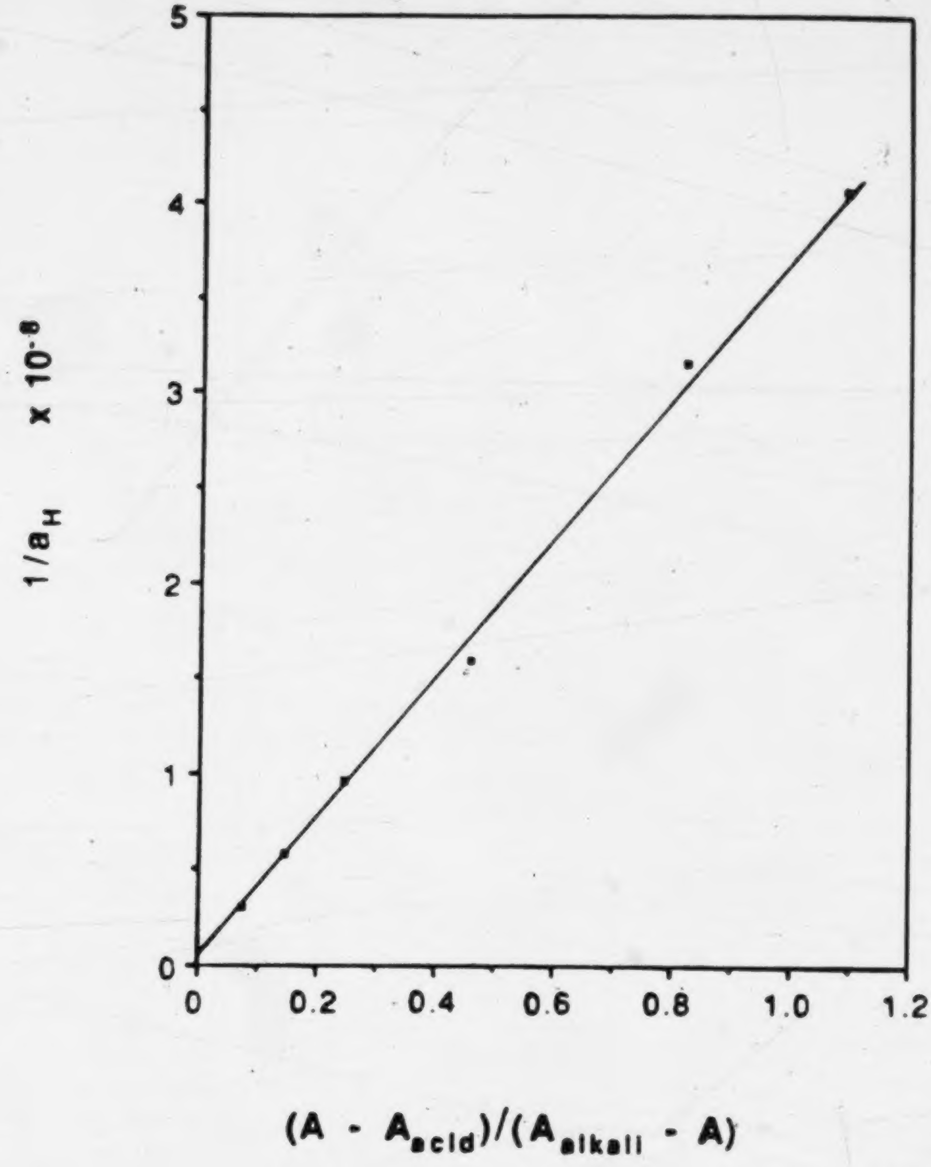

Figure 3.7 : Plot of spectrophotometric data from Run 1 for CPG-Oxine (Batch B) at c = 0.10 M according to Eq. 3.24.

$$\frac{1}{a_H} = \frac{1}{\overline{K'_{a2}}} * \frac{A - A_{acid}}{A_{alkali} - A} \qquad (3.24)$$

Therefore, the reciprocal slope of the line (Figure 3.7) is also equal to $\overline{pK'_{a2}}$ which is found to be 8.57 (Run 1). For Run 2 (Figure 3.8) the slope was $(4.6 \pm 0.1) \times 10^8$, the intercept was $(-5 \pm 7) \times 10^6$ and $\overline{pK'_{a2}}$ was 8.67.

III.4.6 MICROELECTROPHORESIS :

In an attempt to gain more understanding about the electrical properties of the interface of CPG-Oxine and electrolyte solution, microelectrophoresis was used (125,149). The zeta potential (ζ), which relates to the properties at the "surface of shear" between the moving and stationary regions of the double layer, is not equal to Ψ_X, but might be expected to change in a similar way as Ψ_X when experimental variables are changed. Zeta potential cannot be obtained directly from the electrokinetic measurements. It has to be calculated from the Smoluchowski equation (125) by measuring the electrophoretic mobility (u_E).

$$u_E = \frac{\zeta \varepsilon}{\eta} \qquad (3.25)$$

where ε is the permittivity and η is the viscosity of the solution.

The effect of pH on ζ for CPG-Oxine in 0.10 M $NaClO_4$ solution is shown in Table 3.3. Constant ζ was observed between pH 6.51 and 8.01 which suggests that Ψ_X is also independent of pH. This observation agrees with the fact that the plots observed in Figures 3.7 and 3.8 are linear as discussed above.

The probable explanation for the value of Ψ_X remaining constant even though Ψ_O

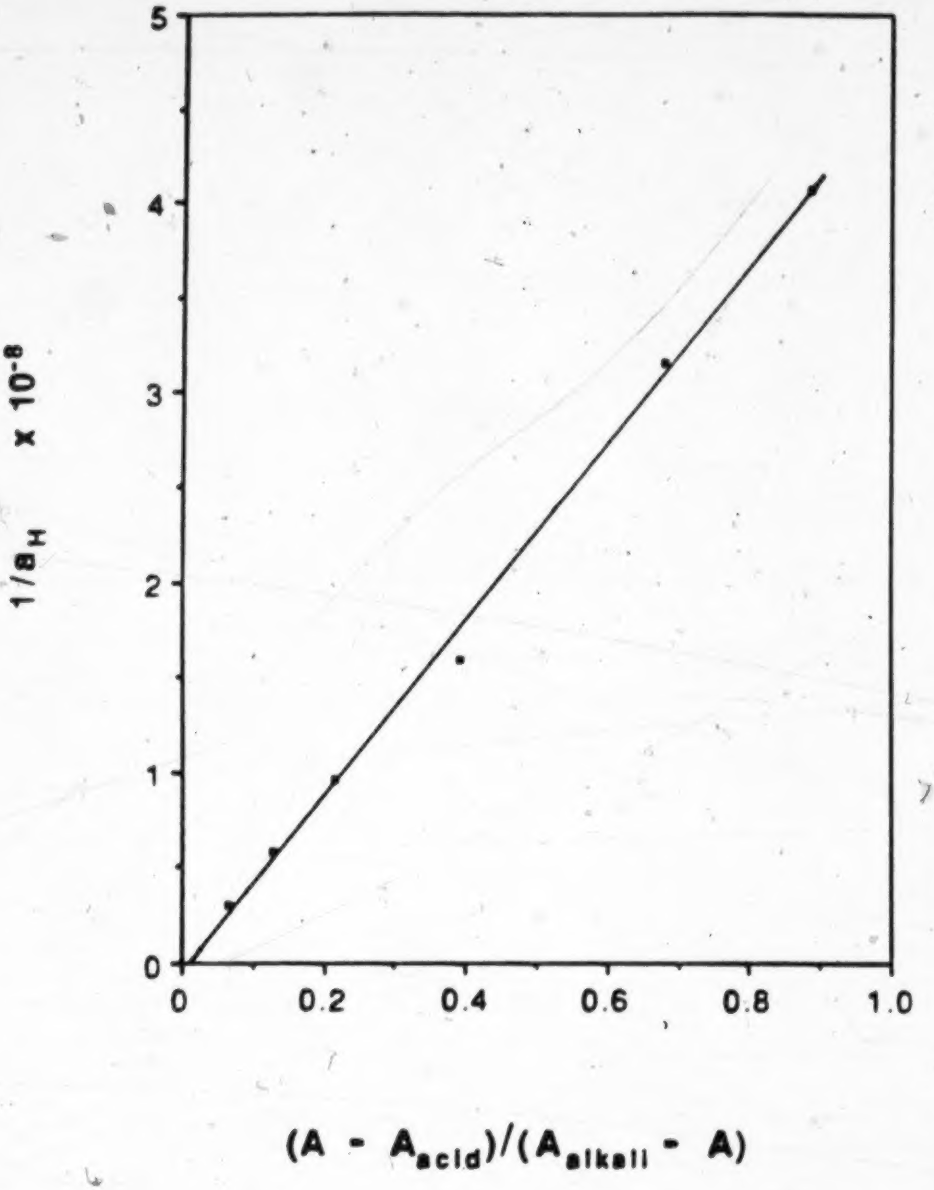

Figure 3.8 : Plot of spectrophotometric data from Run 2 for CPG-Oxine (Batch B) at c = 0.10 M according to Eq. 3.24.

Table 3.3 : Effect of pH on zeta potential at the surface of CPG-Oxine (Batch A) in c = 0.10 M NaClO$_4$.

pH	ζ
6.51	- 44 ± 7 mV
6.75	- 44 ± 7 mV
7.00	- 42 ± 8 mV
7.25	- 42 ± 6 mV
7.50	- 49 ± 8 mV
8.01	- 40 ± 8 mV

changes with pH is that x, the distance between the charge-surface and the phenol/phenolate group on bound 5-P-Oxine, increases as both σ_O and the degree of ionization of bound 5-P-Oxine ($\overline{\alpha_{OX}}$) increase. $\overline{\alpha_{OX}}$ can be calculated by combining Equations 3.15 and 3.24 to give the following expression :

$$\overline{\alpha_{OX}} = \frac{A - A_{acid}}{A_{alkali} - A_{acid}} \qquad (3.26)$$

$\overline{\alpha_{OX}}$ is the degree of ionization and can also be thought of as the fractional charge on a phenol/phenolate group. This group is located at the end of an 1.8 nm long "spacer arm" (111). When $\overline{\alpha_{OX}} \approx 0$ this hydrocarbonaceous arm is more or less folded back on itself rather than being stretched out into the water, in which it is poorly solvated (111). This places the phenol/phenolate group close to the charge-surface giving a small value of x and $\Psi_X \approx \Psi_O$. As both σ_O and $\overline{\alpha_{OX}}$ increase, due to increasing pH (Table 3.2), the electrostatic repulsion of the phenol/phenolate group by the negatively charged surface moves it farther and farther away. Thus, even though Ψ_O changes (Table 3.2), Ψ_X remains nearly constant because x increases (Eq. 3.3). Since the value of Ψ_X is not known, an accurate value of $\overline{pK_{a2}}$ cannot be calculated from $\overline{pK'_{a2}}$.

III.4.7 EFFECT OF pH ON Ca^{2+} SORPTION:

The variation of calcium sorption (as λ_O) with pH at c = 0.10 M is shown in Figure 2.13. The data are presented in the first two columns in the upper half of Table 3.4. Eq. 3.21 predicts λ_O from the site binding model. The validity of this model can be tested by plotting λ_O according to Eq. 3.21. It has been found (Section III.4.6) that Ψ_X and, consequently, $\overline{pK'_{a2}}$ remain constant at c = 0.1 M in the pH range 6.4 - 8.2, even though σ_O and Ψ_O change (columns 6 and 7 in Table 3.4). Thus with c, γ_{Ca} and Ψ_X constant it

Table 3.4 : Surface electrical properties and calcium sorption by CPG-Oxine (Batch A).

pH	λ_o (L/g)	c (M)	γ_{Ca}	Q (mmol/g)	σ_o (coul/cm^2)	ψ_o (volt)	ψ_x (volt)	$\overline{K_{a2}}$	$\overline{\alpha_{OX}}$
6.51	8.8×10^{-4}	0.10	0.354	$9.4_1 \times 10^{-3}$	-1.30×10^{-6}	-0.0176	-	2.4×10^{-9}	0.0077
6.75	1.04×10^{-3}	•	•	1.08×10^{-2}	-1.49×10^{-6}	-0.0201	-	•	0.0133
7.00	1.24×10^{-3}	•	•	1.25×10^{-2}	-1.72×10^{-6}	-0.0231	-	•	0.0234
7.25	1.48×10^{-3}	•	•	1.45×10^{-2}	-2.00×10^{-6}	-0.0265	-	•	0.0409
7.50	2.20×10^{-3}	•	•	1.73×10^{-2}	-2.39×10^{-6}	-0.0311	-	•	0.0705
7.70	3.00×10^{-3}	•	•	2.02×10^{-2}	-2.79×10^{-6}	-0.0357	-	•	0.107
7.87	4.12×10^{-3}	•	•	2.33×10^{-2}	-3.22×10^{-6}	-0.0403	-	•	0.151
8.01	4.72×10^{-3}	•	•	2.61×10^{-2}	-3.60×10^{-6}	-0.0442	-	•	0.197
7.00	1.08×10^{-2}	0.010	0.658	1.25×10^{-2}	-1.72×10^{-6}	-0.0605	-0.0566	6.65×10^{-10}	0.0066
•	5.41×10^{-3}	0.020	0.568	•	•	-0.0467	-0.0426	1.05×10^{-9}	0.0104
•	3.64×10^{-3}	0.030	0.513	•	•	-0.0396	-0.0353	1.37×10^{-9}	0.0135
•	2.40×10^{-3}	0.050	0.443	•	•	-0.0317	-0.0274	1.79×10^{-9}	0.0176
•	1.24×10^{-3}	0.10	0.354	•	•	-0.0231	-0.0188	2.40×10^{-9}	0.0234
•	7.20×10^{-4}	0.20	0.280	•	•	-0.0166	-0.0124	2.92×10^{-9}	0.0284
•	5.60×10^{-4}	0.30	0.249	1.53×10^{-2}	-2.11×10^{-6}	-0.0166	-0.0116	3.06×10^{-9}	0.0297

is predicted from Eq.3.21 that a plot of λ_o *versus* $\overline{\alpha_{OX}}$ should be a straight line with slope $\overline{\beta_1}\ \overline{\alpha_{OX}}\ \overline{v_{Oxine}}\ \gamma_{Ca} \exp(-\frac{2F\psi_x}{RT})$ and intercept k $\gamma_{Ca}\, c^{-1/2}$. Values of $\overline{\alpha_{OX}}$ are calculated from Eq. 3.15 using $\overline{K'_{a2}} = 2.4 \times 10^{-9}$ (i.e. $\overline{pK'_{a2}} = 8.62 \pm 0.07$) measured at c = 0.10 M (Section III.4.5). The values of $\overline{\alpha_{OX}}$ are shown in the last column of Table 3.4. The value of γ_{Ca} calculated *via* the Davies equation (150) :

$$- \log \gamma_{Ca} = \frac{2.046 \sqrt{c}}{1 + \sqrt{c}} - 0.4\ c \qquad (3.27)$$

and the value of Q calculated as described in Section III.4.4 are shown in column 4 and 5 of Table 3.4, respectively. The plot of λ_o *versus* $\overline{\alpha_{OX}}$ is shown in Figure 3.9. It is linear, as predicted, with slope $(2.10 \pm 0.06) \times 10^{-2}$ and intercept $(7.3 \pm 0.6) \times 10^{-4}$ L/g, where ± indicates standard deviation. The value of k is calculated from the intercept to be $(6.5 \pm 0.5) \times 10^{-4}$ L/g.

III.4.8 EFFECT OF IONIC STRENGTH ON Ca^{2+} SORPTION:

In Figure 2.14 it can be seen that λ_o decreases markedly with increasing c at pH 7.00. This behavior can also be understood in terms of the site-binding model.

At pH 7.00, $\overline{\alpha_{OX}} \leq 0.03$ so that the phenol/phenolate group of bound 5-P-Oxine should lie close to the charge-surface. The closest that it can get is the hydrated radius of the negatively charged oxygen on the phenolate group. This is estimated to be equal to the hydrated radius of an OH^- ion, about 0.2 nm (151). Eq. 3.21 can be rearranged to give :

$$\lambda_o - k\,\frac{\gamma_{Ca}}{c^{1/2}} = \overline{\beta_1}\ \overline{\alpha_{OX}}\ \overline{v_{Oxine}}\ \gamma_{Ca} \exp\left(-\frac{2F\psi_x}{RT}\right) \qquad (3.28)$$

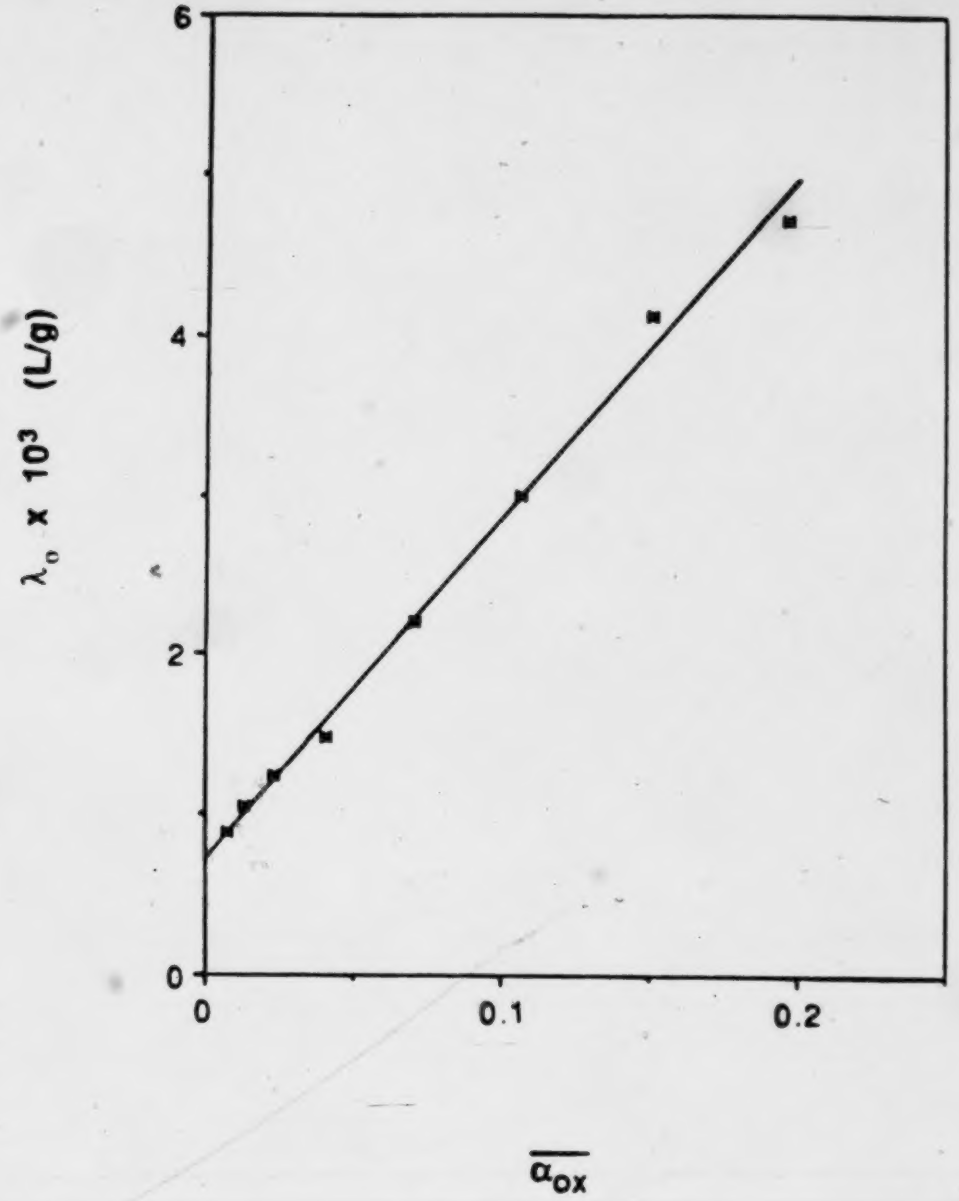

Figure 3.9 : Plot of λ_o versus $\overline{\alpha_{OX}}$ for CPG-Oxine (Batch A) at c = 0.10 M and varying pH for the data in Table 3.4.

from which it is predicted that a plot of $\lambda_0 - k\ \gamma_{Ca}\ c^{-1/2}$ versus $\overline{\alpha_{OX}}\ \gamma_{Ca}\ \exp(-\frac{2F\psi_x}{RT})$ should be linear with slope $\overline{\beta_1}\ \overline{v_{Oxine}}$ and zero intercept. For this plot values of Ψ_x are calculated from Eq. 3.3; values of Ψ_0 are calculated via the Gouy-Chapman equation (Eq. 3.1); values of σ_0 are calculated from titration curves of CPG-Oxine (Figures 3.1-3.5), obtained at the appropriate c, by computation methods previously described in Section III.4.4; and values of $\overline{\alpha_{OX}}$ are calculated from Eq. 3.15, taking into account the change in $\overline{K'_{a2}}$ with c by the following relationship :

$$(\overline{K'_{a2}})_c = 2.4 \times 10^{-9} * \frac{\exp(-\frac{F\psi_x}{RT})}{\exp(-\frac{F\psi_x}{RT})_c} \qquad (3.29)$$

All relevant quantities are presented in the lower half of Table 3.4.

The plot of Eq. 3.28, shown in Figure 3.10, is linear with slope (1.84 ± 0.03) x 10^{-2} and intercept (−1.4 ± 0.5) x 10^{-4}. The intercept is equal to zero, as predicted, within the 99% confidence limits of (−1.4 ± 2.0) x 10^{-4} (152). Dividing the slope by $\overline{v_{Oxine}}$, i.e. 3.6 μmol/g, gives $\overline{\beta_1} = 5.1 \times 10^3$ (i.e. $\log \overline{\beta_1} = 3.71$). No value of $\log \beta_1$ is available for the corresponding calcium complex with 5-phenylazo-8-hydroxyquinoline in homogenous aqueous solution. However, $\log \beta_1$ for the calcium complex with 8-hydroxyquinoline is 3.27 (94).

III.5 CONCLUSIONS :

The ionizable surface-group model can be applied to explain the acid-base behavior of CPG-Oxine. Electrical properties of the surface are obtained by applying the Gouy-Chapman theory to data obtained from capacity measurements and potentiometric titrations of CPG-Oxine. Most of the surface charge comes from residual hydroxyl

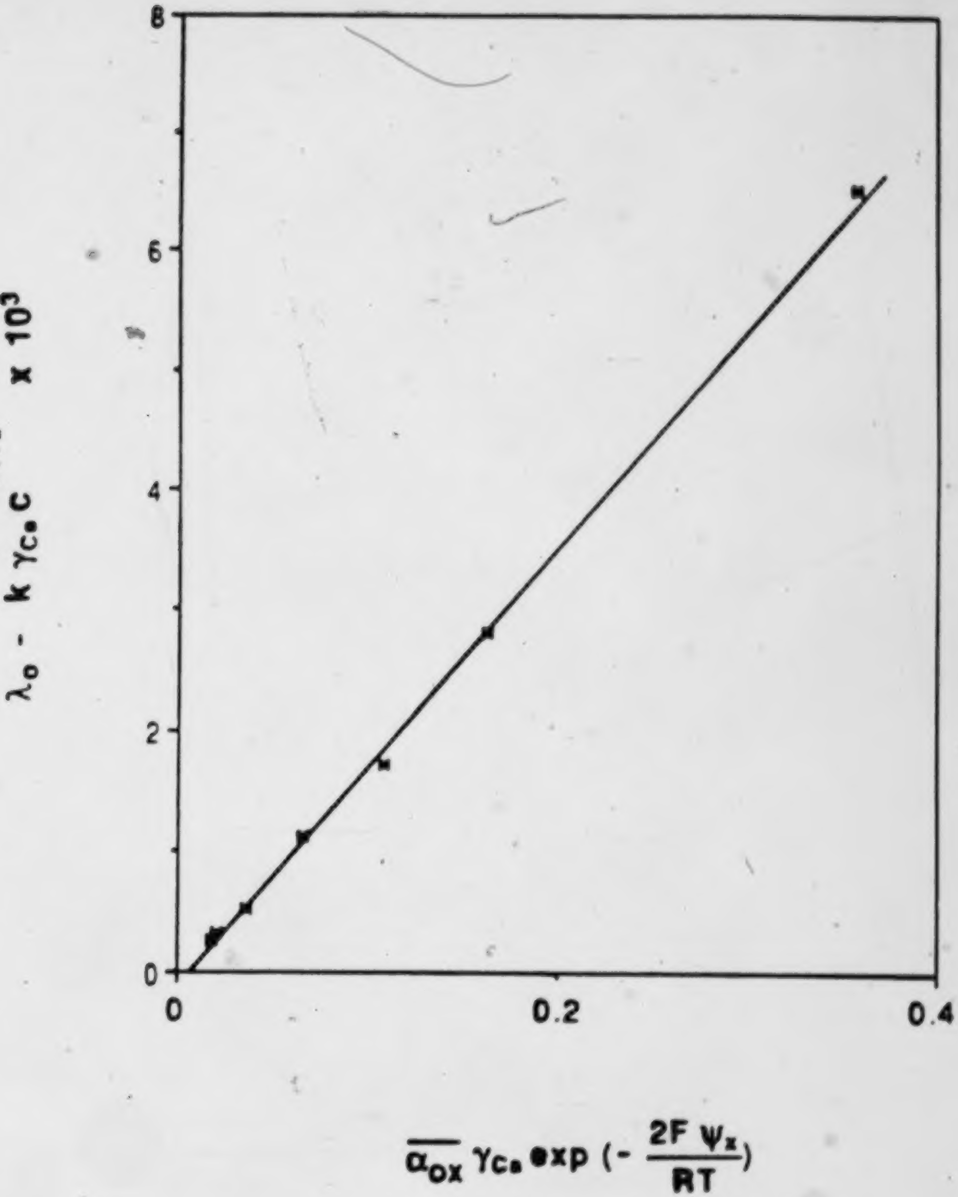

Figure 3.10 : Plot according to Eq. 3.28 for CPG-Oxine (Batch A) at pH 7.00 and varying c for the data in Table 3.4.

groups on the glass surface. Spectrophotometric measurements on the bound 5-P-Oxine give the degree of ionization of the phenolic hydroxyl group as a function of pH. The observed $\overline{pK'_{a2}}$ of 8.62 ± 0.07 for this group is independent of surface potential and is close to that reported in homogeneous aqueous solution (139,153).

The complexation of Ca^{2+} by CPG-Oxine can also be described in terms of a modification of the ionizable surface-group model to include "site-binding". The marked dependence of Ca^{2+} sorption on both pH and ionic strength is quantitatively explained. It appears that the site-binding model can serve as a basis for understanding the sorption behavior of metal ions by CPG-Oxine and for measuring stability constants involving the bound ligand.

CHAPTER FOUR

SPECIFICITY OF THE CPG-OXINE COLUMN EQUILIBRATION / AAS METHOD FOR FREE CALCIUM SPECIES DETERMINATION IN AQUEOUS SOLUTIONS

IV.1 INTRODUCTION :

Measurement of free calcium (Ca^{2+}) concentrations in biological fluids, such as serum, plasma ultrafiltrate and urine by the techniques mentioned in Section I.2.2, has produced a variety of "normal range of values" depending on the method of analysis employed (30,36,46,58,69). Of the three biological fluids, plasma ultrafiltrate is considered the easiest to work with. Free calcium can be determined by a calcium ion selective electrode (ISE) (154) since interfering factors, such as the variability of pH, sodium concentration and protein effects, are minimal in plasma ultrafiltrate. Measurement of Ca^{2+} in urine is difficult and complicated, however, by the facts that the conditions of pH, sodium concentration and ionic strength in urine vary considerably.

The cation exchange column equilibration technique has been used to measure Ca^{2+} in urine (88). The study has shown that this technique is rapid and subject to minimum interference from pH variation among samples. Unfortunately, the study also revealed that the cation exchanger was not completely selective for the Ca^{2+} species. Apparently, other calcium-containing species are also sorbed by the cation exchanger.

In a previous study Landing, et al (93) used oxine immobilized onto Fractogel TSK to obtain information on metal-containing species in ligand-containing aqueous solutions. They apparently did not use a column equilibration method and did not obtain a value for the free metal ion, but rather for "cationic", "anionic" and "particulate" species. In the present study, the specificity of CPG-Oxine is under investigation. The work involves measurements of Ca^{2+} by the column equilibration technique in aqueous solutions containing various labile calcium-ligand species. Furthermore, the limitations and difficulties of using a commercially available calcium ISE in solutions containing interfering chemicals were demonstrated and discussed.

IV.2 EXPERIMENTAL :

IV.2.1 CHEMICALS AND REAGENTS :

CPG-Oxine, batch 071982-81 (Pierce Chemical Co.) with particle size 125 - 177 μm and pore diameter 50 nm, was used for all studies. This material has previously been designated as Batch A.

All solutions were prepared with doubly distilled-deionized water. The following chemicals were used :

$CaCO_3$, HEPES, $NaClO_4$, NaOH, $HClO_4$ and HNO_3 were used for all studies, which have previously been described in Section II.2.1.

KCl and potassium hydrogen phthalate were described in Section III.3.1.

Disodium dihydrogen ethylenediaminetetraacetate, $Na_2H_2 \cdot EDTA \cdot H_2O$, 99.9% (Fisher Scientific Co.).

L-Carnosine, β-alanyl-L-histidine (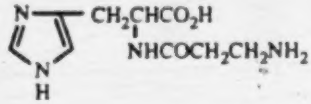), 98% (Aldrich Chemical Co.).

Picolinic acid, 2-pyridinecarboxylic acid (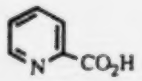), 99% (Sigma Chemical Co.).

Potassium sulfate, K_2SO_4, analytical grade (British Drug Houses).

DL-Malic acid, $HO_2CCH_2CH(OH)CO_2H$, reagent grade (American Chemical Ltd.).

Tartaric acid, $HOOC(CHOH)_2COOH$, reagent grade (Caledon Lab. Ltd.).

Citric acid, $HO_2CCH_2C(OH)(CO_2H)CH_2CO_2H$, analytical grade (British Drug Houses).

IV.2.2 APPARATUS :

The instrument used for the column equilibration experiments has been described previously in Section II.2.3. The eluted calcium was detected by either the Model 290B or the Model 4000 AAS (Perkin-Elmer Corp.). The instrumental parameters for the Model 290B and Model 400 AAS are listed in Table 4.1 and Table 2.1, respectively.

Measurement of solution pH was made with separate glass and calomel electrodes using an Accumet Model 525 digital pH meter (Fisher Scientific Co.). Potentiometric measurement of Ca^{2+} was made with an Orion Model 93-20-01 calcium ion selective electrode and a calomel electrode using the Accumet Model 525 meter in the mV mode.

IV.2.3 PREPARATION OF TEST SOLUTIONS :

Nine ligands were selected for this study. A series of test solutions were prepared at pH 7.00 and at a particular ionic strength. All ionic strengths were controlled by using $NaClO_4$, except for the studies in which the added ligands were phthalate and sulfate, where KCl was used because both ligands were prepared from their potassium salts. Each solution contained 0.010 M HEPES buffer with certain concentrations of total calcium and total ligand to give a known fraction of Ca^{2+}, α_{Ca} (155), which was calculated using ionization and stability constants reported in the literature. In each set of test solutions, a standard calcium solution was prepared similarly at the desired pH and ionic strength but without adding ligand.

For the ISE experiments, three sets of test solutions were prepared. The first set of solutions contained 0, 12.5, 25.0, 50.0, 75.0 and 100 μM Ca^{2+}, respectively, with 0.010 M HEPES at pH 7.00. Ionic strength was adjusted to 0.25 M by adding the necessary amount of $NaClO_4$. The second set of solutions contained 0.020, 0.040 and 0.14 M picolinic acid, respectively, with 0.010 M HEPES at pH 7.00 and the ionic strength was adjusted to 0.10 M $NaClO_4$. The third set of solutions contained Ca^{2+} standards prepared with 0.010 M HEPES at pH 7.00 in 0.10 M $NaClO_4$.

Table 4.1 : Instrumental conditions for measuring calcium with the Model 290B atomic absorption spectrophotometer.

Wavelength	422.7 nm
Spectral Slit Width	0.7 nm
Lamp Current	8 mA
Flame	Oxidizing (lean, blue)
Acetylene Pressure	9 psig
Air Pressure	50 psig
Aspiration Rate	6 mL/min
Pumping Flow Rate	5 mL/min
Recorder Type	Fisher, Series 5000
Voltage Range	10 mV
Chart Speed	1 cm/min

IV.2.4 DETERMINATION OF FREE CALCIUM CONCENTRATION BY THE CPG-OXINE COLUMN EQUILIBRATION METHOD :

The measurement procedures have been described previously in Section II.2.5. Two columns were used for the specificity studies described in this chapter. One of them contained 40 mg of CPG-Oxine (125 - 177 μm particle size) and the other contained 11 mg of CPG-Oxine (125 - 177 μm particle size). These were the same columns used in the studies described in Section II.3.2. When Ca^{2+} concentration was being measured in solutions containing EDTA, carnosine or picolinic acid, the 40 mg column and the Model 290B AAS were used, and loading times of only 4 min (loading flow rate was 5 mL/min) were used in the interest of speed. Although equilibrium has not been achieved in 4 min for this column, the eluted calcium peak height was found to be very reproducible. For the rest of the test solutions, the 11 mg column and the Model 4000 AAS were used and it was loaded completely to equilibrium in 4 min with a loading flow rate of 2 mL/min (Section II.3.2).

IV.3 DETERMINATION OF FREE CALCIUM CONCENTRATION BY THEORETICAL CALCULATIONS :

This subject has been discussed extensively elsewhere (155-160). Theoretical calculations of $[Ca^{2+}]$ involved in all studies were based on the conditional constant method (155,160) by calculating the equilibrium concentrations of all the calcium-ligand species using known values for total calcium and ligand concentrations and published values of the relevant calcium-ligand stability constants (β), as well as the acid dissociation constants (K_a) of ligands. In all the following calculations, hydrolysis of Ca^{2+} at pH 7.00 and all sodium-ligand complexed species were neglected because their stability constants are very small compared to all the calcium-ligand stability constants involved in the studies.

IV.3.1. Ca^{2+} - CaL^{2-} SYSTEM :

In this case, EDTA was used as the complexing ligand. The K_a values for EDTA and the β values for the major calcium-EDTA complexed species are listed in Table 4.2. In fact, CaL^{2-} is the dominant species present under the conditions investigated. Written as concentration constants, the following reactions are involved :

$$Ca^{2+} + L^{4-} \rightleftharpoons CaL^{2-} \qquad \beta'_{CaL^{2-}} = [CaL^{2-}]/[Ca^{2+}][L'] \tag{4.1}$$

$$Ca^{2+} + HL^{3-} \rightleftharpoons CaHL^{-} \qquad \beta'_{CaHL^{-}} = [CaHL^{-}]/[Ca^{2+}][L'] \tag{4.2}$$

where $\beta'_{CaL^{2-}}$ and $\beta'_{CaHL^{-}}$ are the conditional stability constants (155,160) for species CaL^{2-} and $CaHL^{-}$, respectively. $[L']$ is the total concentration of uncomplexed ligand. The total concentration of EDTA added is given by :

$$C_L = [L'] + [CaHL^{-}] + [CaL^{2-}] \tag{4.3}$$

The total concentration of Ca^{2+} added is given by :

$$C_{Ca} = [Ca^{2+}] + [CaHL^{-}] + [CaL^{2-}] \tag{4.4}$$

Combining Equations 4.3 and 4.4 gives :

$$[L'] = C_L - C_{Ca} + [Ca^{2+}] \tag{4.5}$$

The fraction α_{Ca} can be expressed as

$$\alpha_{Ca} = [Ca^{2+}]/C_{Ca} = (1 + \beta'_{CaL^{2-}}[L'] + \beta'_{CaHL^{-}}[L'])^{-1} \tag{4.6}$$

Table 4.2 : Acid dissociation and stability constants for major calcium-EDTA complexes at 25° C.

Ligand	pK_a Value	log β Value	Major Ca Species	Reference
EDTA	$pK_{a1} = 2.0 \pm 0.1$ [a]	$\log \beta_{CaL^{2-}} = 10.61 \pm 0.10$	CaL^{2-} (100%)	161
(c = 0.10 M)	$pK_{a2} = 2.68 \pm 0.02$ [a]	$\log \beta_{CaHL^{-}} = 3.18$ [b]		
	$pK_{a3} = 6.11 \pm 0.02$ [a]			
	$pK_{a4} = 10.17 \pm 0.02$ [a]			

a : Standard deviation at 20° C.

b : At 20° C.

Substituting [L'] from Eq. 4.5 into Eq. 4.6 to give :

$$\alpha_{Ca} = [Ca^{2+}]/C_{Ca} = \{1 + (\beta'_{CaL^{2-}} + \beta'_{CaHL^{-}})(C_L - C_{Ca} + [Ca^{2+}])\}^{-1} \qquad (4.7)$$

In the column equilibration technique, $[Ca^{2+}]$ must be under trace conditions so that λ_o is constant (Section II.1). When designing experiments in which solutions with a certain α_{Ca} value and, simultaneously, with a certain $[Ca^{2+}]$ value (i.e. not above the linear isotherm region) must be prepared, it is necessary to figure out how much ligand (C_L) to add. Since C_{Ca} is specified once $[Ca^{2+}]$ and α_{Ca} are specified, the desired value of C_L can be calculated by rearranging Eq. 4.7. In Table 4.3 are shown the solution compositions (C_{Ca} and C_L) required to give α_{Ca} values of about 0.1, 0.3 and 0.5, all with $[Ca^{2+}]$ about 2.50×10^{-5} M.

IV.3.2 Ca^{2+} - CaL^{+} SYSTEM :

The ligand (L) used in this study is either carnosinate or picolinate. The K_a values for carnosine and picolinic acid, and the β values for their corresponding calcium complexes, are given in Table 4.4. CaL^{+} is the only complexed species formed in this system.

$$Ca^{2+} + L^{-} \rightleftharpoons CaL^{+} \qquad \beta'_{CaL^{+}} = [CaL^{+}]/[Ca^{2+}][L'] \qquad (4.8)$$

where $\beta'_{CaL^{+}}$ is the conditional stability constant for the CaL^{+} species.The total concentration of ligand added is given by :

$$C_L = [L'] + [CaL^{+}] \qquad (4.9)$$

The total concentration of Ca^{2+} added in this case is given by :

Table 4.3 : Complexation of Ca^{2+} with EDTA at pH 7.00.

Ligand	C_L ($\underline{M}$)	C_{Ca} ($\underline{M}$)	$[Ca^{2+}]_{Calc}$ ($\underline{M}$)	α_{Ca}	c ($\underline{M}$)
EDTA	2.48×10^{-5}	5.01×10^{-5}	2.53×10^{-5}	0.50	0.10
EDTA	5.80×10^{-5}	8.39×10^{-5}	2.60×10^{-5}	0.31	0.10
EDTA	2.23×10^{-4}	2.50×10^{-4}	2.73×10^{-5}	0.11	0.10

Table 4.4 : Acid dissociation and stability constants for major calcium-carnosinate and calcium-picolinate complexes at 25° C.

Ligand	pK_a Value	log β Value	Major Ca Species	Reference
Carnosinate (c = 0.10 M)	$pK_{a1} = 6.75 \pm 0.01$ $pK_{a2} = 9.32 \pm 0.04$	$\log \beta_{CaL^+} = 3.22 \pm 0.05$	CaL^+ (100%)	162,163
Carnosinate (c = 0.25 M)	$pK_{a1} = 6.78$ [f] $pK_{a2} = 9.29$ [f]	$\log \beta_{CaL^+} = 3.11$ [f]		
Picolinate (c = 0.10 M)	$pK_{a1} = 1.03$ $pK_{a2} = 5.21 \pm 0.01$	$\log \beta_{CaL^+} = 1.81$ [a]	CaL^+ (100%)	164

a : At 20° C.

f : Calculated from c = 0.10 M to c = 0.25 M.

$$C_{Ca} = [Ca^{2+}] + [CaL^{+}] \qquad (4.10)$$

Therefore, the fraction α_{Ca} can be obtained by combining Equations 4.8, 4.9 and 4.10 to give :

$$\alpha_{Ca} = [Ca^{2+}]/C_{Ca} = \{1 + \beta'_{CaL^{+}}(C_L - C_{Ca} + [Ca^{2+}])\}^{-1} \qquad (4.11)$$

Solution compositions required to give the desired α_{Ca} and $[Ca^{2+}]$ values shown in Table 4.5 were calculated using Eq. 4.11 in a similar manner to that described for EDTA-containing solutions in the preceding section. In the carnosine-containing solutions it was necessary to add high carnosine concentrations in order to allow sufficiently low α_{Ca} values. In these solutions the concentration of the protonated cationic carnosine species was high (e.g. 0.246 $\underline{M}$ H_2L^+ in the solution with C_L = 0.684 $\underline{M}$ and α_{Ca} = 0.26 in Table 4.5). Thus, an ionic strength of 0.1 $\underline{M}$ could not be used and all of the carnosine experiments were performed at an ionic strength of 0.25 $\underline{M}$.

The ligand picolinate has a larger conditional stability constant than carnosinate so that its concentration is smaller and the experiment can be performed at c = 0.10 $\underline{M}$.

IV.3.3 Ca^{2+} - CaL SYSTEM :

In this system, the ligand represents either phthalate or sulfate. The neutral CaL complex is the only species formed in this case. The K_a values for phthalic acid and sulfuric acid, and the β values for their corresponding calcium complexes are given in Table 4.6.

$$Ca^{2+} + L^{2-} \rightleftharpoons CaL \qquad \beta'_{CaL} = [CaL]/[Ca^{2+}][L'] \qquad (4.12)$$

Table 4.5 : Complexation of Ca^{2+} with carnosinate or picolinate at pH 7.00.

Ligand	C_L ($\underline{M}$)	C_{Ca} ($\underline{M}$)	$[Ca^{2+}]_{Calc}$ ($\underline{M}$)	α_{Ca}	c ($\underline{M}$)
Carnosinate	0.108	5.00×10^{-5}	3.45×10^{-5}	0.69	0.25
Carnosinate	0.251	8.25×10^{-5}	4.03×10^{-5}	0.49	0.25
Carnosinate	0.684	1.83×10^{-4}	4.76×10^{-5}	0.26	0.25
Picolinate	0.01576	5.00×10^{-5}	2.50×10^{-5}	0.50	0.10

Table 4.6 : Acid dissociation and stability constants for major calcium-phthalate and calcium-sulfate complexes at 25° C.

Ligand	pK_a Value	log β Value	Major Ca Species	Reference
Phthalate (c = 0)	$pK_{a1} = 2.950$ $pK_{a2} = 5.408$	$\log \beta_{CaL} = 2.42 \pm 0.01$	CaL (100%)	165
Phthalate (c = 0.1 M)	$pK_{a1} = 2.75 \pm 0.02$ $pK_{a2} = 4.92 \pm 0.05$	$\log \beta_{CaL} = 1.6$	"	160,165,166
Phthalate (c = 0.3 M)	$pK_{a1} = 2.80^{d}$ $pK_{a2} = 4.96^{d}$	$\log \beta_{CaL} = 1.21^{d}$	"	
Sulfate (c = 0)	$pK_{a2} = 1.99 \pm 0.01$	$\log \beta_{CaL} = 2.30 \pm 0.01$	CaL (100%)	167,168
Sulfate (c = 0.1 M)	$pK_{a2} = 1.68^{c} \pm 0.12$	$\log \beta_{CaL} = 1.4^{e}$	"	168,169
Sulfate (c = 0.3 M)	$pK_{a2} = 1.54^{d}$	$\log \beta_{CaL} = 1.09^{d}$	"	

d : Calculated from thermodynamic constant to c = 0.3 M.
e : Calculated from thermodynamic constant to c = 0.1 M.
c : Average of the two literature values (168,169).

where β'_{CaL} is the conditional stability constant for the CaL species. The total concentration of ligand added is given by :

$$C_L = [L'] + [CaL] \qquad (4.13)$$

The total concentration of Ca^{2+} added in this case is given by :

$$C_{Ca} = [Ca^{2+}] + [CaL] \qquad (4,14)$$

Finally, α_{Ca} can be obtained by combining Equations 4.12, 4.13 and 4.14 to give :

$$\alpha_{Ca} = [Ca^{2+}]/ C_{Ca} = \{ 1 + \beta'_{CaL}(C_L - C_{Ca} + [Ca^{2+}]) \}^{-1} \qquad (4.15)$$

The values of C_{Ca} and C_L for both ligands are listed in Table 4.7. In this study, solutions of each ligand were prepared at both c = 0.10 M and 0.30 M for comparison.

IV.3.4 Ca^{2+} - CaL - $CaHL^+$ SYSTEM :

In this study, the ligand is either malate acid or tartrate. The K_a values for both acids and the β values for their corresponding calcium complexes are given in Table 4.8. Both CaL and $CaHL^+$ species are present in this system, however the majority is in the form of neutral complexes (~80%).

$$Ca^{2+} + L^{2-} \rightleftharpoons CaL \qquad \beta'_{CaL} = [CaL]/ [Ca^{2+}] [L'] \qquad (4.12)$$

$$Ca^{2+} + HL^- \rightleftharpoons CaHL^+ \qquad \beta'_{CaHL^+} = [CaHL^+]/ [Ca^{2+}] [L'] \qquad (4.16)$$

Table 4.7 : Complexation of Ca^{2+} with phthalate or sulfate at pH 7.00.

Ligand	C_L ($\underline{M}$)	C_{Ca} ($\underline{M}$)	$[Ca^{2+}]_{Calc}$ ($\underline{M}$)	α_{Ca}	c ($\underline{M}$)
Phthalate	0.0308	3.40×10^{-5}	1.54×10^{-5}	0.45	0.10
Phthalate	0.0620	3.40×10^{-5}	1.70×10^{-5}	0.50	0.30
Phthalate	0.0900	3.80×10^{-5}	1.55×10^{-5}	0.41	0.30
Sulfate	0.0150	3.40×10^{-5}	2.47×10^{-5}	0.73	0.10
Sulfate	0.0373	3.60×10^{-5}	2.47×10^{-5}	0.69	0.30
Sulfate	0.0850	5.00×10^{-5}	2.44×10^{-5}	0.49	0.30

Table 4.8 : Acid dissociation and stability constants for major calcium-malate and calcium-tartrate complexes at 25° C.

Ligand	pK_a Value	log β Value	Major Ca Species	Reference
Malate	$pK_{a1} = 3.459$	$\log \beta_{CaL} = 2.66$	CaL (~79%),	165
(c = 0)	$pK_{a2} = 5.097$	$\log \beta_{CaHL^+} = 1.06^{j}$	$CaHL^+$ (~21%)	
Malate	$pK_{a1} = 3.32^{h}$	$\log \beta_{CaL} = 1.55^{h}$	"	165
(c = 0.2 M)	$pK_{a2} = 4.68^{h}$	$\log \beta_{CaHL^+} = 0.958^{a}$		
Malate	$pK_{a1} = 3.31^{d}$	$\log \beta_{CaL} = 1.45^{d}$	"	
(c = 0.3 M)	$pK_{a2} = 4.64^{d}$	$\log \beta_{CaHL^+} = 0.907^{b}$		
Tartrate	$pK_{a1} = 3.036$	$\log \beta_{CaL} = 2.80$	CaL (~82%),	165
(c = 0)	$pK_{a2} = 4.366$		$CaHL^+$ (~18%)	
Tartrate	$pK_{a1} = 2.90^{h}$	$\log \beta_{CaL} = 1.69^{h}$	"	165
(c = 0.2 M)	$pK_{a2} = 3.95^{h}$	$\log \beta_{CaHL^+} = 1.11^{t}$		
Tartrate	$pK_{a1} = 2.89^{d}$	$\log \beta_{CaL} = 1.59^{d}$	"	
(c = 0.3 M)	$pK_{a2} = 3.91^{d}$	$\log \beta_{CaHL^+} = 1.06^{r}$		

a : Calculated from c = 0.1 M to c = 0.2 M.
b : Calculated from c = 0.1 M to c = 0.3 M.
d : Calculated from thermodynamic constant to c = 0.3 M.
h : Calculated from thermodynamic constant to c = 0.2 M.
r : Calculated from c = 0.2 M to c = 0.3 M.
j : At 20° C and c = 0.1 M.
t : Temperature not stated

where β'_{CaL} and β'_{CaHL^+} are the conditional stability constants for species CaL and $CaHL^+$, respectively. The total concentration of ligand added is given by :

$$C_L = [L'] + [CaHL^+] + [CaL] \qquad (4.17)$$

The total concentration of Ca^{2+} added is given by :

$$C_{Ca} = [Ca^{2+}] + [CaHL^+] + [CaL] \qquad (4.18)$$

Finally, α_{Ca} can be obtained by combining the above equations

$$\alpha_{Ca} = [Ca^{2+}]/C_{Ca} = \{1 + (\beta'_{CaL} + \beta'_{CaHL^+})(C_L - C_{Ca} + [Ca^{2+}])\}^{-1} \qquad (4.19)$$

The values of C_{Ca} and C_L for both ligands are listed in Table 4.9. In this study, solutions from each ligand were prepared at both c = 0.20 M and 0.30 M.

IV.3.5 Ca^{2+} - CaH_2L - $CaHL^-$ SYSTEM :

The ligand used for this study is citrate. The K_a values for citric acid and the β values for the major calcium-citrate complexes are listed in Table 4.10. The log β_{CaHL^-} value reported by Smith and Martell (165) is 3.50 at c = 0.1 M. The same value was also reported by Ringbom (160). However it was obtained at c = 0.5 M. Therefore, it was decided to use the calculated value (3.33) which has been converted from the thermodynamic value (170) to the corresponding value at c = 0.1 M. In this case, $CaHL^-$ is the dominant species (~93%).

$$Ca^{2+} + HL^{3-} \rightleftharpoons CaHL^- \qquad \beta'_{CaHL^-} = [CaHL^-]/[Ca^{2+}][L'] \qquad (4.2)$$

Table 4.9 : Complexation of Ca^{2+} with malate or tartrate at pH 7.00.

Ligand	C_L ($\underline{M}$)	C_{Ca} ($\underline{M}$)	$[Ca^{2+}]_{Calc}$ ($\underline{M}$)	α_{Ca}	c ($\underline{M}$)
Malate	9.90×10^{-3}	3.60×10^{-5}	2.50×10^{-5}	0.69	0.20
Malate	0.0225	5.00×10^{-5}	2.50×10^{-5}	0.50	0.20
Malate	0.0524	8.30×10^{-5}	2.50×10^{-5}	0.30	0.20
Malate	0.100	8.35×10^{-5}	1.81×10^{-5}	0.22	0.30
Malate	0.100	5.00×10^{-5}	1.08×10^{-5}	0.22	0.30
Malate	0.100	3.55×10^{-5}	7.70×10^{-6}	0.22	0.30
Tartrate	7.40×10^{-3}	3.60×10^{-5}	2.47×10^{-5}	0.69	0.20
Tartrate	0.0169	5.00×10^{-5}	2.45×10^{-5}	0.49	0.20
Tartrate	0.0392	8.30×10^{-5}	2.43×10^{-5}	0.29	0.20
Tartrate	0.100	8.35×10^{-5}	1.38×10^{-5}	0.16	0.30
Tartrate	0.100	5.00×10^{-5}	8.29×10^{-6}	0.17	0.30
Tartrate	0.100	3.55×10^{-5}	5.88×10^{-6}	0.17	0.30

Table 4.10 : Acid dissociation and stability constants for major calcium-citrate complexes at 25° C.

Ligand	pK_a Value	log β Value	Major Ca Species	Reference
Citrate (c = 0)	$pK_{a1} = 3.128 \pm 0.070$ $pK_{a2} = 4.761 \pm 0.002$ $pK_{a3} = 6.396 \pm 0.004$	$\log \beta_{CaHL^-} = 4.68$ $\log \beta_{CaH_2L} = 3.09$	$CaHL^-$ (~93%), CaH_2L (~7%)	165,170
Citrate (c = 0.1 M)	$pK_{a1} = 2.87 \pm 0.08$ $pK_{a2} = 4.35 \pm 0.05$ $pK_{a3} = 5.69 \pm 0.05$	$\log \beta_{CaHL^-} = 3.33$ [e] $\log \beta_{CaH_2L} = 2.19$ [e]	-	165

e : Calculated from thermodynamic constant to c = 0.1 M.

$$Ca^{2+} + H_2L^{2-} \rightleftharpoons CaH_2L \qquad \beta'_{CaH_2L} = [CaH_2L]/[Ca^{2+}][L'] \qquad (4.20)$$

where β'_{CaHL^-} and β'_{CaH_2L} are the conditional stability constants for species $CaHL^-$ and CaH_2L, respectively. The total concentration of citric acid added is given by :

$$C_L = [L'] + [CaH_2L] + [CaHL^-] \qquad (4.21)$$

The total concentration of Ca^{2+} added is given by :

$$C_{Ca} = [Ca^{2+}] + [CaH_2L] + [CaHL^-] \qquad (4.22)$$

Finally, α_{Ca} can be obtained by combining the above equations

$$\alpha_{Ca} = [Ca^{2+}]/C_{Ca} = \{1 + (\beta'_{CaHL^-} + \beta'_{CaH_2L})(C_L - C_{Ca} + [Ca^{2+}])\}^{-1} \qquad (4.23)$$

The values of C_{Ca} and C_L for both ligands are listed in Table 4.11. All solutions were prepared at c = 0.10 M.

IV.4 RESULTS AND DISCUSSION :

IV.4.1 CALCIUM ISE METHOD :

The measurement procedures were similar to the direct measurement method described in the Orion instruction manual (171), and were performed at ambient temperature (25 ± 1 °C). It is well documented that the Orion calcium ISE is subjected to interference from high Na^+ concentration (73,156) and from ClO_4^- (172,173). The calibration of the Orion 93-20-01 ISE in Ca^{2+} standards containing 0.10 M $NaClO_4$ is shown in Figure 4.1. The electrode response becomes non-linear at about 125 μM Ca^{2+},

Table 4.11 : Complexation of Ca^{2+} with citrate at pH 7.00.

Ligand	C_L ($\underline{M}$)	C_{Ca} ($\underline{M}$)	$[Ca^{2+}]_{Calc}$ ($\underline{M}$)	α_{Ca}	c ($\underline{M}$)
Citrate	3.40×10^{-4}	5.00×10^{-5}	2.94×10^{-5}	0.59	0.10
Citrate	7.90×10^{-4}	8.30×10^{-5}	3.18×10^{-5}	0.38	0.10
Citrate	0.0100	8.35×10^{-5}	3.68×10^{-6}	0.04	0.10
Citrate	0.0100	5.00×10^{-5}	2.20×10^{-6}	0.04	0.10

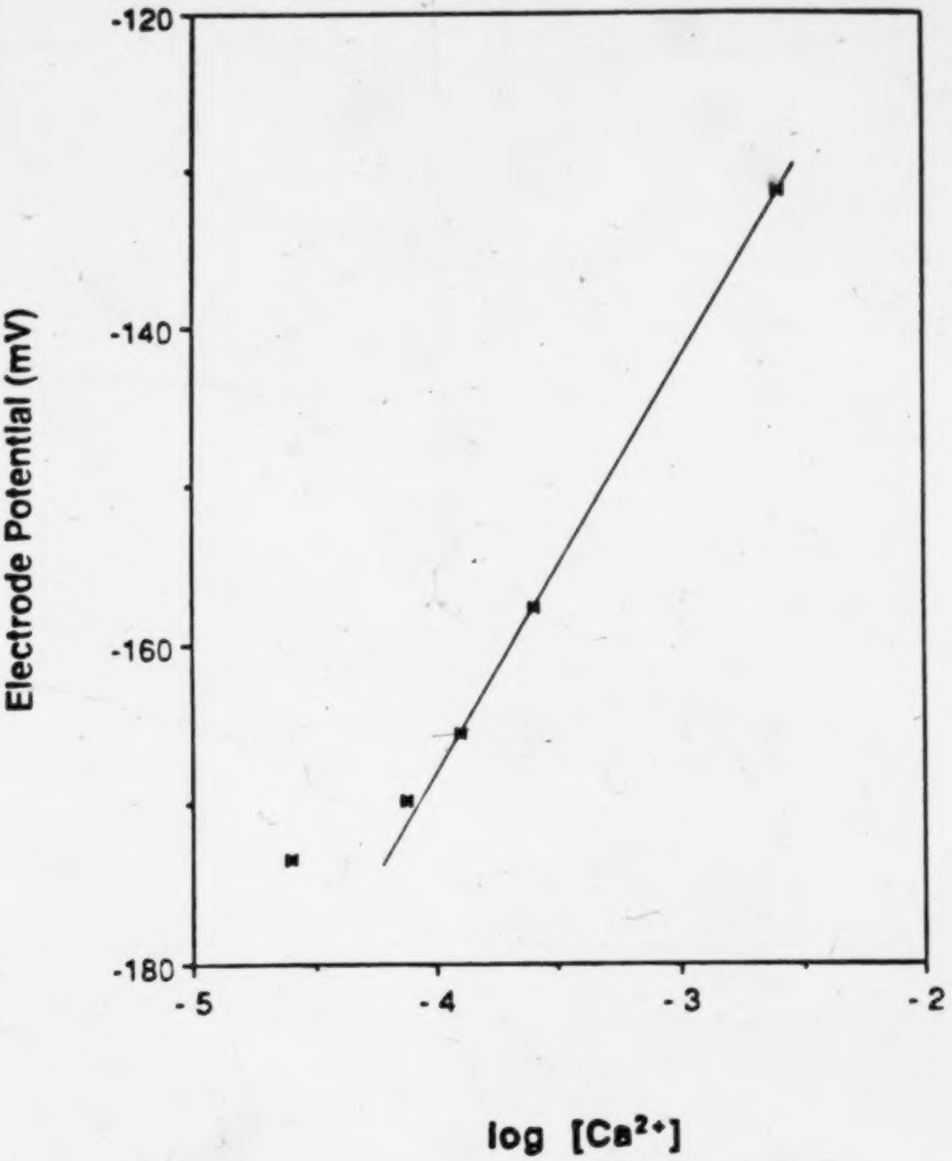

Figure 4.1 : Calibration of the Orion 93-20 calcium ion-selective electrode for Ca^{2+} in 0.10 M $NaClO_4$ (pH 7.00) at 25 ± 1° C.

which is rather poor compared to the manufacturer's value of about 10 μM in pure $CaCl_2$ solutions (171). The interference is even worse in 0.25 M $NaClO_4$, as shown in Table 4.12. When the electrode was calibrated with Ca^{2+} standards containing 0.25 M $NaClO_4$, the potential readings did not change with changing Ca^{2+} concentration. Furthermore, the electrode response drifted and was very sluggish during the measurements in 0.25 M $NaClO_4$. It has been suggested that the interference of high $NaClO_4$ concentration is probably due to its effect on the liquid junction potential (69,74,75) and to salt extraction into the electrode membrane (30,172,174).

Although $[Ca^{2+}]$ measurements by the ISE method have been made in the presence of various ligands, such as EDTA anion (175), phthalate (176), sulfate (177), malate and citrate (173,178), studies of interferences by some naturally occurring organic compounds on the response of Orion 92-20 calcium ISE (174) have shown that phthalate can cause a negative shift in the observed potential readings. Furthermore, in the presence of picolinic acid (Table 4.13) a positive shift in the observed mV readings has been observed for the Orion 93-20-01 calcium ISE, i.e. an apparent increase in the calcium ion activity. Similar behavior has also been reported previously (77) for pyridine and 2-picoline. The interference of organic ligand is probably due to the interaction between the ligand and ion exchange solution in the electrode (174).

The application of commercially available calcium ISE for measuring $[Ca^{2+}]$ is obviously limited to samples which contain low Na^+ concentration and no interfering organic compounds. Furthermore, $NaClO_4$ cannot be used for the purpose of ionic strength adjustment in this kind of measurement. The sorption isotherm for Ca^{2+} on CPG-Oxine under the same conditions (Figure A.2) is non-linear above about 25 μM and the column equilibration has to be performed in the linear region. Because of the interference of ligands and $NaClO_4$ in the ISE measurement of Ca^{2+} at such low concentrations, no attempt was made to measure $[Ca^{2+}]$ by the ISE method in the solutions used for column equilibration measurements.

Table 4.12 : Calibration of the Orion 93-20 calcium ion-selective electrode for Ca^{2+} in 0.25 M $NaClO_4$ (pH 7.00) at 25 ± 1° C.

$[Ca^{2+}]$	Electrode Potential
12.5 uM	- 164.4 mV
25.0 uM	- 164.3 mV
50.0 uM	- 164.0 mV
75.0 uM	- 163.6 mV
100 uM	- 165.9 mV

Table 4.13 : Response of the Orion 93-20 calcium ion-selective electrode in various concentrations of picolinic acid containing 0.10 M $NaClO_4$ at 25 ± 1° C.

Conc. of Picolinic Acid	Electrode Potential
Blank	- 175.5 mV
0.01 M	- 172.3 mV
0.02 M	- 170.1 mV
0.03 M	- 168.0 mV

IV.4.2 COLUMN EQUILIBRATION METHOD :

A sulfonated cation exchanger has been used for the column equilibration method (19,22,88). In principle, it is desirable that the cation exchanger should selectively sorb only free metal ion but not sorb any of its complexes. However, studies have shown that in fact this condition is met when only negatively charged complexed species of the metal ion are present. It is not met in the presence of positively charged and neutral species (22,88).

In this study, specificity of CPG-Oxine for Ca^{2+}, by using the column equilibration method, was tested in the same manner as described for the cation exchanger (19,22). Solutions containing Ca^{2+} and added ligand were prepared at pH 7.00 to contain various α_{Ca} in a particular ionic strength, and were subjected to the column equilibration experiment. All $[Ca^{2+}]$ were expressed in terms of pCa, i.e. the negative logarithm of $[Ca^{2+}]$, because it is commonly used for studies involving complexation equilibria (155,160) and metal speciation (159). The "calculated" pCa values were obtained by the theoretical calculations described in Section IV.3. The reliability of these calculated values can be determined via propagation of error methods, or predicted via the Stolzberg approach (159) which suggested that for the most favorable systems, such as calcium-EDTA where the competitive reactions are unimportant, the expected uncertainty of pCa will be less than 0.1 pCa unit. In other cases where weak complexes are formed, the uncertainties of pCa will be expected to be 0.2 - 1.0 pCa units.

IV.4.2.1 DETERMINATION OF Ca^{2+} IN THE PRESENCE OF CaL^{2-} COMPLEX :

EDTA was used as an added ligand in this study because it forms only the negatively charged complex CaL^{2-} which has a conditional constant (β') of 2.5×10^7 at pH 7.00 and c = 0.1 M (161). The EDTA-containing solutions were prepared at c = 0.10 M to obtain $\alpha_{Ca} = 0.5$, 0.3 and 0.1, i.e. about 50, 30 and 10% of the total dissolved calcium as Ca^{2+} (Table 4.3). Results in Table 4.14 show that agreement between calculated and measured pCa is within the 95% confidence limits. This indicates that CPG-Oxine is selective for Ca^{2+} in the presence of negatively charged species, as is also true for a cation exchanger.

IV.4.2.2 DETERMINATION OF Ca^{2+} IN THE PRESENCE OF CaL^+ COMPLEX :

The dipeptide anion carnosinate and the picolinate anion were used as ligands in this case as they both form the positively charged complex CaL^+ which has a β' value of 4.1 for carnosine at pH 7.00 and c = 0.25 M (162,163), and 63.5 for picolinic acid at pH 7.00 and c = 0.1 M (165). The carnosine-containing solutions were prepared at c = 0.25 M to have about 70, 50 and 30% of the calcium as Ca^{2+} (Table 4.5). On the other hand, the picolinate-containing solutions were prepared at c = 0.10 M to have about 50% Ca^{2+}. The results (Table 4.15) demonstrate that the calculated pCa for both ligands is within the 95% confidence limits of the measured value, suggesting that CPG-Oxine is also selective for Ca^{2+} in the presence of postively charged calcium complexes. The uncertainties of the calculated values of pCa arise from the uncertainties in pK_a and log β values reported at c = 0.1 M and in the calculated activity coefficients that were used to correct these constants to their corresponding values at c = 0.25 M.

IV.4.2.3 DETERMINATION OF Ca^{2+} IN THE PRESENCE OF CaL COMPLEX :

With phthalate and sulfate as ligands, at pH 7.00 the calcium complexes were present as neutral CaL. The phthalate complex has values of β' of 40 and 16 at c = 0.1 and 0.3 M (160,165,166), respectively. For the sulfate complex the β' values are 25 and 12 at c = 0.1 and 0.3 M (167-169), respectively. The solutions for both ligands were prepared at pH 7.00 to contain various α_{Ca}, as indicated in Table 4.7, in either c = 0.10 or 0.30 M. The results in Table 4.16 show that the calculated pCa for both ligands is within the 95%

Table 4.14 : Specificity of CPG-Oxine for Ca^{2+} in the presence of CaL^{2-} species.

Ligand	α_{Ca}	$[Ca^{2+}]_{Calc}$ ($\underline{M}$)	pCa Calculated	$[Ca^{2+}]_{Meas}$ ($\underline{M}$)	pCa Measured
EDTA (c=0.10$\underline{M}$)	0.50	2.53×10^{-5}	4.60 ± 0.00	2.90×10^{-5}	4.54 ± 0.18
EDTA (c=0.10$\underline{M}$)	0.31	2.60×10^{-5}	4.58 ± 0.00	2.98×10^{-5}	4.53 ± 0.09
EDTA (c=0.10$\underline{M}$)	0.11	2.73×10^{-5}	4.56 ± 0.00	3.17×10^{-5}	4.50 ± 0.09

Table 4.15 : Specificity of CPG-Oxine for Ca^{2+} in the presence of CaL^+ species.

Ligand	α_{Ca}	$[Ca^{2+}]_{Calc}$ ($\underline{M}$)	pCa Calculated	$[Ca^{2+}]_{Meas}$ ($\underline{M}$)	pCa Measured
Carnosine (c=0.25$\underline{M}$)	0.69	3.45×10^{-5}	4.46 ± 0.04	2.26×10^{-5}	4.64 ± 0.45
Carnosine (c=0.25$\underline{M}$)	0.49	4.03×10^{-5}	4.39 ± 0.06	2.15×10^{-5}	4.67 ± 0.45
Carnosine (c=0.25$\underline{M}$)	0.26	4.76×10^{-5}	4.32 ± 0.10	3.18×10^{-5}	4.50 ± 0.36
Picolinate (c=0.10$\underline{M}$)	0.50	2.50×10^{-5}	4.60 ± 0.01	3.12×10^{-5}	4.51 ± 0.18

confidence limits of the measured value, suggesting that CPG-Oxine is selective for Ca^{2+} in the presence of neutral calcium complexes as well. The uncertainties of the calculated values of pCa in this case arise from the uncertainties in pK_a and log β values reported at both c = 0 and 0.1 M, and in the calculated activity coefficients that were used to correct the thermodynamic constants to their corresponding values at c = 0.3 M.

IV.4.2.4 DETERMINATION OF Ca^{2+} IN THE PRESENCE OF BOTH CaL AND $CaHL^+$ COMPLEXES :

Malic acid and tartaric acid were used as ligands which form significant amounts of both neutral and cationic complexes with calcium at pH 7.00. The β'_{CaL} and β'_{CaHL^+} values for malate at c = 0.2 M are 1.54 and 4.78 x 10^{-3}, respectively (165); and for tartrate at c = 0.2 M are 1.69 and 1.11 x 10^{-3}, respectively (165). The solutions for both ligands were prepared at pH 7.00 to contain various α_{Ca}, as indicated in Table 4.9, in either c = 0.20 or 0.30 M. The results in Table 4.17 show that the calculated pCa for both ligands is within the 95% confidence limits of the measured value. It is further confirmed that CPG-Oxine is selective for Ca^{2+} in the presence of complexed species which contain about 79% CaL and 21% $CaHL^+$. The uncertainties of the calculated values of pCa in this case arise mainly from the uncertainties in the calculated activity coefficients that were used to correct both K_a and β at either c = 0 or 0.1 M to their corresponding values at c = 0.2 or 0.3 M.

IV.4.2.5 DETERMINATION OF Ca^{2+} IN THE PRESENCE OF BOTH $CaHL^-$ AND CaH_2L COMPLEXES :

With citric acid as a ligand at pH 7.00, the negatively charged species ($CaHL^-$) is the dominant complex. It has a β'_{CaHL^-} value of 2.0 x 10^3 and a rather small β'_{CaH_2L} value of 7.3 at pH 7.00 and c = 0.1 M (165,170). The citrate-containing solutions were prepared at c = 0.10 M to have about 60, 40 and 4% of Ca^{2+} (Table 4.11). The results in Table 4.18 show that the agreement between calculated pCa and measured pCa is generally within the

Table 4.16 : Specificity of CPG-Oxine for Ca^{2+} in the presence of CaL species.

Ligand	α_{Ca}	$[Ca^{2+}]_{Calc}$ (M)	pCa Calculated	$[Ca^{2+}]_{Meas}$ (M)	pCa Measured
Phthalate (c=0.10M)	0.45	1.54×10^{-5}	4.81 ± 0.05	1.25×10^{-5}	4.90 ± 0.18
Phthalate (c=0.30M)	0.50	1.70×10^{-5}	4.77 ± 0.12	4.66×10^{-6}	5.33 ± 0.36
Phthalate (c=0.30M)	0.41	1.55×10^{-5}	4.81 ± 0.12	3.92×10^{-6}	5.41 ± 0.36
Sulfate (c=0.10M)	0.73	2.47×10^{-5}	4.61 ± 0.05	2.79×10^{-5}	4.55 ± 0.18
Sulfate (c=0.30M)	0.69	2.47×10^{-5}	4.61 ± 0.10	2.78×10^{-5}	4.56 ± 0.09
Sulfate (c=0.30M)	0.49	2.44×10^{-5}	4.61 ± 0.10	3.89×10^{-5}	4.41 ± 0.09

Table 4.17 : Specificity of CPG-Oxine for Ca^{2+} in the presence of CaL + $CaHL^+$ species.

Ligand	α_{Ca}	$[Ca^{2+}]_{Calc}$ (M)	pCa Calculated	$[Ca^{2+}]_{Meas}$ (M)	pCa Measured
Malate (c=0.20)	0.69	2.50×10^{-5}	4.60 ± 0.09	2.60×10^{-5}	4.58 ± 0.18
Malate (c=0.20)	0.50	2.50×10^{-5}	4.60 ± 0.09	2.76×10^{-5}	4.56 ± 0.27
Malate (c=0.20)	0.30	2.50×10^{-5}	4.60 ± 0.09	2.86×10^{-5}	4.54 ± 0.27
Malate (c=0.30)	0.22	1.81×10^{-5}	4.74 ± 0.15	2.16×10^{-5}	4.66 ± 0.36
Malate (c=0.30)	0.22	1.08×10^{-5}	4.97 ± 0.15	1.25×10^{-5}	4.90 ± 0.54
Malate (c=0.30)	0.22	7.70×10^{-6}	5.11 ± 0.15	1.02×10^{-5}	4.99 ± 0.45

Table 4.17 : Specificity of CPG-Oxine for Ca^{2+} in the presence of CaL + $CaHL^+$ species (continued).

Ligand	α_{Ca}	$[Ca^{2+}]_{Calc}$ ($\underline{M}$)	pCa Calculated	$[Ca^{2+}]_{Meas}$ ($\underline{M}$)	pCa Measured
Tartrate (c=0.20)	0.69	2.47×10^{-5}	4.61 ± 0.09	2.76×10^{-5}	4.56 ± 0.27
Tartrate (c=0.20)	0.49	2.45×10^{-5}	4.61 ± 0.09	3.07×10^{-5}	4.51 ± 0.18
Tartrate (c=0.20)	0.29	2.43×10^{-5}	4.61 ± 0.09	3.18×10^{-5}	4.50 ± 0.18
Tartrate (c=0.30)	0.16	1.38×10^{-5}	4.86 ± 0.17	2.16×10^{-5}	4.66 ± 0.36
Tartrate (c=0.30)	0.17	8.29×10^{-6}	5.08 ± 0.17	1.36×10^{-5}	4.87 ± 0.36
Tartrate (c=0.30)	0.17	5.88×10^{-6}	5.23 ± 0.17	1.14×10^{-5}	4.94 ± 0.54

Table 4.18 : Specificity of CPG-Oxine for Ca^{2+} in the presence of CaH_2L + $CaHL^-$ species.

Ligand	α_{Ca}	$[Ca^{2+}]_{Calc}$ (M)	pCa Calculated	$[Ca^{2+}]_{Meas}$ (M)	pCa Measured
Citrate (c=0.10M)	0.59	2.94×10^{-5}	4.53 ± 0.10	3.17×10^{-5}	4.50 ± 0.09
Citrate (c=0.10M)	0.38	3.18×10^{-5}	4.50 ± 0.10	3.71×10^{-5}	4.43 ± 0.18
Citrate (c=0.10M)	0.04	3.68×10^{-6}	5.43 ± 0.10	1.62×10^{-5}	4.79 ± 0.27
Citrate (c=0.10M)	0.04	2.20×10^{-6}	5.66 ± 0.10	1.08×10^{-5}	4.97 ± 0.18

95% confidence limits, although there are some discrepancies at $\alpha_{Ca} = 0.04$. Possible reasons for the high experimental values of $[Ca^{2+}]$ at very low α_{Ca} (e.g. $\alpha_{Ca} = 0.04$) are calcium impurities in the citric acid and partial dissociation of the calcium-citrate complex in the pores of the CPG-Oxine during the water washing step. Nevertheless, it is again suggested that CPG-Oxine is selective for Ca^{2+} in the presence of both negatively charged and neutral species. The uncertainties of the calculated values of pCa arise mainly from the uncertainties in pK_a values reported at c = 0.1 M and in the calculated activity coefficients that were used to convert the thermodynamic constants of β to their corresponding values at c = 0.1 M.

IV.5 CONCLUSIONS :

Although calcium ion-selective electrodes have been used for a long time for measuring Ca^{2+} in biological fluids, there is increasing recognition of the limitations and problems relating to the calibration of the electrodes in complex mixtures, such as biological fluids, due to variations in ionic strength, interferences of biochemicals, and consequent difficulties in matching standards to samples. Obviously, questions concerning the clinical and medical uses of these electrodes for accurate and effective Ca^{2+} measurements still remain. It appears that the development of an accurate method to measure Ca^{2+} in biological fluids is necessary and challenging.

The use of CPG-Oxine as a sorbent in this study has proved to be more selective than the conventional cation exchanger (22,88) for measuring free metal ion concentrations by the column equilibration method, in the presence of metal-ligand complexed species. Clearly, further studies employing immobilized ligands in the column equilibration method for free metal ion determination are justified.

CHAPTER FIVE

FEASIBILITY STUDIES OF MEASURING FREE CALCIUM IN REAL SAMPLES BY THE CPG-OXINE COLUMN EQUILIBRATION METHOD :

V.1 INTRODUCTION :

At present determinations of [Ca^{2+}] are frequently done by using the calcium ISE and indicator methods, particularly in the field of biomedical and clinical analysis, even though they are still subject to interference and sensitivity problems. This is because these methods allow measurements for both extracellular and intracellular Ca^{2+} activities. Although the ion-exchange column equilibration method can provide sufficient sensitivity to measure intracellular [Ca^{2+}] from 10^{-5} M to 10^{-8} M, it is probably more practical for measuring [Ca^{2+}] in bulk body fluids, such as urine, because it requires a large sample volume in order to equilibrate the column.

The ion-exchange column equilibration method has been used to determine [Ca^{2+}] in urine (88). However, it was found that the method is not specific for Ca^{2+} and required the addition of a very high concentration of swamping electrolyte in order to obtain a trace loading condition for Ca^{2+} on the sulfonated ion-exchange resin. Unfortunately, increasing ionic strength can reduce the activities of ions, by decreasing the mean activity coefficient (127), which can change the complexation behavior between Ca^{2+} and the ligands in urine, and consequently, perturb all equilibria in the system to a considerable extent: Furthermore, complexation or ion-pair formation between Ca^{2+} and the anion of the electrolyte can also be a serious problem at high electrolyte concentrations because of the decreased activity of the Ca^{2+} species.

In this chapter, studies of the possibilities of using the CPG-Oxine column equilibration / AAS method to determine [Ca^{2+}] in urine and wine samples are reported.

V.2 LIMITATIONS ON THE CPG-OXINE COLUMN EQUILIBRATION METHOD :

Although the use of CPG-Oxine in conjunction with the column equilibration technique has shown better selectivity and more reliable measurements of [Ca^{2+}] than the cation exchanger, there are two major limitations for using CPG-Oxine in the column equilibration technique :

a) The sample volume requirement. It has been shown (Section II.3.2) that about 8 mL of sample was required to equilibrate a 1 cm column. Therefore, it is not practical to apply this technique to samples for which there is a limited supply, such as blood, plasma and intracellular fluids.

b) The trace loading conditions for CPG-Oxine. Measurement of [Ca^{2+}] by the column equilibration method is based on a trace loading condition at which λ_0 is constant. Therefore, in order to use CPG-Oxine as sorbent the [Ca^{2+}] in samples must not be too high (Section II.1). The typical [Ca^{2+}] for blood, serum and urine is between 0.4 and 4 mM (30,36,46,58,69). For intracellular fluids it is between 0.01 μM and 0.1 mM (51,69). In most natural waters, the [Ca^{2+}] is in the range of 0.7 - 10 mM (179-181). In order to use the method on any of these samples trace loading of CPG-Oxine must not be exceeded by solution concentrations of Ca^{2+} in the appropriate ranges.

The normal ionic strength of urine is variable. Typical concentrations for Na^+ and K^+ are 120 - 220 mM and 35 - 80 mM, respectively (69); which contribute to the total ionic strength estimated between 0.08 and 0.15 M with an average of about 0.1 M. The pH of urine is usually between 4.6 and 8 with an average of about 6.0 (182). The studies on sorption isotherms (Section II.3.4.1) have revealed that at normal urinary pH and ionic strength, λ_0 for Ca^{2+} on CPG-Oxine is constant for [Ca^{2+}] below about 0.1 mM (Table 2.5). Obviously, the [Ca^{2+}] for typical urine samples (> 0.5 mM) exceeds the trace loading condition of the CPG-Oxine column equilibration method. Analysis of [Ca^{2+}] for such samples may be possible by measuring $[Ca^{2+}]$ in diluted samples, and then extrapolating to the $[Ca^{2+}]$ in the undiluted sample. Dilution of the urine sample will cause shifting of the natural equilibria in urine and may introduce a determinate error that is not compensated by extrapolation. The magnitude of this error is expected to be influenced by the extent of Ca^{2+} (or species) buffering (83) in the original sample. The effect of dilution on the degree of Ca^{2+} buffering is discussed in this chapter and the possibility of determining $[Ca^{2+}]$ in urine by using dilution is investigated.

V.3 DETERMINATION OF $[Ca^{2+}]$ BY THE DILUTION METHOD :

V.3.1 EXPERIMENTAL :

V.3.1.1 CHEMICALS AND REAGENTS :

The following chemicals were used in this study :

CPG-Oxine (Pierce Chemical Co.) was packed into a 1 cm column which had previously been used for the studies in Chapters Two and Four; $CaCO_3$, HEPES, $NaClO_4$ and KCl, HNO_3, NaOH, $HClO_4$ were as described in Chapter Two. Lanthanum chloride, $LaCl_3 \cdot 7H_2O$ (British Drug Houses) was reagent grade. All solutions were prepared with doubly distilled-deionized water.

V.3.1.2 APPARATUS :

The operating system used for the column equilibration experiment has previously been described in Section II.2.3. The Model 4000 AAS (Perkin-Elmer) was used. The instrumental parameters are listed in Table 2.1, but the pumping flow rate used in the loading step was about 2 mL/min.

pH measurements were made with separate glass and calomel electrodes using an Accumet Model 525 digital pH meter (Fisher Scientific).

V.3.1.3 SAMPLES :

Four urine samples from one individual were collected on four different days. Their pH values were 5.88, 5.92, 5.78 and 6.13, at 37 °C.

A white wine sample, California chablis blanc white wine (Ernest and Julio Gallo) with pH 3.3, was also used in this study. Unlike the situation for urine, no values of [Ca^{2+}] have previously been reported for wine.

V.3.1.4 PREPARATION OF DILUTED SAMPLES AND Ca^{2+} STANDARD SOLUTIONS :

An urine sample was collected and the nominal pH, which is referred to as the pH at human body temperature (37 °C), was taken immediately. After the sample had stood for about 15 min at room temperature, it was diluted with 0.10 M $NaClO_4$ containing 0.010 M HEPES to obtain various dilution factors, and the pH of each diluted sample was adjusted to match the nominal pH value. The consequences of temperature change were ignored.

Ca^{2+} standard solutions containing 0.010 M HEPES were also prepared in 0.10 M $NaClO_4$ with the same nominal pH value as each urine sample.

Diluted urine samples and corresponding Ca^{2+} standard solutions were prepared similarly, except KCl was used to adjust the ionic strength since K^+ is the major cation (about 0.02 M) in the Calfornia white wines (183,184). Also no HEPES buffer was added to the solutions because the pH value for the wine was outside the effective buffer range of HEPES.

V.3.1.5 DETERMINATION OF TOTAL CALCIUM :

Measurements of total calcium (C_{Ca})in urine and wine samples were done by AAS (184-186). The urine and wine samples were diluted 50 times with 1% $LaCl_3$ to insure that concentrations were within a suitable absorbance range. Calcium standards were also prepared in 1% $LaCl_3$, and the lanthanum diluent was used as a blank. The $LaCl_3$ was included to eliminate phosphate interference.

V.3.1.6 DETERMINATION OF COLUMN LOADING TIME FOR URINE :

Diluted urine samples at pH 5.78 were prepared with dilution factors of 50, 100 and 200 times in 0.10 M $NaClO_4$ containing 0.010 M HEPES. These diluted samples were used for the column loading experiments with loading times of 2, 5, 10, 30 and 60 min, as previously described in Section II.3.2. They were not filtered before used.

In order to see if filtration is required, an undiluted urine sample was filtered through a 0.45 μm pore size membrane filter (Ultipor N66). The filtered urine was diluted 50 times in 0.10 M $NaClO_4$ containing 0.010 M HEPES at pH 5.92. A portion of the original unfiltered urine was similarly diluted to prepare another solution. These two diluted samples were used for the column loading experiments.

V.3.1.7 DETERMINATION OF [Ca^{2+}] BY THE COLUMN EQUILIBRATION METHOD :

The measurement procedures have previously been described in Section II.2.5. Four minutes loading time was used for all Ca^{2+} standard solutions because previously it has been observed that this column reached equilibrium in less than 4 min even at pH 7.00 and c = 0.10 M (Figure 2.12).

V.3.2 RESULTS AND DISCUSSION :

V.3.2.1 TOTAL CALCIUM :

The concentrations of total calcium in the urine and wine samples are presented in Table 5.1. The calcium content in urine was found to vary with pH and between samples. If about 50% of the total calcium in urine was present as Ca^{2+} (47), then it would be

Table 5.1 : Total calcium content in urine and wine samples.

Sample	Total Calcium
Urine (pH 5.78)	4.11 (± 0.07) mM
Urine (pH 5.92)	1.15 (± 0.04) mM
Urine (pH 5.88)	6.05 (± 0.07) mM
Urine (pH 6.13)	2.40 (± 0.04) mM
Wine (pH 3.30)	2.14 (± 0.06) mM

expected that [Ca^{2+}] in these urine samples would be in the range of 0.5 - 3 mM. Although there is no literature value for [Ca^{2+}] in wine, it might be expected that α_{Ca} would be large at the low pH of about 3. Therefore, as predicted, both urine and wine have [Ca^{2+}] too high to be determined directly by the CPG-Oxine column equilibration method.

V.3.2.2 LOADING STUDY FOR DILUTED URINE SAMPLES :

In Chapter Two it was shown that a 4 min loading time was more than enough to equilibrate Ca^{2+}-containing solutions with the 11 mg CPG-Oxine column. Because urine may contain particulate and colloidal matter, the loading study was repeated for diluted urine samples. The results in Table 5.2 show that when the unfiltered urine sample is diluted ≥ 100 fold the loading time required to achieve equilibrium is the same as that for Ca^{2+} standards. However, samples diluted ≤ 50 fold are not yet equilibrated in 60 min. The loading curve for the sample diluted 50 fold is given in Figure 5.1. This effect is probably due to the presence of crystals (187) or colloidal particles in the urine. Some of the urine samples were cloudy, especially after refrigeration. The fact that the peak height continues to increase, though slowly at longer loading times in Figure 5.1 suggests that the particles containing calcium were being "filtered" out of the solution by the column. Similar behavior has previously been observed when loading solutions containing filterable, colloidal complexed species to a cation exchange column (22).

In order to determine whether the calcium-containing particles can be removed from urine by filtration, loading curves were obtained for two portions of the same urine solution, one filtered and one unfiltered, after 50 fold dilution. The loading curves, which are shown in Figures 5.2 and 5.3 are nearly identical. Even the filtered sample is not equilibrated after 50 min. Although typical crystals in urine are in the size range of 4 to 40 μm (27), it seems that the majority of the calcium-containing particles are small enough to pass throught the 0.45 μm filter. Evidently, from the results in Table 5.2, 50 fold dilution is not enough to dissolve all of these small particles but ≥ 100 fold dilution is.

Table 5.2 : Loading times for unfiltered urine samples (pH 5.78) with various dilutions. Sample loading flow rate of 2 mL/min.

Dilution Factor	Loading Time Required for Equilibration
50	> 60 min*
100	≤ 2 min
200	≤ 2 min

* : See Figure 5.1.

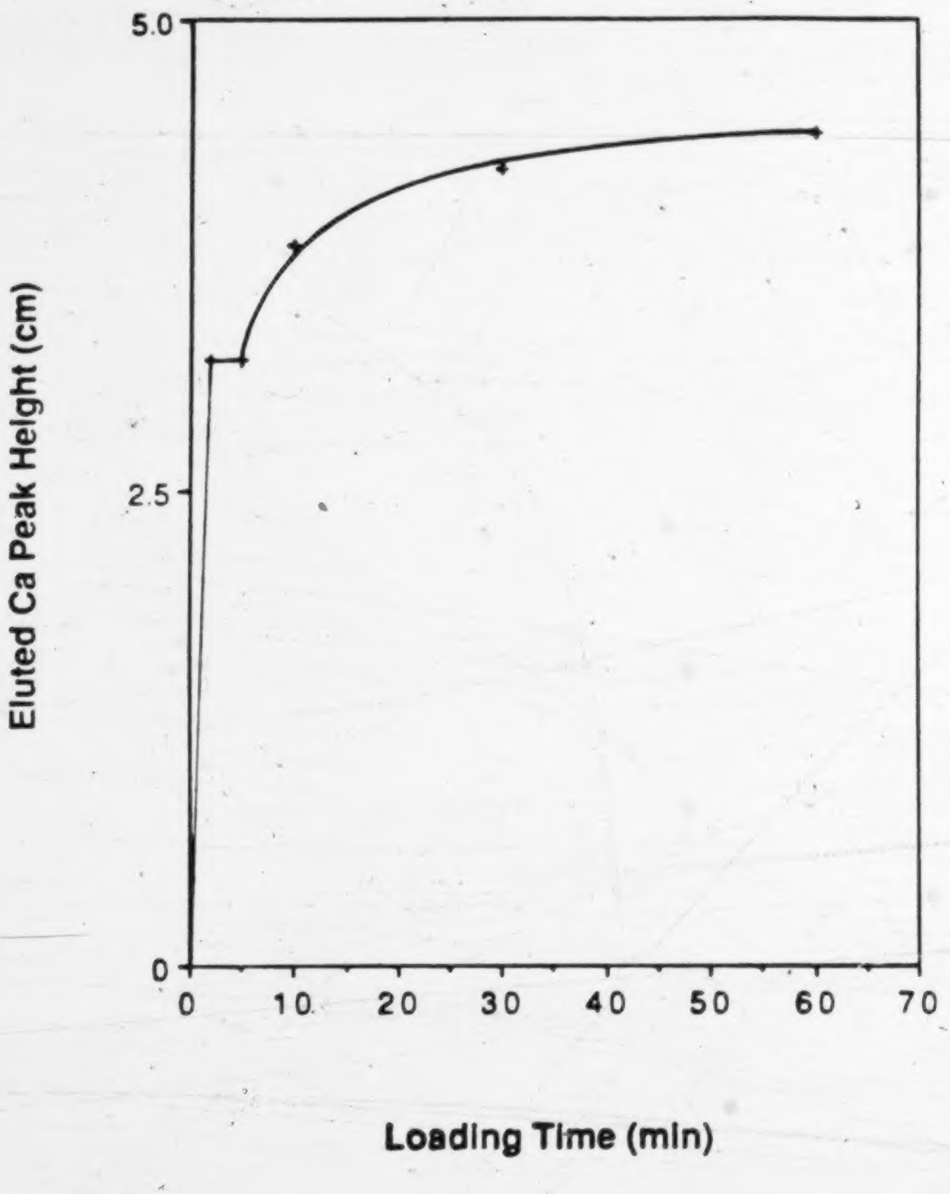

Figure 5.1 : Loading curve for unfiltered urine sample (pH 5.78) with 50 fold dilution.

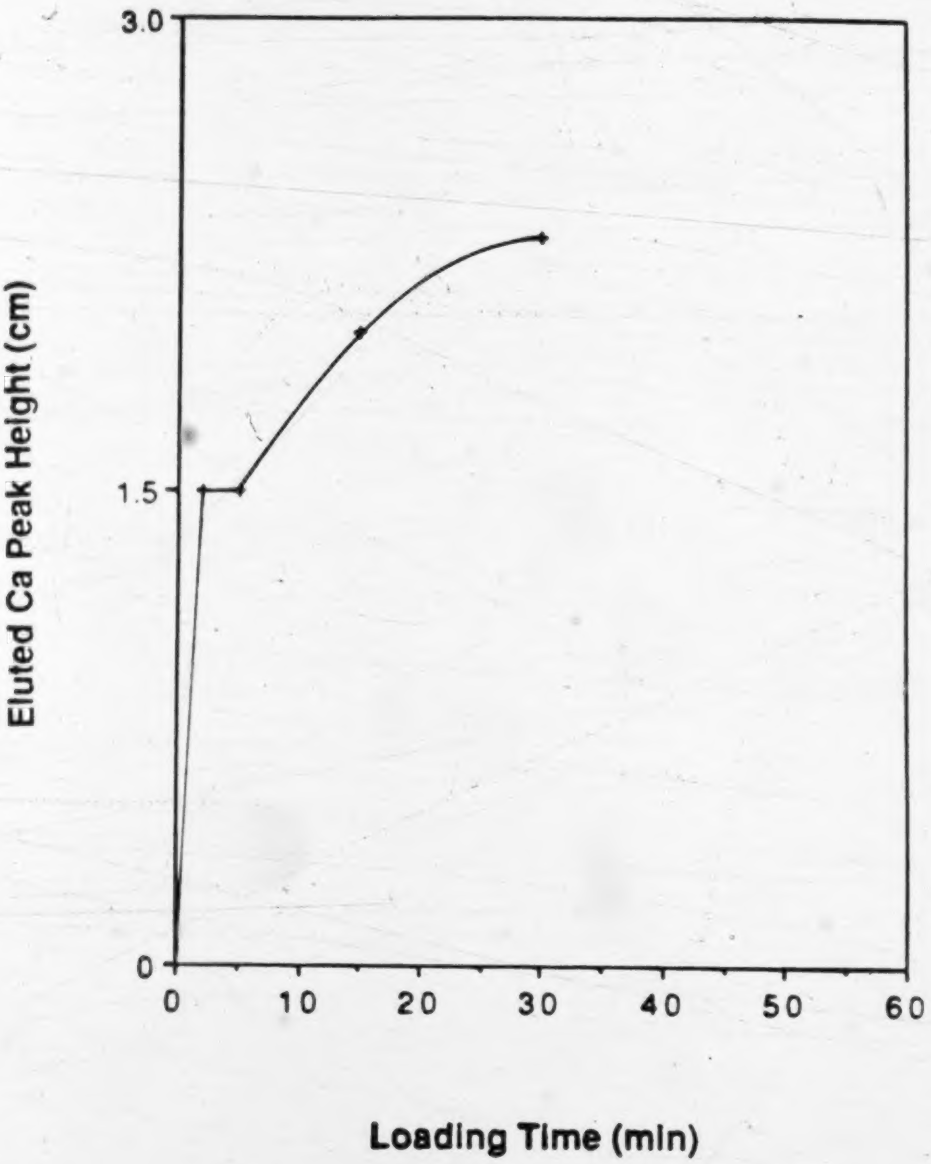

Figure 5.2 : Loading curve for unfiltered urine sample (pH 5.92) with 50 fold dilution.

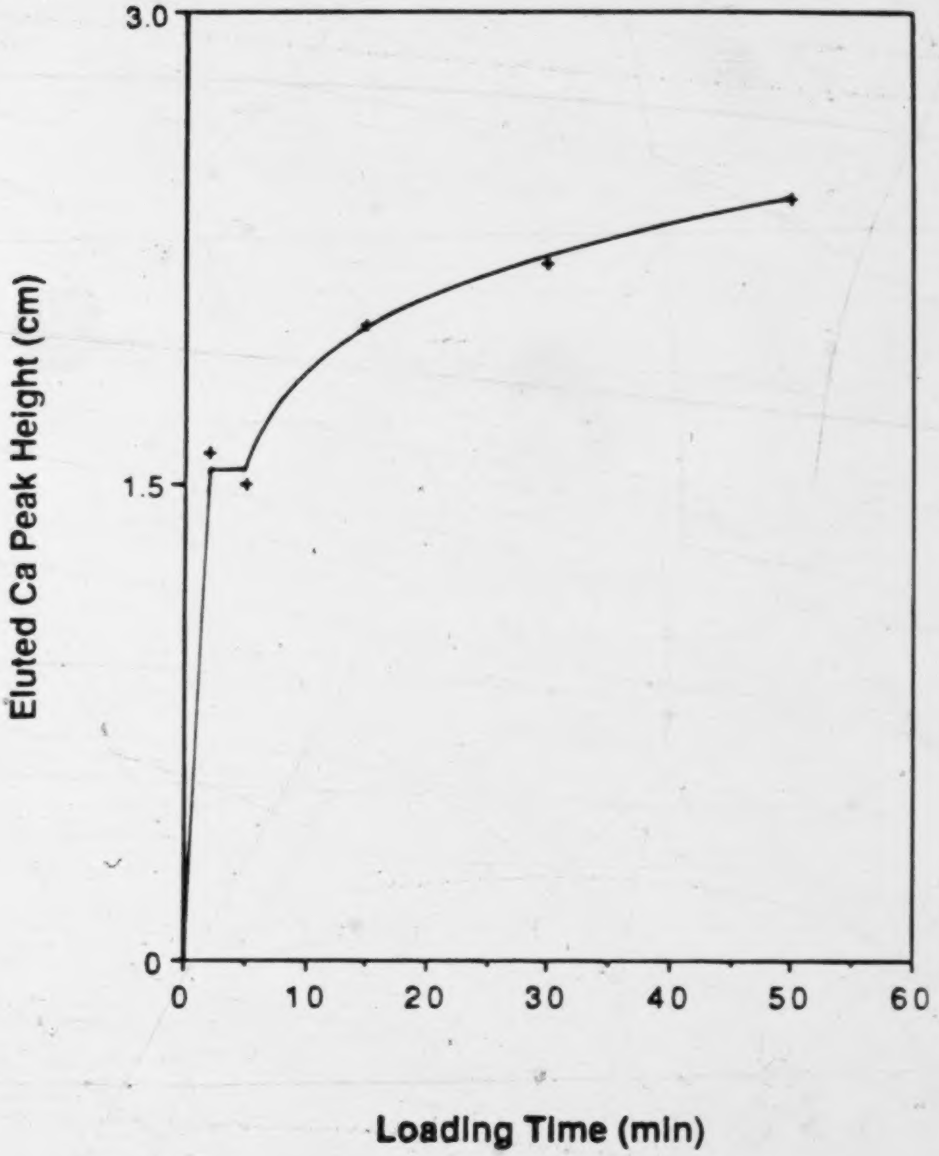

Figure 5.3 : Loading curve for filtered urine sample (pH 5.92) with 50 fold dilution.

On the assumption that the slow equilibration of an urine sample diluted ≤ 50 fold is, in fact, due to calcium-containing particles, and because calcium in the particles is not Ca^{2+} in solution, it was decided to employ the 4 min equilibration time in all subsequent studies since this time is sufficient to equilibrate Ca^{2+} in standard solution. This shorter time will also minimize erroneously high values of measured $[Ca^{2+}]$ for urine samples since the accumulation rate of calcium on the column due to the particles is obviously slow as seen from the small slope of the loading curve after 4 min in Figures 5.1-5.3.

V.3.2.3 EFFECT OF DILUTION ON $[Ca^{2+}]$:

In the second columns of Tables 5.3-5.5 are presented the values of $[Ca^{2+}]$ obtained for diluted urine and in the second column of Table 5.6 is presented the $[Ca^{2+}]$ value for diluted wine. For the entries with an asterisk next to the corresponding dilution factor, the column loading exceeded trace conditions as shown by the fact that peak heights corresponded to concentrations above the linear part of the Ca^{2+} sorption isotherm on CPG-Oxine. For these cases the standard calibration curve was also measured into the non-linear region.

In the third columns of Tables 5.3-5.6 are shown the values of $[Ca^{2+}]$ obtained from those in the second columns by simply multiplying by the dilution factors. These values for $[Ca^{2+}]$ in the undiluted samples are also plotted versus dilution factor in Figures 5.4-5.7. The fact that the values of $[Ca^{2+}]$ for the undiluted samples obtained in this way increase with increasing dilution factor suggests that dilution of the sample converts more calcium into the Ca^{2+} form. This could result from dissociation of calcium-ligand complexes and from dissolution of calcium-containing particles. It is clear that Ca^{2+} in these urine and wine samples is poorly buffered (83).

A study was undertaken to see if an accurate value for $[Ca^{2+}]$ in the original undiluted sample could be obtained from values measured in diluted samples by extrapolating the data to zero dilution. This approach will work if the data can be accurately

Table 5.3 : Analysis of [Ca^{2+}] in diluted urine (unfiltered, pH 5.78). Total calcium content in the original, undiluted urine was 4.11 (± 0.07) mM.

Dilution Factor	[Ca^{2+}] in Diluted Sample	[Ca^{2+}] Calculated [a] for Undiluted Sample
50	7.48×10^{-5} M	3.74 (±0.19) mM
66.7	6.03×10^{-5} M	4.02 (±0.20) mM
100	4.12×10^{-5} M	4.12 (±0.25) mM
200	$2.24_5 \times 10^{-5}$ M	4.49 (±0.36) mM

a : [Ca^{2+}] calculated for undiluted sample by multiplying [Ca^{2+}] from diluted sample by the dilution factor.

Table 5.4 : Analysis of [Ca^{2+}] in diluted urine (unfiltered, pH 5.88). Total calcium content in the original, undiluted urine was 6.05 (± 0.07) mM.

Dilution Factor	[Ca^{2+}] in Diluted Sample	[Ca^{2+}] Calculated [a] for Undiluted Sample
50*	9.44×10^{-5} M	4.72 (±0.21) mM
100	5.61×10^{-5} M	5.61 (±0.00) mM
133.3	4.44×10^{-5} M	5.92 (±0.00) mM
200	$3.24_5 \times 10^{-5}$ M	6.49 (±0.45) mM

a : [Ca^{2+}] calculated for undiluted sample by multiplying [Ca^{2+}] from diluted sample by the dilution factor.

Table 5.5 : Analysis of [Ca^{2+}] in diluted urine (unfiltered, pH 6.13). Total calcium content in the original, undiluted urine was 2.40 (± 0.04) mM.

Dilution Factor	[Ca^{2+}] in Diluted Sample	[Ca^{2+}] Calculated [a] for Undiluted Sample
14.3*	1.27×10^{-4} M	1.82 (±0.07) mM
20*	9.80×10^{-5} M	1.96 (±0.08) mM
22.2*	9.55×10^{-5} M	2.12 (±0.08) mM
25*	8.84×10^{-5} M	2.21 (±0.09) mM
28.6*	7.94×10^{-5} M	2.27 (±0.11) mM
33.3*	6.85×10^{-5} M	2.28 (±0.11) mM

a : [Ca^{2+}] calculated for undiluted sample by multiplying [Ca^{2+}] from diluted sample by the dilution factor.

Table 5.6 : Analysis of [Ca^{2+}] in diluted wine (unfiltered, pH 3.30). Total calcium content in the original, undiluted wine was 2.14 (± 0.06) mM.

Dilution Factor	[Ca^{2+}] in Diluted Sample	[Ca^{2+}] Calculated [a] for Undiluted Sample
25	7.24×10^{-5} M	1.81 (±0.31) mM
33.3	6.49×10^{-5} M	2.16 (±0.39) mM
40	5.75×10^{-5} M	2.30 (±0.44) mM
50	5.00×10^{-5} M	2.50 (±0.50) mM

[a] : [Ca^{2+}] calculated for undiluted sample by multiplying [Ca^{2+}] from diluted sample by the dilution factor.

Table 5.7 : Mean values of maximum and minimum concentrations of some major components in typical urine sample (36).

	Concentration (mM)		
Major Component	Maximum	Minimum	Mean
Calcium	6.26	1.45	3.86 ± 2.40
Magnesium	5.96	1.44	3.70 ± 2.26
Phosphate	13.3	3.05	8.18 ± 5.12
Citrate	3.33	0.833	2.08 ± 1.25
Oxalate	0.284	0.136	0.210 ± 0.074

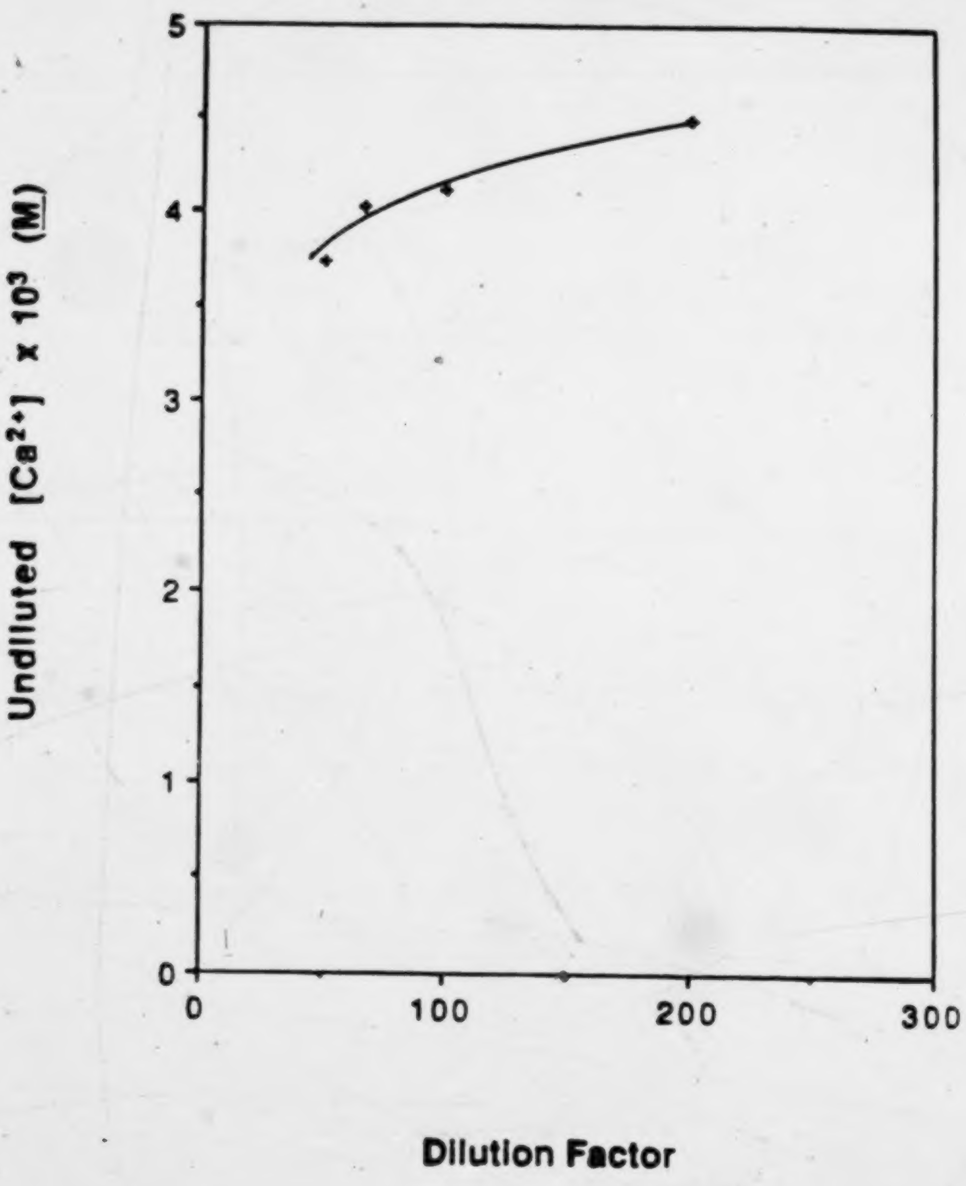

Figure 5.4 : Plot of undiluted [Ca^{2+}] versus dilution factor for urine sample at pH 5.78. Value of undiluted [Ca^{2+}] was obtained by multiplying the value of [Ca^{2+}] in the diluted urine by the corresponding dilution factor.

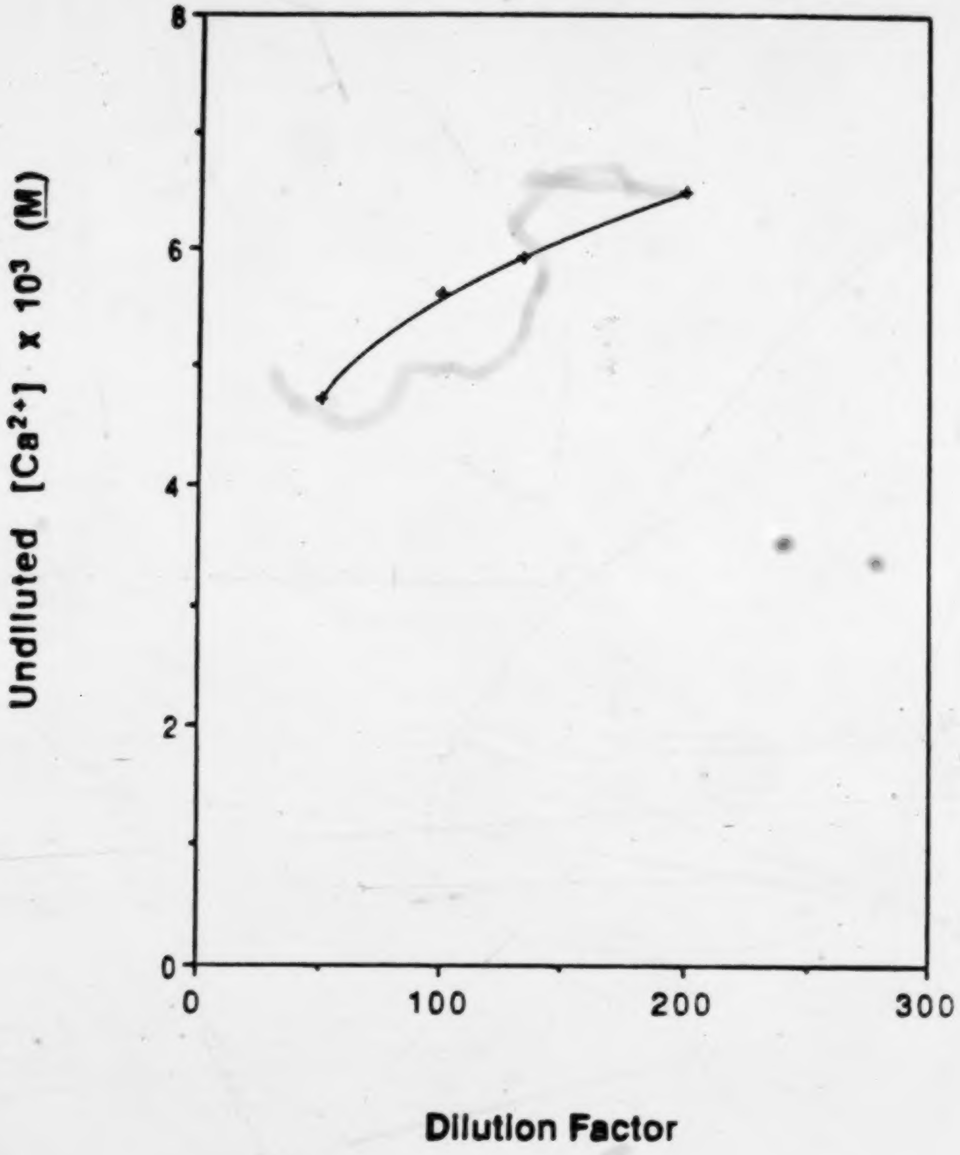

Figure 5.5 : Plot of undiluted [Ca^{2+}] versus dilution factor for urine sample at pH 5.88. Value of undiluted [Ca^{2+}] was obtained by multiplying the value of [Ca^{2+}] in the diluted urine by the corresponding dilution factor.

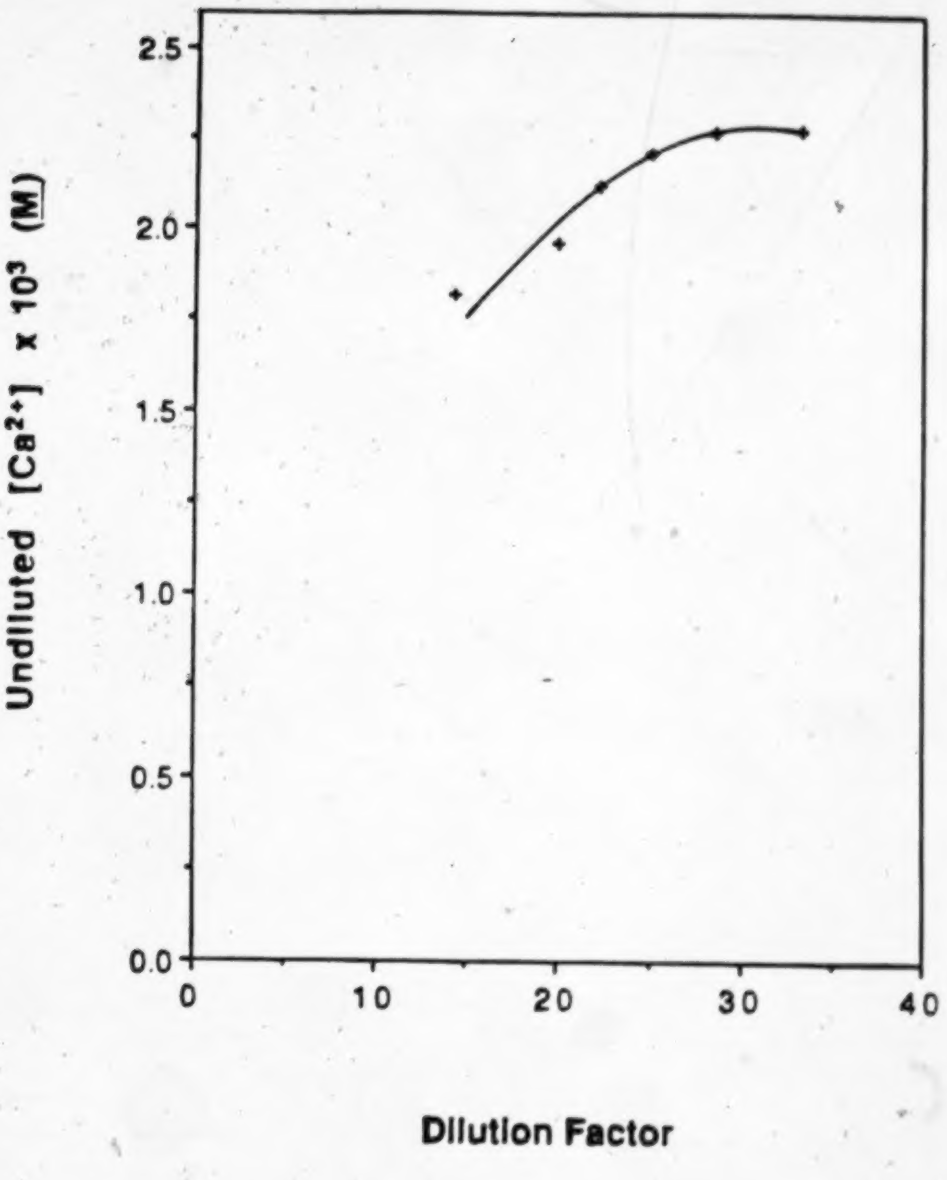

Figure 5.6 : Plot of undiluted [Ca^{2+}] _versus_ dilution factor for urine sample at pH 6.13. Value of undiluted [Ca^{2+}] was obtained by multiplying the value of [Ca^{2+}] in the diluted urine by the corresponding dilution factor.

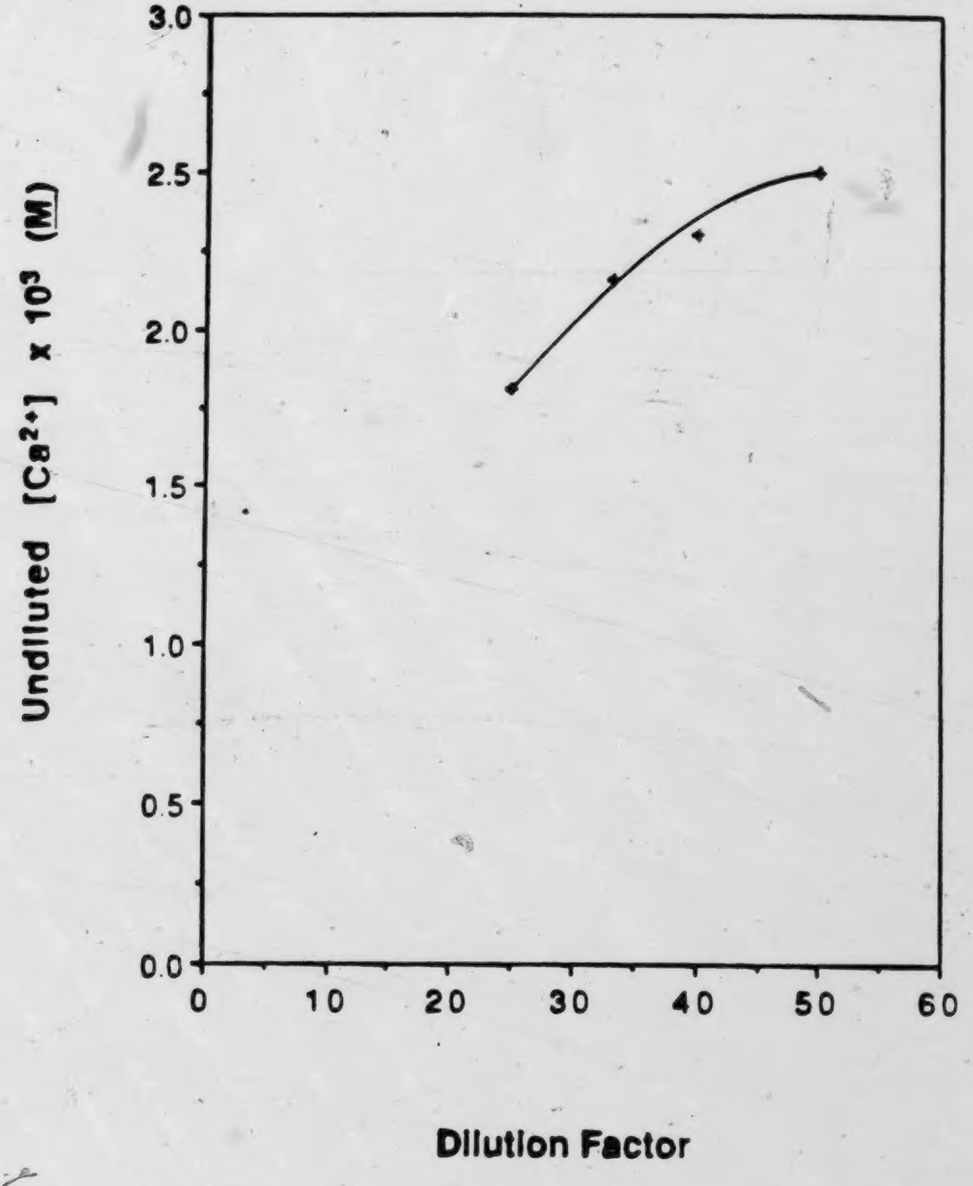

Figure 5.7 : Plot of undiluted [Ca^{2+}] versus dilution factor for wine sample at pH 3.30. Value of undiluted [Ca^{2+}] was obtained by multiplying the value of [Ca^{2+}] in the diluted wine by the corresponding dilution factor.

represented by a mathematical function (e.g. polynomial). In order to investigate the possibilities of using this approach, theoretical calculations were performed to predict the effect of dilution on [Ca^{2+}] in model solution.

V.3.3 COMPUTER SIMULATION STUDIES OF DILUTION EFFECT ON [Ca^{2+}] IN MODEL SOLUTIONS:

V.3.3.1 SIMULATED URINE SYSTEM:

With the known composition of urine (36,66) and the available quantitative stability constants, it is possible to use the "speciation" computer program COMICS to estimate the [Ca^{2+}] in diluted urine, and consequently predict the variation of [Ca^{2+}] with dilution.

The COMICS program is discussed in Appendix II. The iterative calculations give the concentrations of all calcium-containing species as a function of pH and component concentration.

The model solution chosen to represent urine was made to contain calcium and magnesium, at the mean concentrations reported for typical urine samples (Table 5.7). It also contained phosphate, citrate and oxalate ligands at the mean concentrations reported for typical urine samples (Table 5.7). The pH range investigated was between 5.5 and 6.0 in order to simulate the pH values for the urine samples listed in Table 5.1. The equilibrium constants used in the COMICS program are presented in Table A.1 in Appendix II.

When calculations were carried out for complexation of both calcium and magnesium with the three ligands, it was found about 33% of the total calcium was complexed, most of it by citrate and a much smaller amount by oxalate, and about 20% of the total magnesium was complexed, most of it by citrate and a much smaller amount by oxalate. Only negligible amounts of calcium and magnesium were complexed by phosphate. Therefore, in the remaining studies citrate was used as the only ligand in the model solution to study the effects of dilution on Ca^{2+}.

V.3.3.2 RESULTS AND DISCUSSION :

Figures 5.8 and 5.9 show the computer simulated plots of [Ca^{2+}] in the undiluted solution versus dilution factor for citrate to calcium ratios of 0.2, 0.7, 1.5, 3.0 and 6.0 at pH 5.5 and 6.0, respectively. The value of [Ca^{2+}] was obtained by multiplying the value of [Ca^{2+}] calculated via COMICS for the diluted solution by its dilution factor. The curves in Figures 5.8 and 5.9 at high citrate to calcium ratios are extremely non-linear and show dramatic changes of slope at dilutions of ≤ 50 fold. It is clear that successful curve fitting to permit accurate extrapolation to zero dilution would require the collection of data at dilution ≤ 50 fold. However, as discussed above, these low dilutions produce calcium loading in the distinctly non-linear part of the Ca^{2+} sorption isotherm where the results are imprecise and where Mg^{2+} uptake would alter the measured value of λ_0 (Section II.3.4.4).

Furthermore, from the curves obtained at various citrate to calcium ratios in Figures 5.8 and 5.9 it can be seen that a mathematical equation which would describe the curve at one ratio would not describe it at other ratios. Thus, it would be necessary to determine the citrate content of a sample in order to determine [Ca^{2+}]. Obviously, it would also be necessary to determine oxalate and magnesium and perhaps other components as well.

The need to determine many components in addition to measuring [Ca^{2+}] at several dilutions and the need to collect data at non-trace (low dilution) conditions make the "dilution" approach for measuring [Ca^{2+}] unattractive.

V.4 CONCLUSIONS :

Due to the restriction of trace loading in the column equilibration technique, the use of a CPG-Oxine column for direct measurement of Ca^{2+} in biological and water samples containing high [Ca^{2+}] (e.g. ≥ 0.1 mM) is probably impossible at this stage.

The use of a dilution / extrapolation technique to obtain accurate values of [Ca^{2+}] in such samples also seems not to work, mainly because the minimum degree of dilution

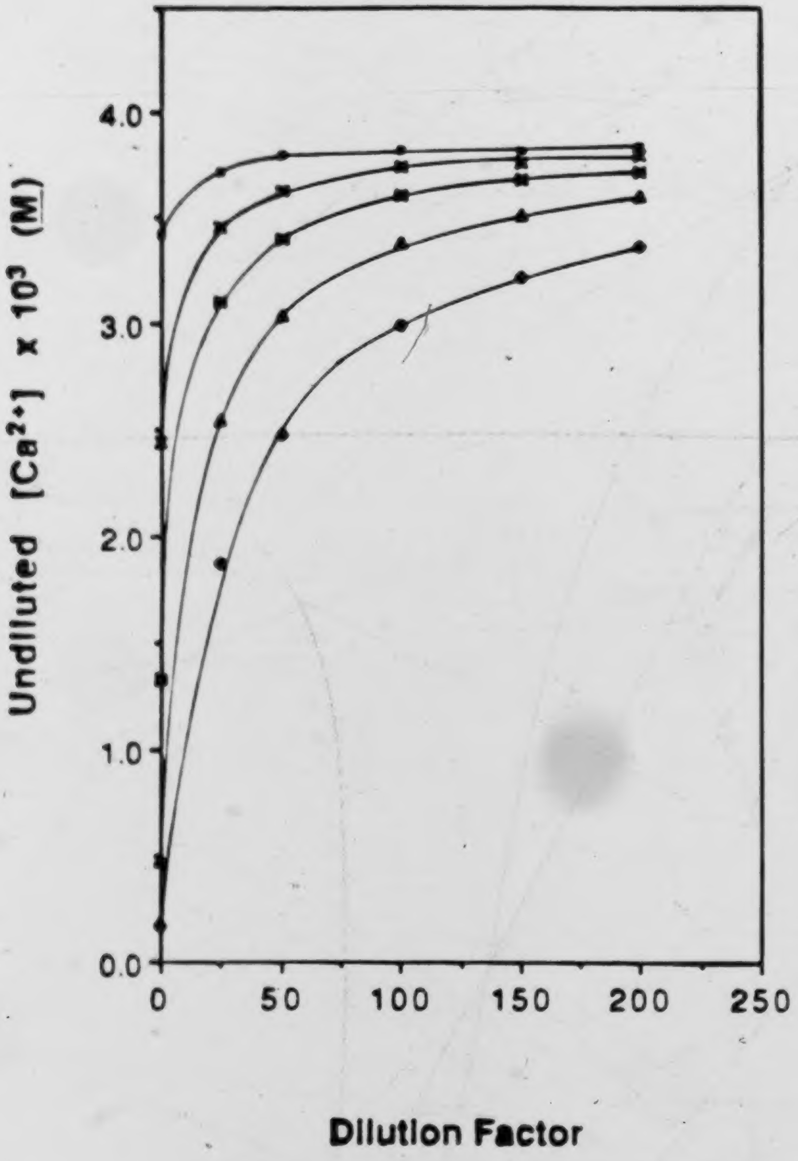

Figure 5.8 : Plots of undiluted [Ca^{2+}] versus dilution factor for simulated urine samples, with citrate to calcium ratios of 0.2 (■), 0.7 (x), 1.5 (⌘), 3.0 (▲) and 6.0 (◆), at pH 5.5. Value of undiluted [Ca^{2+}] was obtained by multiplying the value of [Ca^{2+}] in the diluted urine by the corresponding dilution factor.

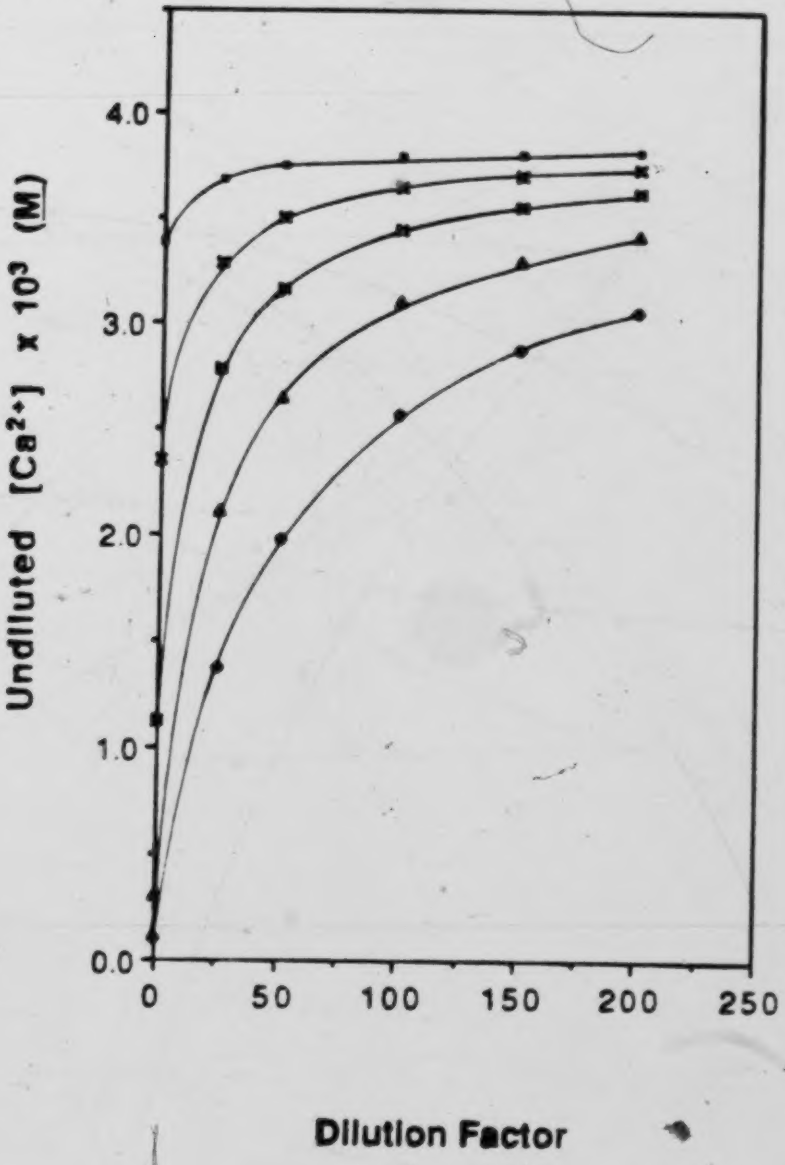

Figure 5.9 : Plots of undiluted [Ca^{2+}] *versus* dilution factor for simulated urine samples, with citrate to calcium ratios of 0.2 (■), 0.7 (×), 1.5 (⁕), 3.0 (▲) and 6.0 (◆), at pH 6.0. Value of undiluted [Ca^{2+}] was obtained by multiplying the value of [Ca^{2+}] in the diluted urine by the corresponding dilution factor.

(> 50 fold) needed to achieve trace loading conditions on CPG-Oxine is too great to permit accurate extrapolation to zero dilution.

The solution to this problem, as will be discussed in Chapter Six , is to replace "oxine" as immobilized ligand with another ligand which has a much smaller conditional stability constant for Ca^{2+} at pH ≈ 6. The result would be that the trace loading region would be raised to include much higher [Ca^{2+}].

CHAPTER SIX

FUTURE STUDIES

In the present investigation, in which CPG-Oxine was substituted for conventional cation exchange resins in the column equilibration / AAS method for measuring Ca^{2+}, the results are promising. The major advantage of using a CPG-Oxine column is that it is more specific for Ca^{2+}, especially in the presence of cationic calcium-containing species. The column equilibration / AAS method, in general, seems to be less subject to interference than other techniques, such as ISE potentiometry.

Direct measurement of Ca^{2+} in biological fluids using the column equilibration / AAS method should be possible if an immobilized ligand having a lower conditional stability constant than "oxine" is used. The main emphasis of future work should be the identification of such a ligand and binding of the ligand to a suitable support. Ligands such as α-aminopropionate, aminoacetate and glycylglycinate might be tried.

As far as supports are concerned, one consideration is the hydrolytic stability of the ligand-support bond and another is the amount of residual ionizable surface groups (e.g. silanol). Porous glass (e.g. CPG) seems to be a suitable support but it cannot be used in high or low pH solutions (115,118) due to hydrolysis and furthermore, it has a lot of residual ionizable surface groups. Chemically modified silica, in which the residual silanol groups are "end-capped" with an organic group should have far fewer residual ionizable groups. In addition, porous organic polymers such as amberlyst XAD-2 (styrene-divinylbenzene copolymer) (194-198) would be expected to have fewer residual ionizable groups than glass or silica. The polymer Fractogel-TSK (93), which is a vinyl polymer, has also been used as a support for immobilized ligand. In general, a high ligand capacity is probably desirable in order to yield good sensitivity which remaining under trace metal ion loading conditions.

It is also recommended that the role of the water washing step in the column equilibration method be more thoroughly investigated. Because of the possibility of dissociation of the metal-ligand complexes in solution in the pores, it might be better to eliminate the water washing step. In this case, it would be necessary to measure accurately the void volume of the column, valve and associated tubing in order to subtract the contribution of calcium in solution from the observed AA signal for a sample.

REFERENCES

1. T.M. Florence and G.E. Batley, CRC Crit. Rev. Anal. Chem. 9 : 219 (1980).
2. T.M. Florence, Talanta 29 : 345 (1982).
3. G.G. Leppard (Ed.), " Trace Element Speciation in Surface Waters and its Ecological Implications ", Plenum Press, New York, 1983.
4. D.T.E. Hunt and A.L. Wilson (Eds.), " The Chemical Analysis of Water - General Principles and Techniques ", The Royal Society of Chemistry, London, 1986; pp. 559.
5. A. Mizuike, Pure and Appl. Chem. 59 : 555 (1987).
6. R.S. Braman, in D.F.S. Natusch and P.K. Hopke (Eds.), "Analytical Aspects of Environmental Chemistry", Wiley-Interscience, New York, 1983; pp. 1.
7. D.D. Perrin and I.G. Sayce, Talanta 14 : 833 (1967).
8. E.A. Jenne (Ed.), " Chemical Modeling in Aqueous Systems ", ACS Symposium Series No. 93, American Chemical Society, Washington D.C., 1979.
9. E.H. Hansen, J. Ruzicka and A.K. Ghose, Anal. Chim. Acta 100 : 151 (1978).
10. W.G. Sunda and P.J. Hanson, in E.A. Jenne (Ed.), " Chemical Modeling in Aqueous Systems ", ACS Symposium Series No. 93, American Chemical Society, Washington D.C., 1979; pp. 147.
11. J. Buffle, F.L. Greter, G. Nembrini, J. Paul and W. Haerdi, Fresenius' Z. Anal. Chem. 282 : 339 (1976).
12. W. Davison, J. Electroanal. Chem. 87 : 395 (1978).
13. D.P.H. Laxen and R.M. Harrison, Sci. Total Environ. 19 : 59 (1981).
14. E.Steinnes, in G.G. Leppard (Ed.), " Trace Element Speciation in Surface Waters and its Ecological Implications ", Plenum Press, New York, 1983; pp. 37.

15. S.J. de Mora and R.M. Harrison, Water Res. 17 : 723 (1983).

16. K. Matsunaga, M. Negishi, S. Fukase and K. Hasebe, Geochem. Cosmochim. Acta, 44 : 1615 (1980).

17. P.G.C. Campbell, M. Bisson, R. Bougie, A. Tessier and J.P. Villeneuve, Anal. Chem. 55 : 2246 (1983).

18. C.T. Driscoll, Int. J. Environ. Anal. Chem. 16 : 267 (1984).

19. F.F. Cantwell, J.S. Nielsen and S.E. Hrudey, Anal. Chem. 54 : 1498 (1982).

20. J. Treit, J.S. Nielsen, B. Kratochvil and F.F. Cantwell, Anal. Chem. 55 : 1650 (1983).

21. J.S. Nielsen, S.E. Hrudey and F.F. Cantwell, Environ. Sci. Technol. 18 : 883 (1984).

22. J.A. Sweileh, D. Lucyk, B. Kratochvil and F.F. Cantwell, Anal. Chem. 59 : 586 (1987).

23. N.G. Zorkin, E.V. Grill and A.G. Lewis, Anal. Chim. Acta 183 : 163 (1986).

24. D.F. Martin, in R.F. Gould (Ed.), " Equilibrium Concepts in Natural Water Systems ", Advances in Chemistry Series No. 67, American Chemical Society, Washington D.C., 1967. pp. 255.

25. J.W. Morse and R.C. Berner, in E.A. Jenne (Ed.), " Chemical Modeling in Aqueous Systems ", ACS Symposium Series No. 93, American Chemical Society, Washington D.C., 1979; pp. 499.

26. R.F. Gould (Ed.), " Equilibrium Concepts in Natural Water Systems ", Advances in Chemistry Series No. 67, American Chemical Society, Washington D.C., 1967.

27. B.E.C. Nordin (Ed.), " Calcium, Phosphate, and Magnesium Metabolism : Clinical Physiology and Diagnostic Procedures ", Churchill Livingstone, Edinburgh, 1976.

28. F.C. McLean and A.B. Hastings, J. Biol. Chem. 108 : 285 (1935).

29. E.W. Moore, Ann. N. Y. Acad. Sci., 148 : 93 (1968).

30. J.A. Lott, CRC Crit. Rev. Anal. Chem. 3 : 41 (1972).

31. E. Carafoli, F. Clementi, W. Drabikowski and A. Margreth (Eds.), " Calcium Transport in Contraction and Secretion ", North-Holland/American Elsevier, Amsterdam, 1975.

32. C.O. Brostrom, F.L. Hunkeler and E.G. Krebs, J. Biol. Chem. 246 : 1961 (1971).

33. R.H. Wasserman, R.A. Corradino, E. Carafoli, R.H. Kretsinger, D.H. MacLennan and F.L. Siegel (Eds.), " Calcium-Binding Proteins and Calcium Function ", Elsevier North-Holland, New York, 1977.

34. R. Eckert and D. Tillotson, Science 200 : 437 (1978).

35. S.T. Ohnishi and M. Endo (Eds.), " The Mechanism of Gated Calcium Transport Across Biological Membranes ", Academic Press, New York, 1981.

36. R.W. Marshall, M. Cochran, W.G. Robertson, A. Hodgkinson and B.E.C. Nordin, Clin. Sci. 43 : 433 (1972).

37. M. Modlin, J. Urol. 97 : 567 (1967).

38. J.H. Ladenson, J.M. McDonald, J. Aguanno and M. Goren, Clin. Chem. 25 : 1821 (1979).

39. B.W. Renoe, J.M. McDonald and J.H. Ladenson, Clin. Chem. 25 : 1766 (1979).

40. B.W. Renoe, J.M. McDonald and J.H. Ladenson, Clin. Chim. Acta 103 : 91 (1980).

41. L.J. Anghileri and A.M. Tuffet-Anghileri (Eds.), " The Role of Calcium in Biological Systems - Volumes I, II and III ", CRC Press, Florida, 1982.

42. R.G. Rahwan and D.T. Witiak (Eds.), " Calcium Regulation by Calcium Antagonists ", ACS Symposium Series No. 201, American Chemical Society, Washington D.C., 1982.

43. A.K. Campbell (Ed.), " Intracellular Calcium, Its Universal Role as Regulator ", John Wiley and Sons, Chichester, 1983.

44. D. Marme (Ed.), " Calcium and Cell Physiology ", Springer-Verlag, Berlin, 1985.

45. W.Y. Cheung (Ed.), " Calcium and Cell Function", Academic Press, New York, 1980 - 1987.

46. D.E. Frizel, A.G. Malleson and V. Marks, Clin. Chim. Acta 16 : 45 (1967).

47. W.G. Robertson, Clin. Chim. Acta 24 : 149 (1969).

48. D. Ammann, P.C. Meier and W. Simon, In C.C. Ashley and A.K. Campbell (Eds.), " Detection and Measurement of Free Ca^{2+} in Cells ", Elsevier/North-Holland, Amsterdam, 1979; pp. 117.

49. D. Erne and D. Ammann, in L.J. Anghileri and A.M. Tuffet-Anghileri (Eds.), " The Role of Calcium in Biological Systems, Volume I ", CRC Press, Florida, 1982; pp. 71.

50. H. Husden, M. Leung, D. Oreopoulos and A. Rapoport, Clin. Chem. 23 : 1775 (1977).

51. Y. Hamaguchi, in L.J. Anghileri and A.M. Tuffet-Anghileri (Eds.), " The Role of Calcium in Biological Systems, Volume I ", CRC Press, Florida, 1982; pp. 85.

52. A.K. Campbell, T.J. lea and C.C. Ashley, in C.C. Ashley and A.K. Campbell (Eds.), " Detection and Measurement of Free Ca^{2+} in Cells ", Elsevier/North-Holland, Amsterdam, 1979; pp. 13.

53. O. Shimomura and F.H. Johnson, in C.C. Ashley and A.K. Campbell (Eds.), " Detection and Measurement of Free Ca^{2+} in Cells ", Elsevier/North-Holland, Amsterdam, 1979; pp. 73.

54. A. Scarpa, in C.C. Ashley and A.K. Campbell (Eds.), " Detection and Measurement of Free Ca^{2+} in Cells ", Elsevier/North-Holland, Amsterdam, 1979;

pp. 85.

55. S.T. Ohnishi, Anal. Biochem. 85 : 165 (1978).

56. M. Walser, Anal. Chem. 32 : 711 (1960).

57. A.B. Borle and K.W. Snowdowne, in Ref. (45); pp.159.

58. B.E.C. Nordin and D.A. Smith (Eds.), " Diagnostic Produres in Disorders of Calcium Metabolism ", Churchill, London, 1965; pp. 12.

59. K.A. Munday and B.W. Mahy, Clin. Chim. Acta 10 : 144 (1964).

60. J.H. Eckfeldt and D.F. Koehler, Clin. Chem. 26 : 1871 (1980).

61. J. Toffaletti, D. Tompkins and G. Hoff, Clin. Chem. 27 : 466 (1981).

62. M. D'Costa and P.T. Cheng, Clin. Chem. 29 : 519 (1983).

63. G. Christianson, R. Jenness and S.T. Coulter, Anal. Chem. 26 : 1923 (1954).

64. L.D. MacLeod, Biochem. J. 91 : 29P (1964).

65. P.J. Muldoon and B.J. Liska, J. Dairy Sci. 52 : 460 (1969).

66. M. Rubin, R. Gohil, A.E. Martell, R.J. Motekaitis, J.C. Penhos and P. Weiss, in A.E. Martell (Ed.), " Inorganic Chemistry in Biology and Medicine ", ACS Symposium Series No. 140, American Chemical Society, Washington D.C., 1980; pp. 381.

67. J. Koryta, Anal. Chim. Acta 183 : 1 (1986).

68. G.J. Moody, J.D.R. Thomas, Prog. Med. Chem. 14 : 51 (1977).

69. P.C. Meier, D. Ammann, W.E. Morf and W. Simon, in J. Koryta (Ed.), "Medical and Biological Applications of Electrochemical Devices ", John Wiley and Sons, New York, 1980; pp. 13.

70. R.Y. Tsien and T.J. Rink, Biochem. Biophys. Acta 599 : 623 (1980).

71. E.W. Moore, in R.A. Durst (Ed.), "Ion-Selective Electrodes", Special Publication 314, National Bureau of Standards, Washington, D.C., 1969; pp. 215.

72. L. Keil, G.J. Moody and J.D.R. Thomas, Anal. Chim. Acta 96 : 171 (1978).

73. M. Whitfield and J.V. Leyendekkers, Anal. Chem. 42 : 444 (1970).

74. P.C. Meier, D. Ammann, H.F. Osswald and W. Simon, Med. Progr. Techn. 5 : 1 (1977).

75. W.E. Morf, Anal. Chem. 49 : 810 (1977).

76. H.B. Collier, Anal. Chem. 42 : 1443 (1970).

77. R.G. Burr, Clin. Chim. Acta 43 : 311 (1973).

78. S.A.H. Khalil, G.J. Moody and J.D.R. Thomas, Analyst 110 : 353 (1985).

79. R.A. Llenado, Anal. Chem. 47 : 2243 (1975).

80. A. Craggs, G.J. Moody, J.D.R. Thomas and B.J. Birch, Analyst 105 : 426 (1980).

81. A.J. Frend, G.J. Moody, J.D.R. Thomas and B.J. Birch, Analyst 108 : 1357 (1983).

82. J.R. Blinks, F.G. Prendergast and D.G. Allen, Pharmacol. Rev. 28 : 1 (1976).

83. R.B. Fulton and B. Kratochvil, Anal. Chem. 52 : 546 (1980).

84. J. Toffaletti, Clin. Chem. 27 : 1095 (1981).

85. J. Schubert, J. Phys. Colloid Chem. 52 : 340 (1948).

86. M. Schnitzer and S.I.M. Skinner, Soil Sci. 103 : 247 (1967).

87. K.N. Pearce and L.K. Creamer, Anal. Chem. 46 : 457 (1974).

88. V.P. Mutucumarana, M.Sc. Thesis, Department of Chemistry, University of Alberta, Edmonton, Alberta, Canada, 1988.

89. D.E. Leyden and W. Wegscheider, Anal. Chem. 53 : 1059A (1981).

90. S.K. Sahni and J. Reedijk, Coord. Chem. Rev. 59 : 1 (1984).

91. H.P. Gregor, M. Taifer, L. Citarel and E.I. Becker, Ind. Engng. Chem. 44 : 2834 (1952).

92. G.V. Myasoedova and S.B. Savvin, CRC Crit. Rev. Anal. Chem. 17 : 1 (1986).

93. W.M. Landing, C. Haraldsson, and N. Paxeus, Anal. Chem. 58 : 3031 (1986).

94. R.M. Smith and A.E. Martell (Eds.), "Critical Stability Constants, Volume 2 :

Amines ", Plenum Press, New York, 1975; Section IV.

95. J. Stary, Y.A. Zolotov and O.M. Petrukhin (Eds.), " Critical Evaluation of Equilibrium Constants involving 8-Hydroxyquinoline and its Metal Chelates ", IUPAC Chemical Data Series No. 24, Pergamon Press, Oxford, 1979.

96. E.D. Moorhead and P.H. Davis, Anal. Chem. 46 : 1879 (1974).

97. F. Malamas, M. Bengtsson and G. Johansson, Anal. Chim. Acta 160 : 1 (1984).

98. M.M. Guedes da Mota, F.G. Romer and B. Griepink, Fresenius' Z. Anal. Chem. 287 : 19 (1977).

99. R.E. Sturgeon, S.S. Berman, S.N. Willie and J.A.H. Desaulniers, Anal. Chem. 53 : 2337 (1981).

100. E.A. Allen, P.K.N. Bartlett and G. Ingram, Analyst 109 : 1075 (1984).

101. Z. Fang, J. Ruzicka and E.H. Hansen, Anal. Chim. Acta 164 : 23 (1984).

102. J.W. McLaren, A.P. Mykytiuk, S.N. Willie and S.S. Berman, Anal. Chem. 57 : 2907 (1985).

103. M.A. Marshall and H.A. Mottola, Anal. Chem. 57 : 729 (1985).

104. D.K. Ryan and J.H. Weber, Talanta 32 : 859 (1985).

105. E.A. Allen, M.C. Boardman and B.A. Plunkett, Anal. Chim. Acta 196 : 323 (1987).

106. J.R. Jezorek and H. Freiser, Anal. Chem. 51 : 366 (1979).

107. M.-S. Kuo and H.A. Mottola, Anal. Chim. Acta 120 : 255 (1980).

108. J.M. Hill, J. Chromatogr. 76 : 455 (1973).

109. G.J. Shahwan and J.R. Jezorek, J. Chromatogr. 256 : 39 (1983).

110. C.H. Risner and J.R. Jezorek, Anal. Chim. Acta 186 : 233 (1986).

111. M.A. Marshall and H.A. Mottola, Anal. Chem. 55 : 2089 (1983).

112. M.A. Marshall and H.A. Mottola, Anal. Chim. Acta 158 : 369 (1984).

113. J.R. Jezorek, K.H. Faltynski, L.G. Blackburn, P.J. Henderson and H.D. Medina, Talanta 32 : 763 (1985).

114. C. Fulcher, M.A. Crowell, R. Bayliss, K.B. Holland and J.R. Jezorek, Anal. Chim. Acta 129 : 29 (1981).

115. Product Bulletin, Pierce Chem. Co., Rockford, Ill., 1986.

116. D.E. Leyden, in D.E. Leyden and W.T. Collins (Eds.), "Silylated Surfaces", Gordon and Breach, New York, 1980; pp. 321.

117. D.E. Leyden and G.H. Luttrell, Anal. Chem. 47 : 1612 (1975).

118. K.F. Sugawara, H.H. Weetall and G.D. Schucker, Anal. Chem. 46 : 489 (1974).

119. Pierce, Private Communication, 1984.

120. Pierce, Private Communication, 1986.

121. T.W. Healy and L.R. White, Adv. Coll. Interface Sci. 9 : 303 (1978).

122. I.H. Harding and T.W. Healy, J. Coll. Interface Sci. 107 : 362 (1985).

123. I.H. Harding and T.W. Healy, J. Coll. Interface Sci. 107 : 371 (1985).

124. R.S. Chow and K. Takamura, J. Coll. Interface Sci., in press, Jan. 1988.

125. D.J. Shaw (Ed.), " Introduction to Colloid and Surface Chemistry ", Butterworths, London, 1980; Chapter 7.

126. N.E. Good, G.D. Winget, W. Winter, T.N. Connolly, S. Izawa and R.M.M. Singh, Biochem. 5 : 467 (1966).

127. R.H. Stokes and R.A. Robinson, J. Amer. Chem. Soc. 70 : 1870 (1948).

128. K. Takamura and R.S. Chow, Coll. and Surfaces 15 : 35 (1985).

129. I.H. Harding and T.W. Healy, J. Coll. Interface Sci. 107 : 382 (1985).

130. E.J. Verwey and J.T. Overbeck (Eds.), " Theory of the Stability of Lyophobic Colloids", Elsevier, Amsterdam, 1948.

131. M. Honda, J. Am. Chem. Soc. 73 : 2943 (1951).

132. I. Altug and M.L. Hair, J. Phys. Chem. 71 : 4260 (1967).

133. F. Helfferich (Ed.), "Ion Exchange", McGraw-Hill, New York, 1962; Chapter 5.

134. J.A. Marinsky, in J.A. Marinsky (Ed.), "Ion Exchange : A Series of Advances,

Vol. 1", Marcel Dekker, New York, 1966; Chapter 9.

135. J.A. Marinsky, A. Wolf and K. Bunzl, Talanta 27 : 461 (1980).

136. J.A. Marinsky, J. Phys. Chem. 89 : 5294 (1985).

137. D.C. Grahame, Chem. Rev. 41 : 441 (1947).

138. F.F. Cantwell and S. Puon, Anal. Chem. 51 : 623 (1979).

139. M.M. Khater, Y.M. Issa, A.F. Shoukry, J. f. prakt. Chemie 322 : 470 (1980).

140. J.R. Jezorek, C. Fulcher, M.A. Crowell, R. Bayliss, B. Greenwood and J. Lyon, Anal. Chim. Acta 131 : 223 (1981).

141. B.A. Utkelov, Ye.Ye. Yergozhin, B.A. Mukhitdinova and S.R. Rafikov, Polymer Sci. U.S.S.R. 20 : 532 (1978).

142. W.J. Blaedel, W.B. Lewis and J.W. Thomas, Anal. Chem. 24 : 509 (1952).

143. R.K. Iler (Ed.), "The Chemistry of Silica", John Wiley, New York, 1979; pp. 672.

144. B.S. Mustafin and O.V. Sivanova, Tr. Kom. Anal. Khim. Akad. Nauk. SSSR 17 : 131 (1969).

145. A. Albert and E.P. Serjeant (Eds.), "The Determination of Ionization Constants", 3 rd. ed., Chapman and Hall, New York, 1984; Chapter 9.

146. D. Cukman, J. Jednacak-Biscan, Z. Veksli and W. Haller, J. Coll.Interface Sci. 115 : 357 (1987).

147. A. Dawidowicz, W. Janusz, J. Szczypa and A. Waksmundzki, J. Coll. Interface Sci. 115 : 555 (1987).

148. Y.G. Berube and P.L. de Bruyn, J. Coll. Interface Sci. 27 : 305 (1968).

149. D.J. Shaw (Ed.), "Electrophoresis", Academic Press Inc., London, 1969.

150. C.W. Davies, J. Chem. Soc., 2093 (1938).

151. J. Kielland, J. Amer. Chem. Soc. 59 : 1675 (1937).

152. H.A. Laitinen and W.E. Harris, "Chemical Analysis", 2 nd. ed., McGraw-Hill, Toronto, 1975; Chapter 26.

153. S. Takamoto, Q. Fernando and H. Freiser, Anal. Chem. 37 : 1249 (1965).

154. E.W. Moore, J. Clin. Invest. 49 : 318 (1970).

155. H.A. Laitinen and W.E. Harris, "Chemical Analysis", 2 nd. ed., McGraw-Hill, Toronto, 1975; Chapter 11.

156. G.J. Moody and J.D.R. Thomas, Ion-Selective Electrode Rev. 1 : 3 (1979).

157. E.H. Hansen, C.G. Lamm and J. Ruzicka, Anal. Chim. Acta 59 : 403 (1972).

158. R. Guevremont and D.L. Rabenstein, Can. J. Chem. 55 : 4211 (1977).

159. R.J. Stolzberg, Anal. Chem. 53 : 1286 (1981).

160. A. Ringbom, " Complexation in Analytical Chemistry", Interscience, New York, 1963; Chapter 2.

161. R.M. Smith and A.E. Martell (Eds.), "Critical Stability Constants", Volume 1 : Amino Acids, Plenum Press, New York, 1974; Section III.

162. G.R. Lenz and A.E. Martell, Biochem. 3 : 750 (1964).

163. R.M. Smith and A.E. Martell (Eds.), "Critical Stability Constants", Volume 1 : Amino Acids, Plenum Press, New York, 1974; Section IV.

164. R.M. Smith and A.E. Martell (Eds.), "Critical Stability Constants", Volume 1 : Amino Acids, Plenum Press, New York, 1974; Section VI.

165. R.M. Smith and A.E. Martell (Eds.), "Critical Stability Constants", Volume 3 : Other Organic Ligands, Plenum Press, New York, 1977; Section II.

166. N.E. Topp and C.W. Davies, J. Chem. Soc. 87 (1940).

167. R.P. Bell and J.H.B. George, Trans. Faraday Soc. 49 : 619 (1953).

168. R.M. Smith and A.E. Martell (Eds.), "Critical Stability Constants", Volume 4 : Inorganic Complexes, Plenum Press, New York, 1976; Section II.

169. J. Bjerrum, G. Schwarzenbach and L.G. Sillen (Eds.), "Stability Constants", Chem. Soc. Spec. Publ. No. 7, London, 1958.

170. C.W. Davies and B.E. Hoyle, J. Chem. Soc. 1038 (1955).

171. Instruction Manual for Model 93-20 Calcium Ion Selective Electrode, Orion

Research Incorporated, Cambridge, Massachusetts, 1983.

172. G.A. Rechnitz and Z.F. Lin, Anal. Chem. 40 : 696 (1968).

173. B.J. Birch, A. Craggs, G.J. Moody and J.D.R. Thomas, J. Chem. Ed. 55 : 740 (1978).

174. G.K. Pagenkopf and K.A. Buell, Water Res. 8 : 375 (1974).

175. M. Otto, P.M. May, K. Murray and J.D.R. Thomas, Anal. Chem. 57 : 1511 (1985).

176. N.A. Farid, A.M. Wasfi, M.A. Fezel-Arab, H.M. Abd El-bary and M.M. Emara, Indian J. Chem. 25A : 817 (1986).

177. F.S. Nakayama and B.A. Rasnick, Anal. Chem. 39 : 1022 (1967).

178. G.A. Rechnitz and T.M. Hseu, Anal. Chem. 41 : 111 (1969).

179. J.R. Kramer, in R.F. Gould (Ed.), " Equilibrium Concepts in Natural Water Systems ", Advances in Chemistry Series No. 67, American Chemical Society, Washington D.C., 1967. pp. 243.

180. A. Lerman and C.W. Childs, in P.C. Singer (Ed.) "Trace Metals and Metal-Organic Interactions in Natural Waters", Ann Arbor Science, Michigan, 1974; pp. 201.

181. H.C. Claassen and A.F. White, in E.A. Jenne (Ed.), " Chemical Modeling in Aqueous Systems ", ACS Symposium Series No. 93, American Chemical Society, Washington D.C., 1979. pp. 771.

182. A.L. Jacobson, P.C. Singhal, H. Mandin and J.B. Hyne, Biochem. Med. 22 : 383 (1979).

183. M.A. Amerine and C.S. Ough (Eds.), " Wine and Must Analysis", Wiley, New York, 1974.

184. R.J. Cox, R.R. Eitenmiller and J.J. Powers, 42 : 849 (1977).

185. J.B. Willis, Anal. Chem. 33 : 556 (1961).

186. C. Baluja-Santos, A. Gonzalez-Portal and F. Bermejo-Martinez, Analyst 109 :

797 (1984).

187. Urinalysis News 3 : 3 (1987).

188. C.W. Davies and B.E. Hoyle, J. Chem. Soc. 4134 (1953).

189. N. Bjerrum and A. Unmack, Mat. Fys. Medd. Dan. Vid. Selsk., 9 : 1 (1929).

190. E. Gelles and A. Salama, J. Chem. Soc. 3683 (1958).

191. I. Greenwald, J. Redish and A.C. Kibrick, J. Biol. Chem. 135 : 65 (1940).

192. N.C. Li, A. Lindenbaum and J.M. White, J. Inorg. Nucl. Chem. 12 :122 (1959).

193. C.W. Davies, Trans. Faraday Soc. 23 : 351 (1927).

194. J.R. Parrish, Chem. Ind. 137 (1956).

195. F. Vernon and H. Eccles, Anal. Chim. Acta 63 : 403 (1973).

196. J.R. Parrish and R. Stevenson, Anal. Chim. Acta 70 : 189 (1974).

197. J.A. Buono, R.W. Karin and J.L. Fasching, Anal. Chim. Acta 80 : 327 (1975).

198. S.N. Willie, R.E. Sturgeon and S.S. Berman, Anal. Chim. Acta 149 : 59 (1983).

APPENDIX I

The sorption isotherms for Ca^{2+} on CPG-Oxine (Batch A) under various solution pH values and ionic strengths are presented in the following figures :

FIGURE PAGE

A.1 Sorption isotherm for Ca^{2+} in 0.10 M $NaClO_4$ at pH 8.01 on the 11 mg CPG-Oxine column................................ 164

A.2 Sorption isotherm for Ca^{2+} in 0.10 M $NaClO_4$ at pH 7.00 on the 11 mg CPG-Oxine column................................ 165

A.3 Sorption isotherm for Ca^{2+} in 0.10 M $NaClO_4$ at pH 6.00 on the 11 mg CPG-Oxine column................................ 166

A.4 Sorption isotherm for Ca^{2+} in 0.10 M $NaClO_4$ at pH 5.00 on the 11 mg CPG-Oxine column................................ 167

A.5 Sorption isotherm for Ca^{2+} in 0.010 M $NaClO_4$ at pH 8.01 on the 11 mg CPG-Oxine column................................ 168

A.6 Sorption isotherm for Ca^{2+} in 0.010 M $NaClO_4$ at pH 5.00 on the 11 mg CPG-Oxine column................................ 169

A.7 Sorption isotherm for Ca^{2+} in 0.75 M $NaClO_4$ at pH 7.00 on the 11 mg CPG-Oxine column................................ 170

A.8 Sorption isotherm for Ca^{2+} in 0.10 M $NaClO_4$ at pH 8.01 on the 40 mg CPG-Oxine column................................ 171

A.9 Sorption isotherm for Ca^{2+} in 0.10 M $NaClO_4$ at pH 7.00 on the 40 mg CPG-Oxine column which has not been equilibrated....... 172

A.10 Sorption isotherm for Ca^{2+} in 0.10 M KCl at pH 5.00 on the

11 mg CPG-Oxine column.................................. 173

A.11 Sorption isotherm for Ca^{2+} in 0.10 M KCl at pH 3.00 on the 11 mg CPG-Oxine column.................................. 174

A.12 Sorption isotherm for Ca^{2+} in 0.30 M $NaClO_4$ at pH 6.00 and pH 7.40 on the 11 mg CPG-Oxine column.......................... 175

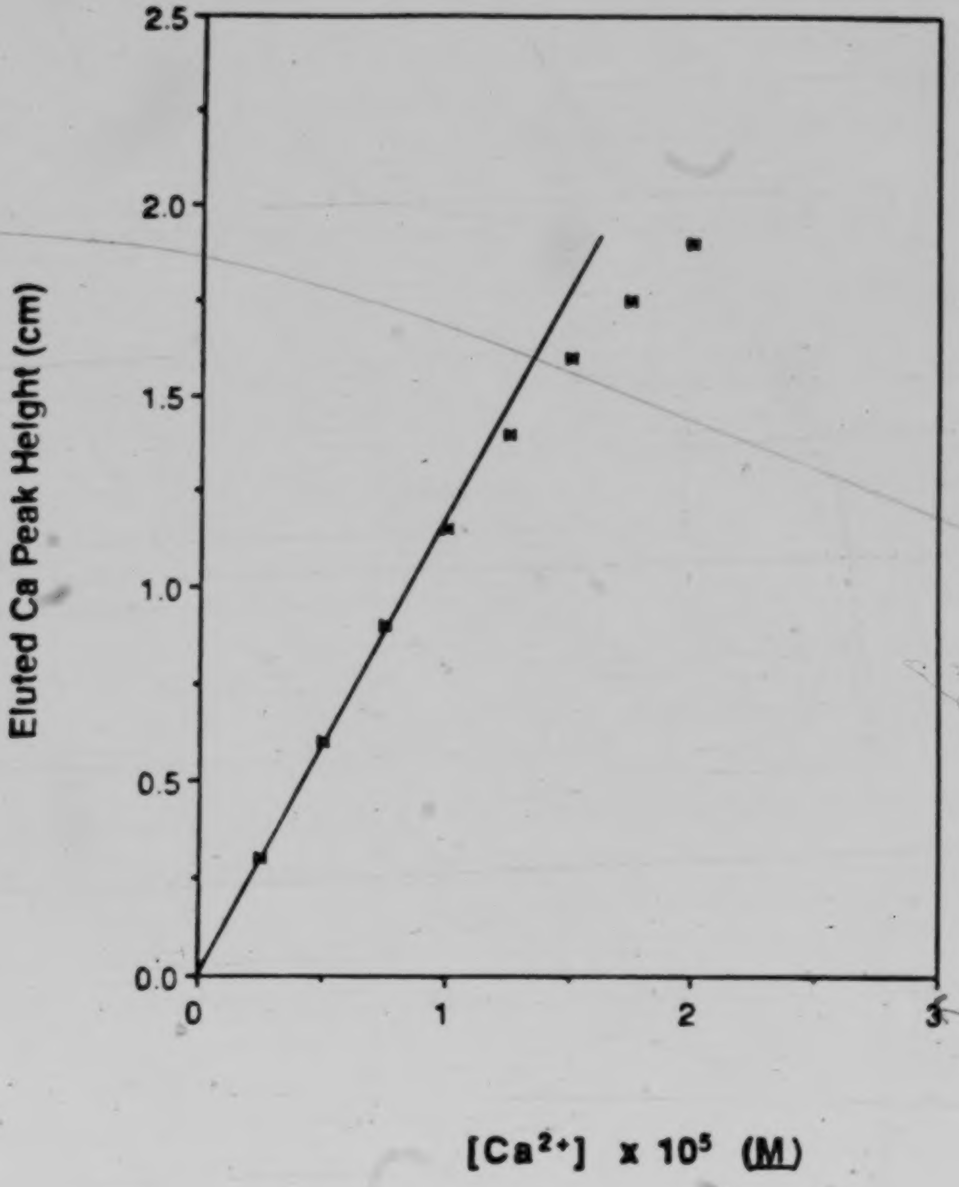

Figure A.1 : Sorption isotherm for Ca^{2+} in 0.10 M $NaClO_4$ at pH 8.01 on the 11 mg CPG-Oxine column.

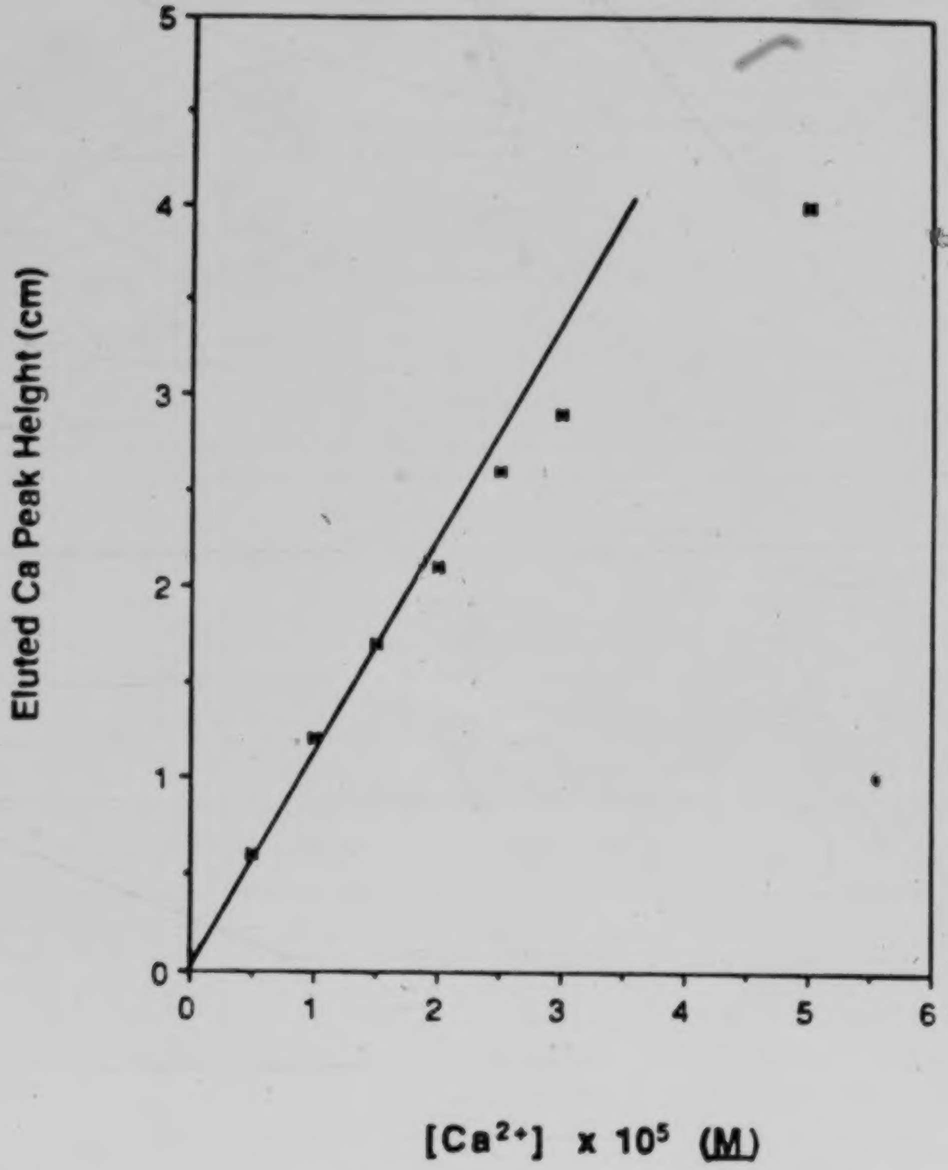

Figure A.2 : Sorption isotherm for Ca^{2+} in 0.10 M NaClO$_4$ at pH 7.00 on the 11 mg CPG-Oxine column.

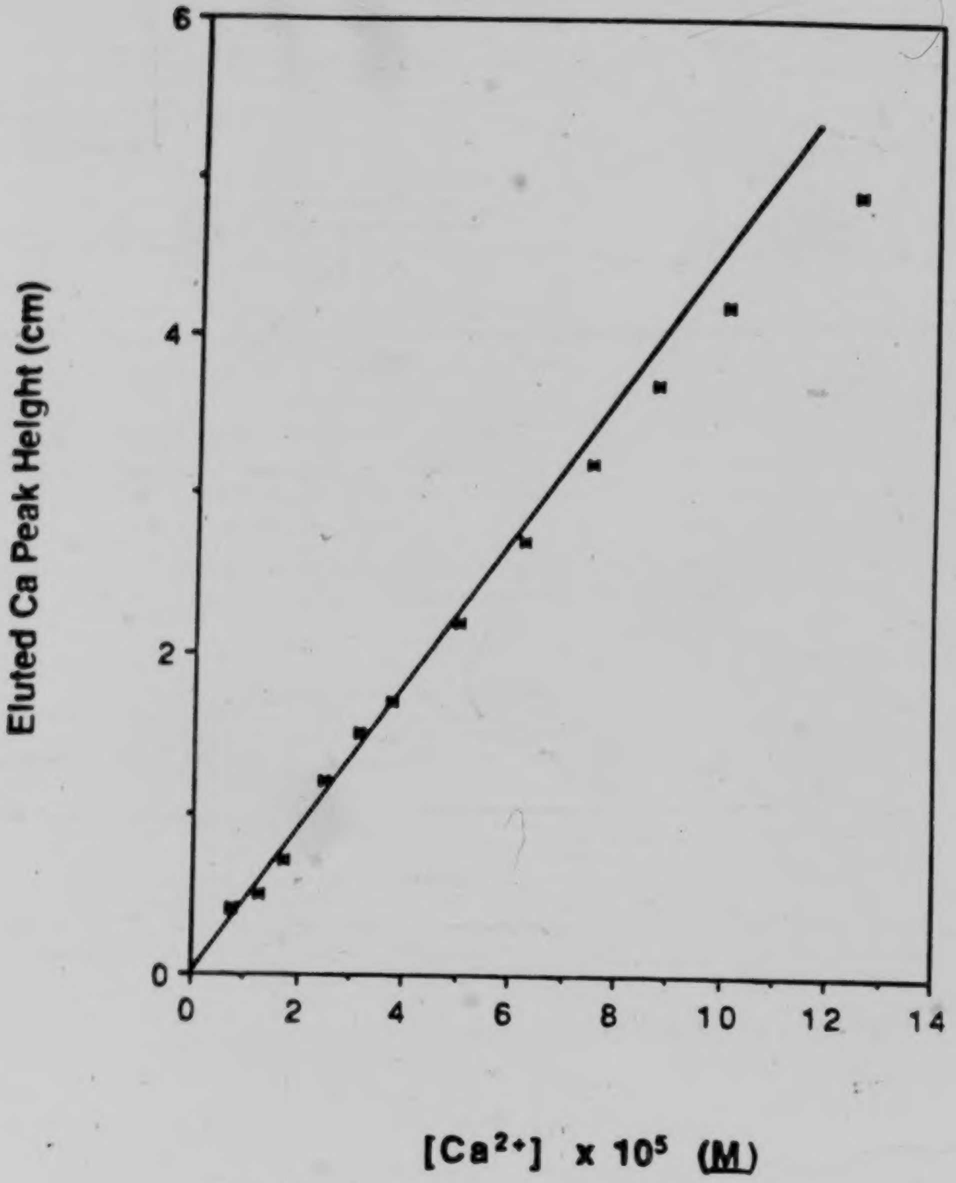

Figure A.3 : Sorption isotherm for Ca^{2+} in 0.10 M $NaClO_4$ at pH 6.00 on the 11 mg CPG-Oxine column.

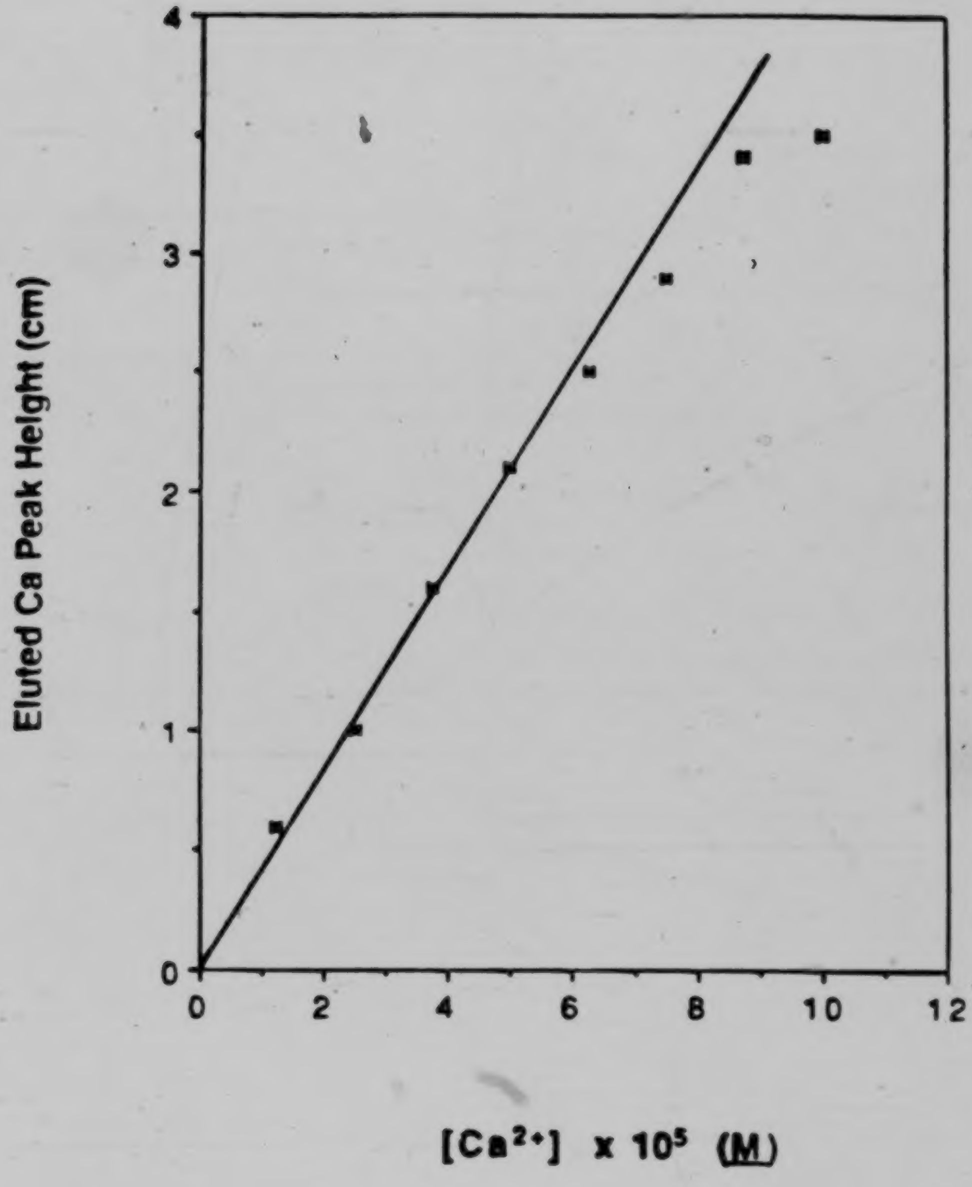

Figure A.4 : Sorption isotherm for Ca^{2+} in 0.10 M $NaClO_4$ at pH 5.00 on the 11 mg CPG-Oxine column.

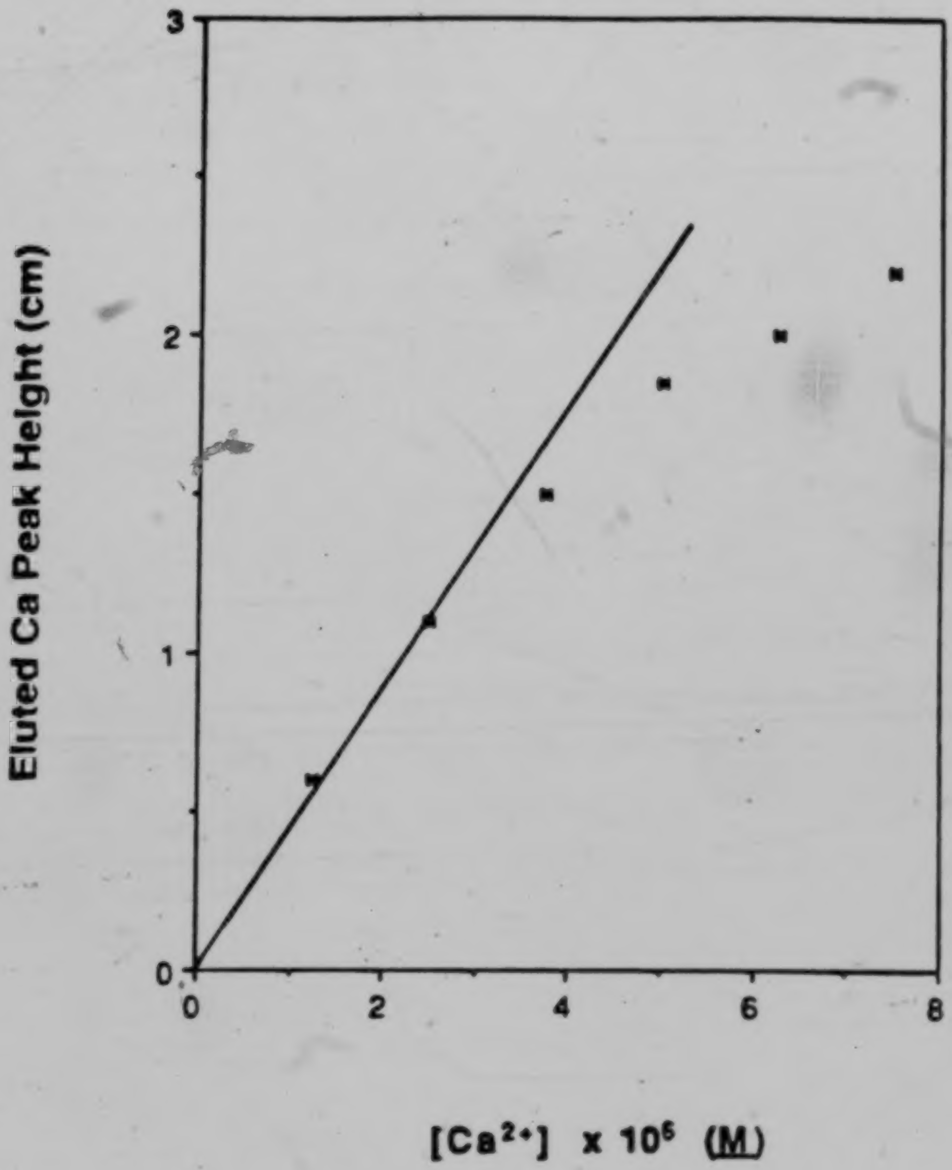

Figure A.5 : Sorption isotherm for Ca^{2+} in 0.010 M NaClO$_4$ at pH 8.01 on the 11 mg CPG-Oxine column.

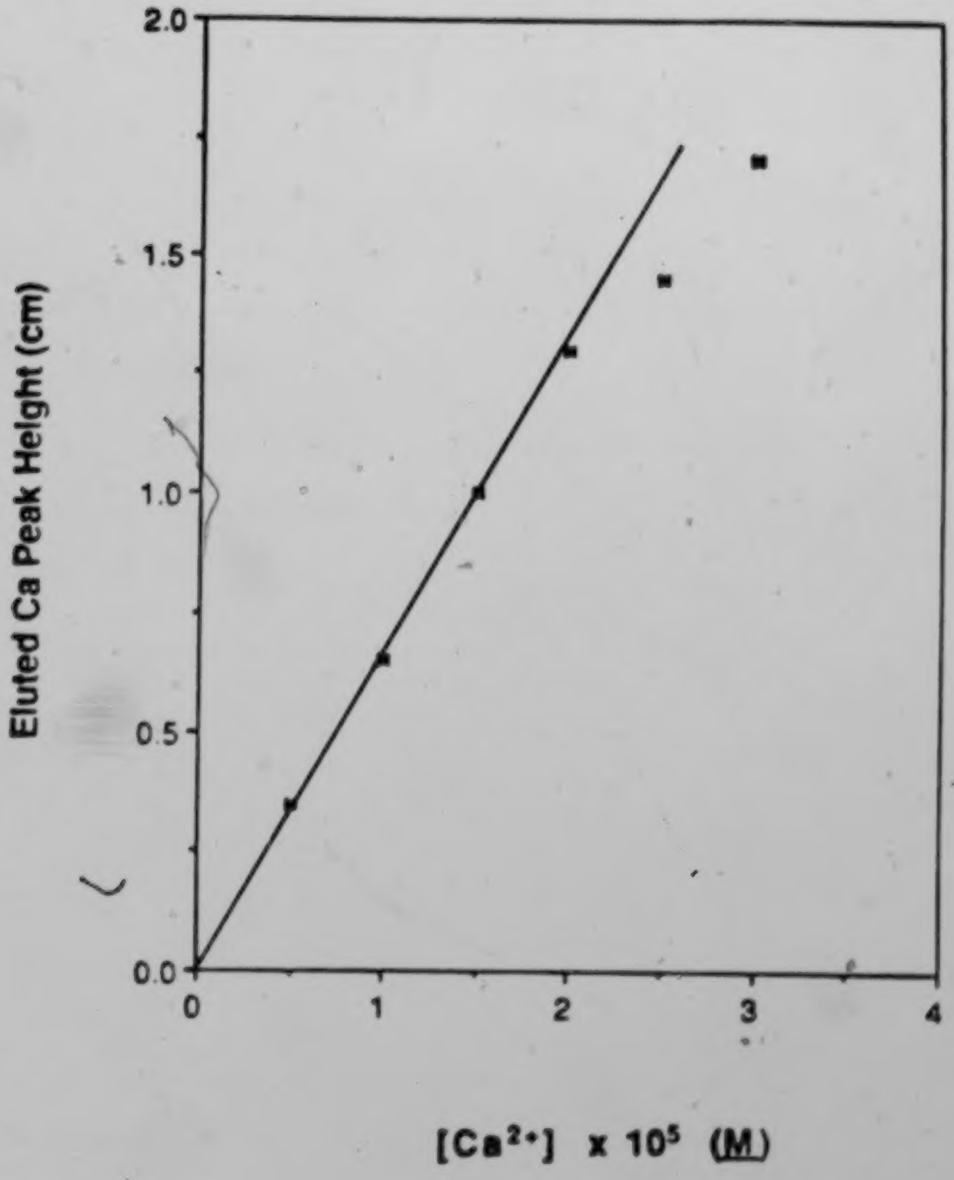

Figure A.6 : Sorption isotherm for Ca^{2+} in 0.010 M $NaClO_4$ at pH 5.00 on the 11 mg CPG-Oxine column.

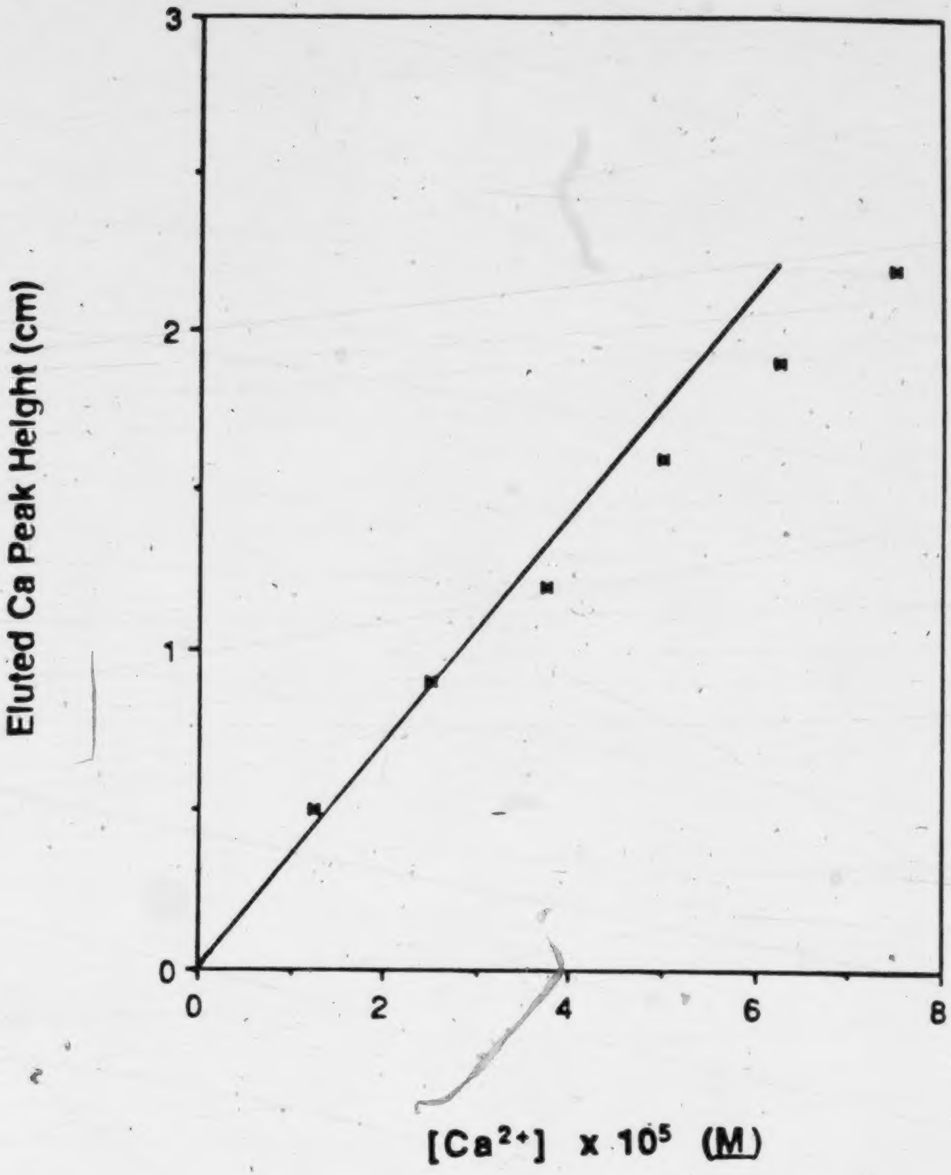

Figure A.7 : Sorption isotherm for Ca^{2+} in 0.75 M $NaClO_4$ at pH 7.00 on the 11 mg CPG-Oxine column.

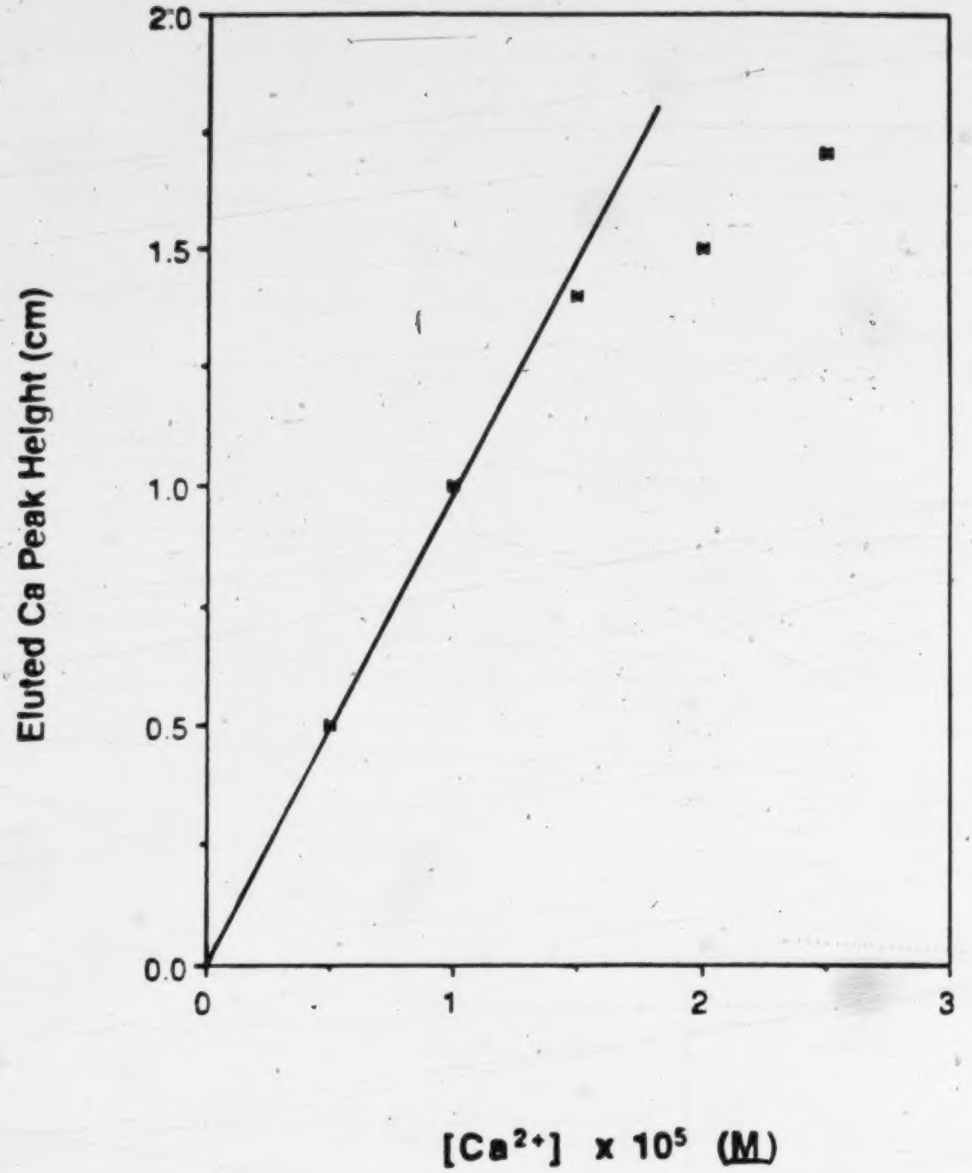

Figure A.8 : Sorption isotherm for Ca^{2+} in 0.10 M $NaClO_4$ at pH 8.01 on the 40 mg CPG-Oxine column.

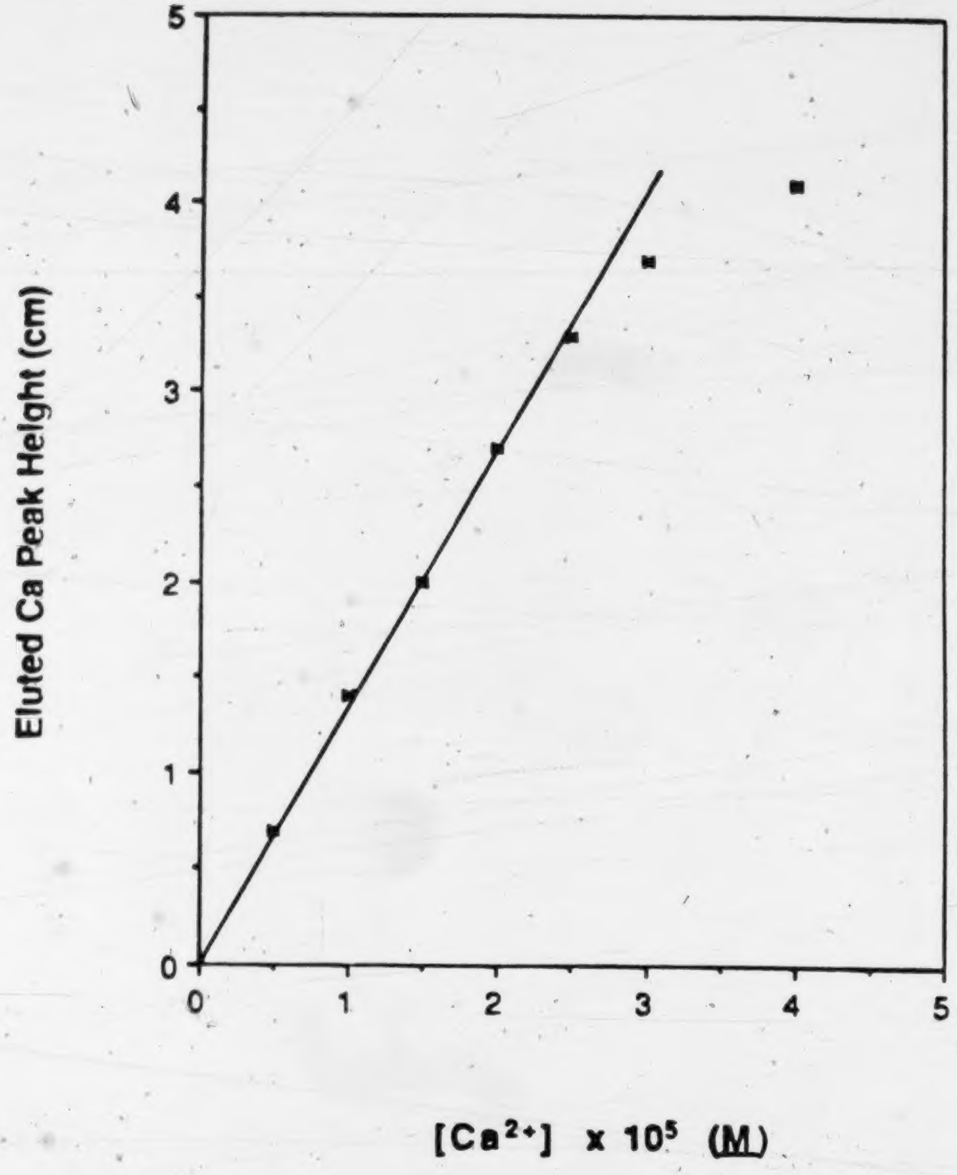

Figure A.9 : Sorption isotherm for Ca^{2+} in 0.10 M $NaClO_4$ at pH 7.00 on the 40 mg CPG-Oxine column which has not been equilibrated.

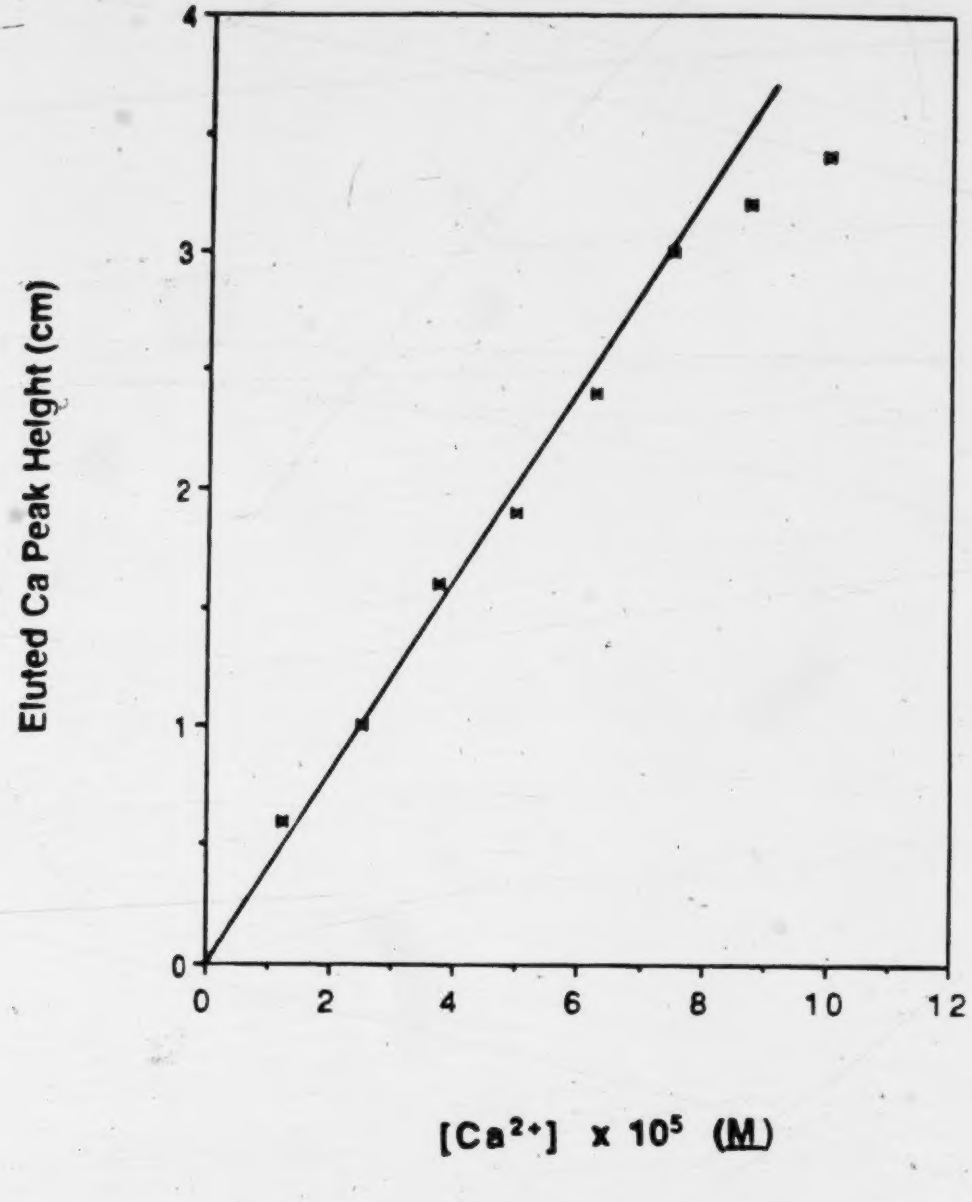

Figure A.10 : Sorption isotherm for Ca^{2+} in 0.10 M KCl at pH 5.00 on the 11 mg CPG-Oxine column.

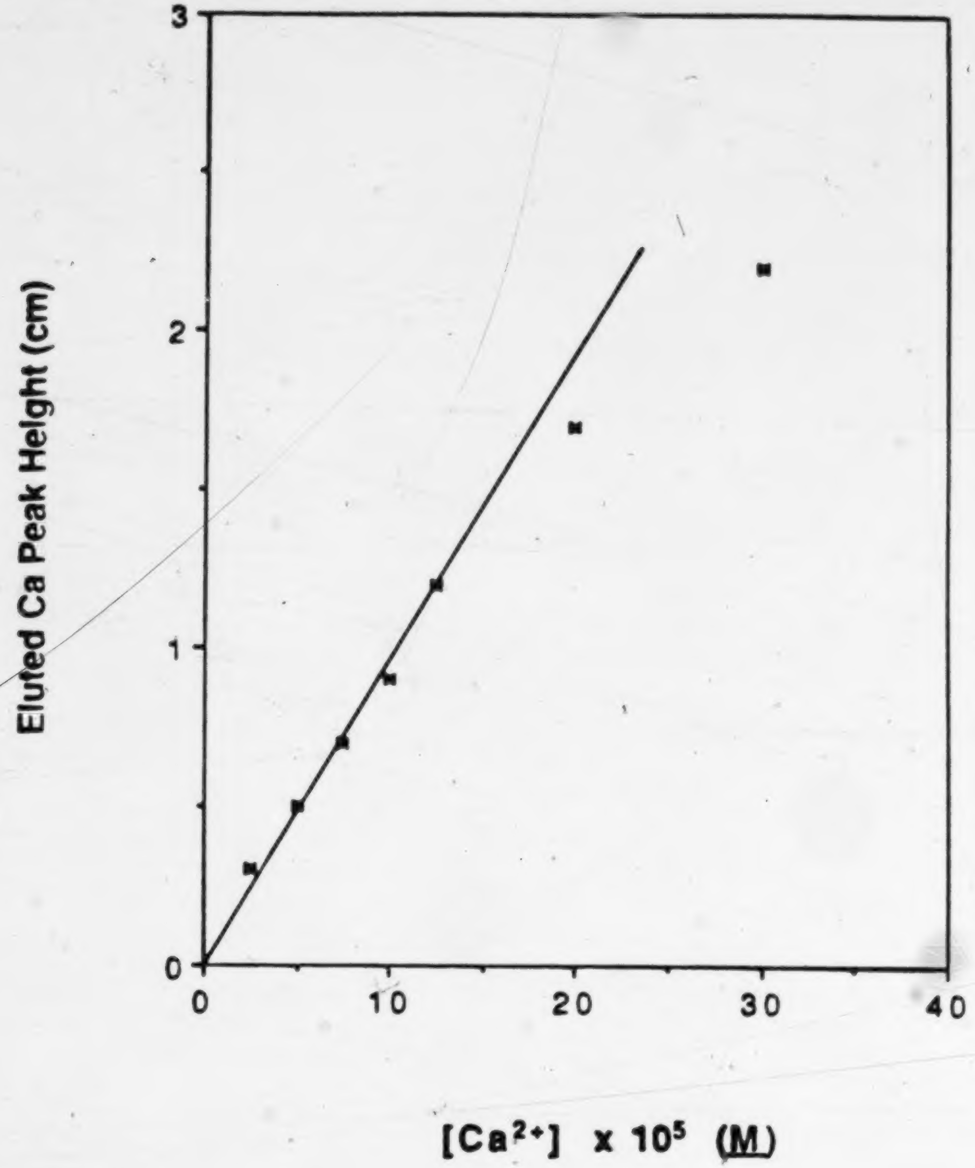

Figure A.11 : Sorption isotherm for Ca^{2+} in 0.10 M KCl at pH 3.00 on the 11 mg CPG-Oxine column.

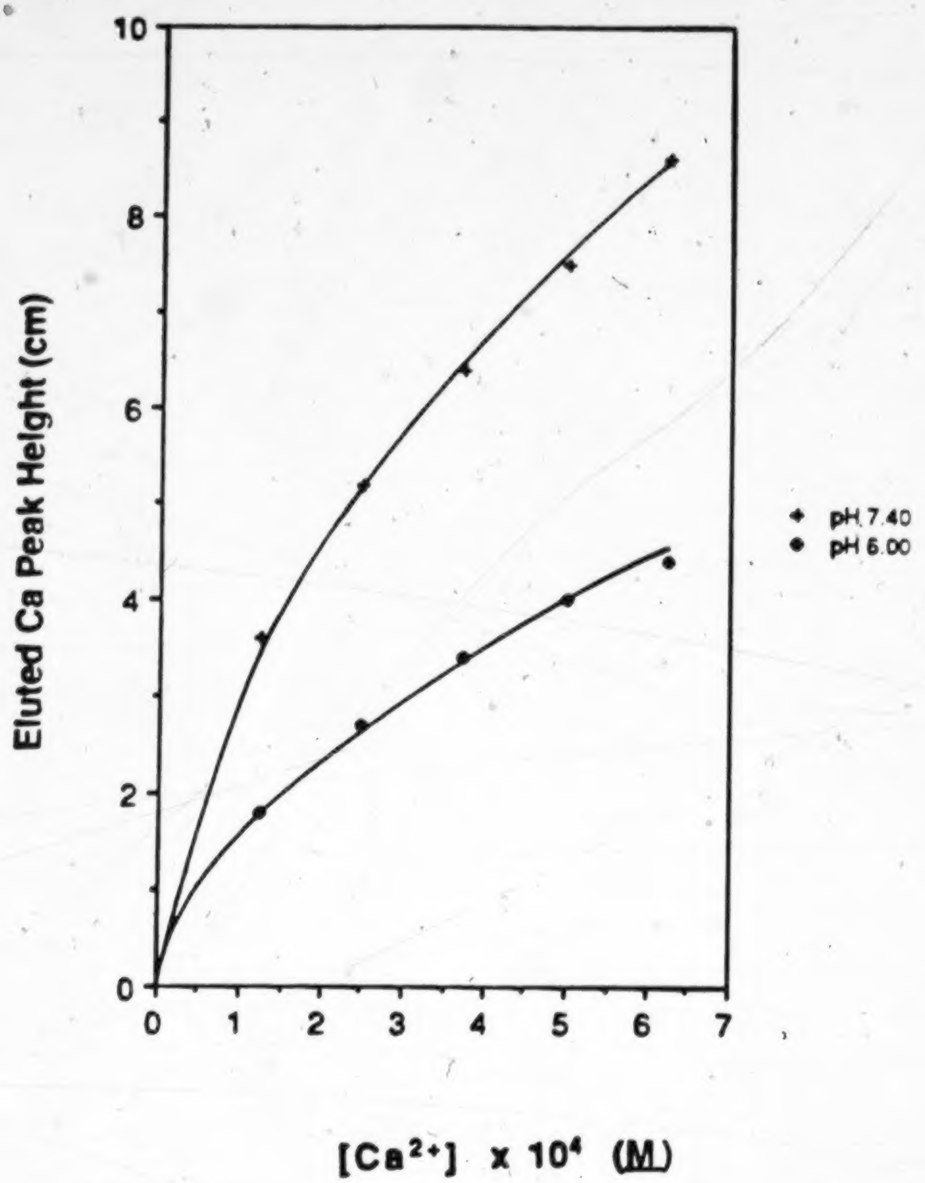

Figure A.12 : Sorption isotherm for Ca^{2+} in 0.30 M $NaClO_4$ at pH 6.00 and pH 7.40 on the 11 mg CPG-Oxine column.

APPENDIX II

COMICS PROGRAM

Values of $[Ca^{2+}]$ for solution containing several metal ions and several ligands, as in Section IV.3, were calculated using a slightly modified version of the speciation program called "COMICS" (7). The program was written in FORTRAN and stored in the Michigan Terminal System (MTS) of computing services, the University of Alberta.

COMICS is one of the commercially available programs designed for the calculation of equilibrium concentrations in solution. The calculation involves a simple species distribution routine using iteration (Figure A.13). The modified program included an additional subroutine which provided fractional species distributions of the metal in a tabular form. The scheme of the COMICS method (Figure A.13) is discussed briefly below (7.180):

A general form of a complexed species (J) that contains the metal-ion (M_i) and ligand (L_i) is given by

$$[M_{a,i}\, L_{b,i}\, H_d]_J \qquad (A.1)$$

where subscripts a, b and d denote stoichiometric coefficients for M_i, L_i and proton (H), respectively. a and b may be either positive or zero integers, whereas d may be a positive integer for hydrolyzed species, zero or a negative integer for protonated species.

The concentration of J, C_J, characterized by a stability constant (β_J), may be written as

$$C_J = \beta_J\, [M_i]^a\, [L_i]^b\, [H]^d \qquad (A.2)$$

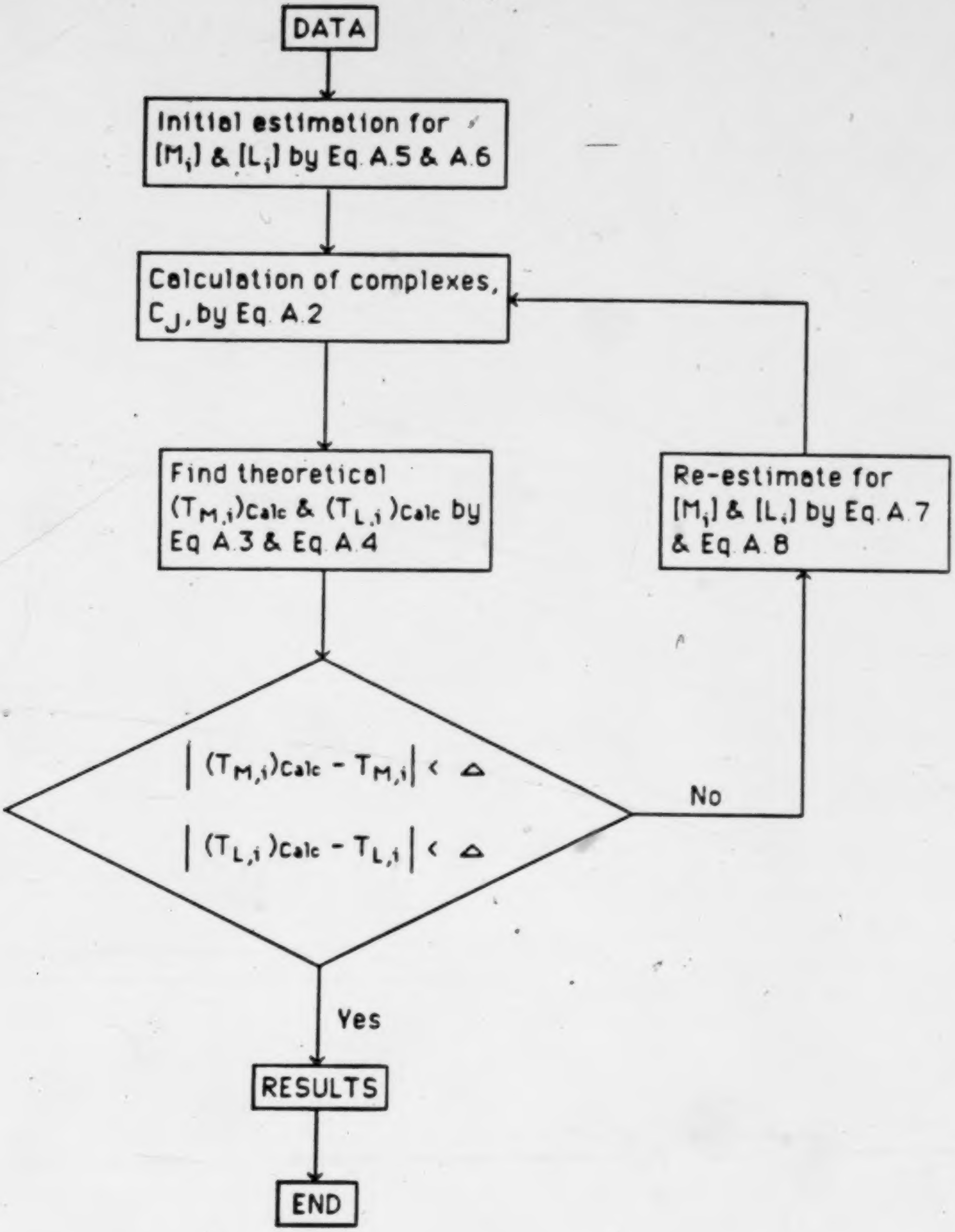
DATA
Initial estimation for $[M_i]$ & $[L_i]$ by Eq. A.5 & A.6
Calculation of complexes, C_J, by Eq. A.2
Find theoretical $(T_{M,i})_{Calc}$ & $(T_{L,i})_{Calc}$ by Eq A.3 & Eq A.4
$|(T_{M,i})_{Calc} - T_{M,i}| < \Delta$
$|(T_{L,i})_{Calc} - T_{L,i}| < \Delta$
No
Re-estimate for $[M_i]$ & $[L_i]$ by Eq. A.7 & Eq. A.8
Yes
RESULTS
END

Figure A.13 : Schemes of COMICS method.

The total concentration of M_i ($T_{M,i}$) is then

$$T_{M,i} = [M_i] + \sum_{J=1}^{n} aC_J \qquad (A.3)$$

The total concentration of L_i ($T_{L,i}$) is given by

$$T_{L,i} = [L_i] + \sum_{J=1}^{n} bC_J \qquad (A.4)$$

where n is the total number of complexed species containing M_i in the system.

The computer reads from input data and sets the values a, b and d for all species, the corresponding β_J, $T_{M,i}$ for each metal ion and $T_{L,i}$ for each ligand, the pH values at which the distributions of the species are to be computed, and then estimates the initial $[M_i]$ and $[L_i]$ by assuming

$$[M_i] = T_{M,i} \qquad (A.5)$$

and

$$[L_i] = T_{L,i} / (1 + \sum_{J=1}^{n} \beta_J [H]^d) \qquad (A.6)$$

The quantity on the right hand side of Eq. A.5 is computed for each kind of metal ion and, similarly for each ligand (Eq. A.6), to give the first approximation quantities that can be designated $(T_{M,i})_{Calc}$ and $(T_{L,i})_{Calc}$. The initial estimates of the free metals ($[M_i]$) and ligands ($[L_i]$) are then replaced by

$$[M_i]' = [M_i] \{ T_{M,i} / (T_{M,i})_{Calc} \}^{1/2} \qquad (A.7)$$

$$[L_i]' = [L_i] \{ T_{L,i} / (T_{L,i})_{Calc} \}^{1/2} \qquad (A.8)$$

With these new values ($[M_i]'$ and $[L_i]'$) the calculations are repeated to obtain better estimates of $[M_i]$ and $[L_i]$. The process is repeated until all values of $(T_{M,i})_{Calc}$ and $(T_{L,i})_{Calc}$ differ from the corresponding values of $T_{M,i}$ and $T_{L,i}$ by less than a specified quantity (Δ), usually 0.001%. Within this accuracy, the final values of $[M_i]$ and $[L_i]$ satisfy all the equations for metal ion and ligand concentrations. These final values are used to compute the equilibrium concentrations of all species, and the results are printed out in tabular form.

The data input for COMICS includes (i) stoichiometric descriptions of all complex species to be considered, such as metal-ligand complexes, and hydrolyzed and protonated species, along with their stability constants; (ii) total concentration of each component; and (iii) pH values under investigation. The stability constants, only for those components which participate in complexation, used for all studies were taken from data compilations or from specific literature references. Correction for ionic strength, if necessary, was made by using the calculated mean activity coefficients based on the Davies equation (150). The data input and output of a sample calculation (e.g. calcium speciation in urine) are given in Figures A.14 and A.15, respectively. The data input procedures for Figure A.14 are illustrated in Figure A.16. It is important to input data in the correct format as specified in Figure A.16.

```
list pat1

   1      1
   2     CALCIUM SPECIATION IN URINE
   3      3 2 17
   4      1 0 0 0 0 0 0 0 0 0 1 0 0 0 0 0 0 0 0 0 0          0.6434
   5      1 0 0 0 0 0 0 0 0 0 1 0 0 0 0 0 0 0 0 0 0          1.8182
   6      1 0 0 0 0 0 0 0 0 0 0 0 0 0 0 0 0 0 0 0-1         11.7399
   7      1 0 0 0 0 0 0 0 0 0 0 0 0 0 0 0 0 0 0 0-2         17.4612
   8      1 0 0 0 0 0 0 0 0 0 0 0 0 0 0 0 0 0 0 0-3         19.4612
   9      0 1 0 0 0 0 0 0 0 0 1 0 0 0 0 0 0 0 0 0 0          2.2090
  10      0 1 0 0 0 0 0 0 0 0 1 0 0 0 0 0 0 0 0 0 0          3.5291
  11      0 1 0 0 0 0 0 0 0 0 0 0 0 0 0 0 0 0 0 0-1          5.6904
  12      0 1 0 0 0 0 0 0 0 0 0 0 0 0 0 0 0 0 0 0-2         10.0401
  13      0 1 0 0 0 0 0 0 0 0 0 0 0 0 0 0 0 0 0 0-3         12.9097
  14      0 0 1 0 0 0 0 0 0 0 1 0 0 0 0 0 0 0 0 0 0          2.9684
  15      0 0 1 0 0 0 0 0 0 0 0 0 0 0 0 0 0 0 0 0-1          3.8210
  16      0 0 1 0 0 0 0 0 0 0 0 0 0 0 0 0 0 0 0 0-2          4.8610
  17      1 0 0 0 0 0 0 0 0 0 0 1 0 0 0 0 0 0 0 0 0          1.6187
  18      0 1 0 0 0 0 0 0 0 0 0 1 0 0 0 0 0 0 0 0 0          1.5784
  19      0 1 0 0 0 0 0 0 0 0 0 1 0 0 0 0 0 0 0 0 0          3.2490
  20      0 0 1 0 0 0 0 0 0 0 0 1 0 0 0 0 0 0 0 0 0          2.5488
  21     8.18E-032.08E-032.10E-04
  22     3.86E-033.70E-03
  23         5.50000
  24         5.60000
  25         5.70000
  26         5.80000
  27         5.90000
  28         6.00001
```

Figure A.14 : Data input of "CALCIUM SPECIATION IN URINE" for the COMICS program.

```
list patl.outl

 #
  CALCIUM SPECIATION IN URINE


          L1  L2  L3  L4  L5  L6  L7  L8  L9  L10 M1  M2  M3  M4  M5  M6  M7  M8  M9  M10  OH   LOG.BETA
      1    1   0   0   0   0   0   0   0   0   0   1   0   0   0   0   0   0   0   0   0   0     0.6434
      2    1   0   0   0   0   0   0   0   0   0   1   0   0   0   0   0   0   0   0   0   0     1.8182
      3    1   0   0   0   0   0   0   0   0   0   0   0   0   0   0   0   0   0   0   0  -1    11.7399
      4    1   0   0   0   0   0   0   0   0   0   0   0   0   0   0   0   0   0   0   0  -2    17.4612
      5    1   0   0   0   0   0   0   0   0   0   0   0   0   0   0   0   0   0   0   0  -3    19.4612
      6    0   1   0   0   0   0   0   0   0   0   1   0   0   0   0   0   0   0   0   0   0     2.2090
      7    0   1   0   0   0   0   0   0   0   0   1   0   0   0   0   0   0   0   0   0   0     3.5291
      8    0   1   0   0   0   0   0   0   0   0   0   0   0   0   0   0   0   0   0   0  -1     5.6904
      9    0   1   0   0   0   0   0   0   0   0   0   0   0   0   0   0   0   0   0   0  -2    10.0401
     10    0   1   0   0   0   0   0   0   0   0   0   0   0   0   0   0   0   0   0   0  -3    12.9097
     11    0   0   1   0   0   0   0   0   0   0   1   0   0   0   0   0   0   0   0   0   0     2.9684
     12    0   0   1   0   0   0   0   0   0   0   0   0   0   0   0   0   0   0   0   0  -1     3.8210
     13    0   0   1   0   0   0   0   0   0   0   0   0   0   0   0   0   0   0   0   0  -2     4.8610
     14    1   0   0   0   0   0   0   0   0   0   0   1   0   0   0   0   0   0   0   0   0     1.6187
     15    0   1   0   0   0   0   0   0   0   0   0   1   0   0   0   0   0   0   0   0   0     1.5784
     16    0   1   0   0   0   0   0   0   0   0   0   1   0   0   0   0   0   0   0   0   0     3.2490
     17    0   0   1   0   0   0   0   0   0   0   0   1   0   0   0   0   0   0   0   0   0     2.5400
 TOTAL CONCN. OF LIGAND ( 1)=   0.818E-02
 TOTAL CONCN. OF LIGAND ( 2)=   0.208E-02
 TOTAL CONCN. OF LIGAND ( 3)=   0.210E-03
 TOTAL CONCN. OF METAL ( 1)=   0.386E-02
 TOTAL CONCN. OF METAL ( 2)=   0.370E-02



PH = 5.500
NUMBER OF ITERATIONS =   37
           C1          C2          C3          C4          C5          C6          C7          C8          C9          C10
FREE METALS
        2.633E-03   3.002E-03
FREE LIGANDS
        1.767E-09   1.193E-04   4.634E-05
COMPLEX SPECIES
   1- 10  2.047E-11   3.061E-10   3.069E-03   5.109E-03   1.616E-06   5.085E-05   1.063E-03   1.850E-04   1.309E-05   3.065E-08
  11- 17  1.135E-04   9.705E-07   3.365E-11   2.704E-10   1.357E-05   6.356E-04   4.922E-05

```

Figure A.15 : Data output of "CALCIUM SPECIATION IN URINE" for the COMICS program.

```
PH = 5.600
NUMBER OF ITERATIONS =   25
              C1          C2          C3          C4          C5          C6          C7          C8          C9          C10
FREE METALS
           2.612E-03  2.987E-03
FREE LIGANDS
           2.552E-09  1.226E-04  4.664E-05
COMPLEX SPECIES
   1- 10   2.933E-11  4.386E-10  3.522E-03  4.657E-03  1.170E-06  5.181E-05  1.083E-03  1.509E-04  8.482E-06  1.578E-08
  11- 17   1.133E-04  7.758E-07  2.137E-11  3.169E-10  1.387E-05  6.496E-04  4.930E-05


PH = 5.700
NUMBER OF ITERATIONS =   24
              C1          C2          C3          C4          C5          C6          C7          C8          C9          C10

FREE METALS
           2.595E-03  2.975E-03
FREE LIGANDS
           3.639E-09  1.252E-04  4.688E-05
COMPLEX SPECIES
   1- 10   4.155E-11  6.714E-10  3.989E-03  4.190E-03  8.360E-07  5.259E-05  1.099E-03  1.275E-04  5.468E-06  8.080E-09
  11- 17   1.131E-04  6.195E-07  1.355E-11  4.500E-10  1.411E-05  6.611E-04  4.936E-05


PH = 5.800
NUMBER OF ITERATIONS =   24
              C1          C2          C3          C4          C5          C6          C7          C8          C9          C10
FREE METALS
           2.582E-03  2.966E-03
FREE LIGANDS
           5.121E-09  1.274E-04  4.708E-05
COMPLEX SPECIES
   1- 10   5.816E-11  8.699E-10  4.459E-03  3.720E-03  5.896E-07  5.322E-05  1.112E-03  9.899E-05  3.510E-06  4.120E-09
  11- 17   1.130E-04  4.941E-07  8.587E-12  6.313E-10  1.431E-05  6.704E-04  4.941E-05
```

Figure A.15 : Data output of "CALCIUM SPECIATION IN URINE" for the COMICS program (continued).

```

   PH = 5.900
   NUMBER OF ITERATIONS =    23
             C1          C2          C3          C4          C5          C6          C7          C8          C9          C10
   FREE METALS
          2.571E-03   2.958E-03
   FREE LIGANDS
          7.113E-09   1.292E-04   4.724E-05
   COMPLEX SPECIES
      1- 10  8.044E-11   1.203E-09   4.920E-03   3.760E-03   4.104E-07   5.373E-05   1.123E-03   7.972E-05   2.245E-06   2.093E-09
     11- 17  1.129E-04   3.938E-07   5.437E-12   8.745E-10   1.447E-05   6.779E-04   4.945E-05



   PH = 6.000
   NUMBER OF ITERATIONS =    23
             C1          C2          C3          C4          C5          C6          C7          C8          C9          C10
   FREE METALS
          2.562E-03   2.952E-03
   FREE LIGANDS
          9.754E-09   1.306E-04   4.737E-05
   COMPLEX SPECIES
      1- 10  1.099E-10   1.644E-09   5.359E-03   2.821E-03   2.821E-07   5.413E-05   1.131E-03   6.402E-05   1.432E-06   1.061E-09
     11- 17  1.128E-04   3.137E-07   3.440E-12   1.197E-09   1.460E-05   6.840E-04   4.948E-05
   8

list pat1.out2



   9
   CALCIUM SPECIATION IN URINE

    LIGAND CONC. =  8.180E-03
    METAL CONC. =  3.860E-03

           FREE
     PH    METAL   C1     C2     C3     C4     C5     C6     C7     C8     C9

    5.500  0.682  0.000  0.000  0.013  0.275  0.029
    5.600  0.677  0.000  0.000  0.013  0.280  0.029
    5.700  0.672  0.000  0.000  0.014  0.285  0.029
    5.800  0.669  0.000  0.000  0.014  0.288  0.029
    5.900  0.666  0.000  0.000  0.014  0.291  0.029
    6.000  0.664  0.000  0.000  0.014  0.293  0.029
```

Figure A.15 : Data output of "CALCIUM SPECIATION IN URINE" for the COMICS program (continued).

DATA INPUT PROCEDURES:

I) Creat a data file, e.g. Pat1 (See Figure A.14).

II) Edit Pat1 in the following format :

1. Line #1 : Number of jobs to be run. Start at Column #2 for less than 10 jobs.
2. Line #2 : Title of the job. Start at Column #1.
3. Line #3 : Number of ligands, metals and equilibria involved.
    - Column #1-2 : Number of ligands (maximum 10 ligands), i.e. 3 for phosphate, citrate and oxalate.
    - Column #3-4 : Number of metals (maximum 10 metals), i.e. 2 for calcium and magnesium.
    - Column #5-7 : Number of equilibria, i.e. 17 (See Table A.1).
4. Line #4-20 : Stoichiometric coefficients of ligands, metals and proton.
    - Column #2 -20 : Stoichiometric coefficient of ligand in each species (See Table A.1). Use Column #2 for phosphates and Column #4 for citrates, etc.
    - Column #22-40 : Stoichiometric coefficient of metal ion in each species (See Table A.1). Use Column #22 for calcium and Column #24 magnesium.
    - Column #41-42 : Stoichiometric coefficient of proton in each species (See Table A.1).
    - Column #53-59 : Value of log β for each species (See Table A.1). Fix decimal point at Column #55.

Figure A.16 : Data input procedures for the COMICS program.

5. Line #21 : Total concentration of each ligand. Enter ligand concentrations in the order previously assigned, i.e. phosphate, citrate, oxalate. Use 3 significant figures only and without any spacing between each concentration.

6. Line #22 : Total concentration of each metal. Enter metal ion concentrations in the order previously assigned, i.e. calcium, magnesium. Use 3 significant figures only and without any spacing between each concentration.

7. Line #23-28 : Values of pH. Start from Column #5, enter the pH values under investigation on separate lines. Use 6 significant figures for each pH and the last pH value should be ended with a number 1.

III) Create two output files, e.g. Pat1.Out1 and Pat2.Out2.

IV) Run the COMICS program by using the following command :

```
RUN MODCOM.1 1=Pat1 3=Pat1.Out1 4=Pat1.Out2
```

V) List Pat1 (Figure A.14); Pat1.Out1 and Pat1.Out2 (Figure A.15).

Figure A.16 : Data input procedures for the COMICS program (continued).

Table A 1 : Equilibria in the simulated urine system (Section V.3.3.1).

	Stoichiometric Coefficient				
Equilibrium	M_i	L_i	H	log β_j	Reference
$Ca^{2+} + H_2PO_4^- \rightleftharpoons CaH_2PO_4^+$	1	1	0	0.6434 [a]	179
$Ca^{2+} + HPO_4^{2-} \rightleftharpoons CaHPO_4$	1	1	0	1.8182 [a]	179
$H^+ + PO_4^{3-} \rightleftharpoons HPO_4^{2-}$	0	1	-1	11.7399	169
$2H^+ + PO_4^{3-} \rightleftharpoons H_2PO_4^-$	0	1	-2	17.4612	169
$3H^+ + PO_4^{3-} \rightleftharpoons H_3PO_4$	0	1	-3	19.4612	169
$Ca^{2+} + HCit^{2-} \rightleftharpoons CaHCit$	1	1	0	2.2090 [a]	171
$Ca^{2+} + Cit^{3-} \rightleftharpoons CaCit^-$	1	1	0	3.5291 [a]	180
$H^+ + Cit^{3-} \rightleftharpoons HCit^{2-}$	0	1	-1	5.6904	166
$2H^+ + Cit^{3-} \rightleftharpoons H_2Cit^-$	0	1	-2	10.0401	166
$3H^+ + Cit^{3-} \rightleftharpoons H_3Cit$	0	1	-3	12.9097	166
$Ca^{2+} + C_2O_4^{2-} \rightleftharpoons CaC_2O_4$	1	1	0	2.9684 [a]	181
$H^+ + C_2O_4^{2-} \rightleftharpoons HC_2O_4^-$	0	1	-1	3.8210	166
$2H^+ + C_2O_4^{2-} \rightleftharpoons H_2C_2O_4$	0	1	-2	4.8610	166
$Mg^{2+} + HPO_4^{2-} \rightleftharpoons MgHPO_4$	1	1	0	1.6187 [a]	182
$Mg^{2+} + HCit^{2-} \rightleftharpoons MgHCit$	1	1	0	1.5784 [a]	183
$Mg^{2+} + Cit^{3-} \rightleftharpoons MgCit^-$	1	1	0	3.2490 [a]	183
$Mg^{2+} + C_2O_4^{2-} \rightleftharpoons MgC_2O_4$	1	1	0	2.5488 [a]	184

a : Calculated from thermodynamic constant to c = 0.1 M

Cit^{3-} : Citrate, i.e. $C_6H_5O_7^{3-}$